

**Phosphoribosyltransferases in *Toxoplasma gondii*:
Targets for Structure-based Inhibitor Design**

by

Darrick A. Carter


A DISSERTATION

Presented to the Department of Biochemistry and Molecular Biology and the
Oregon Health Sciences University
School of Medicine
in partial fulfillment of
the requirements for the degree of
Doctor of Philosophy
November 1997

School of Medicine
Oregon Health Sciences University

CERTIFICATE OF APPROVAL

This is to certify that the Ph.D. thesis of
Darrick A. Carter
has been approved



Professor in charge of thesis



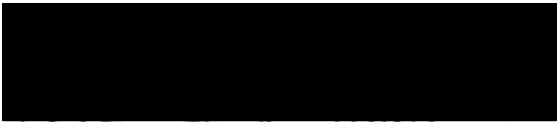
Member



Member



Member



Associate Dean for Graduate Studies

Table of Contents

Catalog of Figures.....	iii
Acknowledgments	viii
Abstract	x

I. Introduction

1. <i>Toxoplasma gondii</i> , an Overview.....	1
1.1. History.....	1
1.2. Life Cycle.....	4
1.3. Cell Culture and Biology.....	6
1.4. Pathogenesis and Treatment of Toxoplasmosis.....	7
1.5. Purine and Pyrimidine Metabolism in <i>T. gondii</i>	13
1.5.1. Purine Metabolism.....	13
1.5.2. Pyrimidine Metabolism.....	14
2. Phosphoribosyltransferases.....	17
2.1. Phosphoribosyltransferases in Metabolism.....	17
2.2. Biochemistry of Phosphoribosyltransfer.....	19
2.3. Structural Features of Phosphoribosyltransferases.....	23
2.4. Phosphoribosyltransferases as Drug Targets.....	30
3. Rational Inhibitor Design.....	33
4. Literature Cited.....	39

II. Main

1. Overexpression and Characterization of HGXPRT isoforms.....	48
2. Characterization of HGXPRT-I.....	60
2.1. Expression, purification, and biochemical properties.....	60
2.2. Structural studies.....	78
2.3. Kinetic studies (forward, reverse, mechanism).....	88
2.4. Site-directed mutagenesis	
2.4.1. Aromatic mutations in <i>L. donovani</i> HGPRT (Manuscript).....	100
2.4.2. D206 mutants.....	120
3. Inhibitor design against HGXPRT-I.....	131
4. Uracil phosphoribosyltransferase	
4.1. Expression and characterization of UPRT (Manuscript).....	143
4.2. Chemical Modification of UPRT and C128V mutant.....	166
5. Future directions.....	178

III. Appendix

A. Cloning and overexpression of <i>P. falciparum</i> HGXPRT in <i>E. coli</i>	179
B. Cloning, overexpression and purification of <i>T. gondii</i> DHFR-TS in <i>E. coli</i>	189

Catalog of Figures

Introduction

Figure 1	Phylogenetic tree for <i>Toxoplasma gondii</i>	03
Figure 2	Life cycle of <i>Toxoplasma gondii</i>	05
Figure 3	Tachyzoite ultrastructure.....	08
Figure 4	Commonly used drugs for toxoplasmosis.....	12
Figure 5	Purine metabolism in <i>T. gondii</i>	15
Figure 6	Pyrimidine metabolism in <i>T. gondii</i>	16
Figure 7	Chemistry of the purine / pyrimidine phosphoribosyltransferase reaction.....	20
Figure 8	Kinetic mechanism of the hypoxanthine-(xanthine)-guanine phosphoribosyltransferases.....	22
Figure 9a	Alignment of HG(X)PRT enzymes.....	25
Figure 9b	Alignment of APRT enzymes.	26
Figure 9c	Alignment of OPRT enzymes.....	27
Figure 9d	Alignment of UPRT enzymes.....	28
Figure 10	Structural conservation among phosphoribosyltransferases.....	29
Figure 11	Subversive substrates of phosphoribosyltransferases.....	31
Figure 12	The DOCK suite of programs.....	37
Figure 13	Iterative structure determination and inhibitor testing for the discovery of tight binding inhibitors.....	38
Table 1	Phosphoribosyltransferases and their functions.....	17

Chapter 1: Overexpression and Characterization of HGXPRT Isoforms

Figure 1	Alignment of HGXPRT-I and HGXPRT-II.....	49
Figure 2	Expression and affinity purification of recombinant HGXPRT isoforms.....	53
Figure 3	Western blot of <i>T. gondii</i> lysates.....	54
Figure 4a	Densitometric analyses of fractionated RH strain <i>Toxoplasma</i> lysates.....	57
Figure 4b	Degradation of <i>T. gondii</i> HGXPRT isoforms.....	58
Table 1	Kinetic parameters for recombinant <i>T. gondii</i> HGXPRT isoforms.....	55

Chapter 2.1: Expression, purification, and biochemical characterization of the *T. gondii* HGXPRT-I

Figure 1	Map of the pBAce-HGXPRTI construct.....	67
Figure 2	DEAE Chromatography of HGXPRT-I.....	68
Figure 3	Ammonium sulfate precipitation of HGXPRT-I.....	69
Figure 4	Gel permeation chromatography of HGXPRT-I	70
Figure 5	Purification of HGXPRT-I	71
Figure 6	Divalent Cation usage by HGXPRT-I	72
Figure 7	Arrhenius plot of reaction rates for HGXPRT-I	73
Figure 8	Effect of Cysteine modifying reagents on HGXPRT-I	74
Figure 9	GMP dialdehyde dependant inactivation of HGXPRT-I	75

Chapter 2.2: Structural studies on the *T. gondii* HGXPRT-I enzyme

Figure 1	HPLC size exclusion chromatography of HGXPRT-I.....	84
Figure 2	Disassociation of HGXPRT-I as a function of concentration	85
Figure 3	Circular dichroism studies on HGXPRT-I	86
Table 1	Changes in calculated Stoke's radii with PRPP	82

Chapter 2.3: Kinetic Studies on the *T. gondii* HGXPRT-I enzyme

Figure 1	Magnesium dependent rates of the HGXPRT-I.....	95
Figure 2	Steady-state kinetics of the HGXPRT-I in the forward direction.....	96
Figure 3	Steady-state kinetics of the HGXPRT-I in the reverse direction.....	97
Figure 4	Secondary plot of hypoxanthine and PRPP kinetics.....	98

Chapter 2.4.1: The Active Site Aromatic Residue Stabilizes Substrate Binding to the *Leishmania donovani* Hypoxanthine-Guanine Phosphoribosyltransferase (Manuscript)

Figure 1	Complementation analysis for wild type and mutant <i>hgprt</i> constructs	118
Figure 2	Tryptophan fluorescence of wild type, F178W, and F178L HGPRTs.....	119

Chapter 2.4.2: Site-directed Mutagenesis at Asp206 Reveals the Role of the Conserved Aspartate in Purine Specificity of HG(X)PRT proteins

Figure 1	Representative purification of the expressed HGXPRT proteins.....	126
Figure 2	Complementation analysis of mutant constructs.....	127
Figure 3	Alignment of the purine binding regions from various HG(X)PRT proteins and their specificities.....	128
Table 1	Kinetic parameters for D206 mutants.....	129

Chapter 3: Inhibitor Design Targeting the *T. gondii* HGXPRT-I enzyme

Figure 1	Efficacy of purine analogs in the recombinant bacterial screen.....	137
Figure 2	Inhibition of bacterial growth by different concentrations of 2-amino-6-isothiocyanopurine.....	138
Figure 3	Inhibition kinetics of cPRPP.....	139
Figure 4	Primary screen of inhibitors discovered by DOCK 3.5.....	140
Figure 5	Strong inhibitors identified by DOCK 3.5 and their K_i values.....	141

Chapter 4.1: Expression, Purification, and Characterization of Uracil Phosphoribosyltransferase from *Toxoplasma gondii* (Manuscript)

Figure 1	Fractionation of UPRT by SDS-PAGE	161
Figure 2	Size-exclusion chromatography of purified UPRT.....	162
Figure 3	Heat inactivation of <i>T. gondii</i> UPRT.....	163
Figure 4	Effects of sundry divalent cations on UPRT activity.....	164
Figure 5	Hanes analysis of UPRT activity as a function of substrate concentration.....	165

Chapter 4.2: Chemical modifications and mutagenesis of the *T. gondii* UPRT enzyme

Figure 1	Purification of the UPRT protein by hydrophobic interaction chromatography.....	173
Figure 2	Time dependent inactivation of the <i>T. gondii</i> UPRT by the protein modifying reagent tetranitromethane.....	174
Figure 3	Fluorescent tagging of the UPRT enzyme by CPM.....	175
Figure 4	Hanes analysis of kinetic studies on the UPRT ^{C128V} mutant.....	176
Table 1	Chemical modifiers of the UPRT enzyme.....	170

Appendix A: Cloning and expression of the *P. falciparum* HGXPRT enzyme

Figure 1	rtPCR products using the <i>P. falciparum</i> <i>hgxprt</i> primers.....	183
Figure 2	Restriction map of the pBAce-PFHGXPRT expression construct..	184
Figure 3	Fractionation of the overexpressed <i>P. falciparum</i> HGXPRT protein by SDS-PAGE.....	185
Figure 4	Alignment of the <i>T. gondii</i> and <i>P. falciparum</i> HGXPRT peptide sequences.....	186

Appendix B: Subcloning, expression and purification of the *T. gondii* dihydrofolate reductase thymidylate synthase enzyme

Figure 1	Vector map of the DHFR-TS expression construct.....	192
Figure 2	Purification of the DHFR-TS.....	193

Acknowledgments

To truly thank all the people involved in making my dissertation possible would necessitate an essay longer than this thesis itself, but I want to mention some of the people who were a great help in my development and learning. First of all, my parents, who have put up with tear gas, strange scents from the basement, and exploding bedrooms. Their infinite patience, love, and guidance have been a constant companion throughout my life and have buoyed me through difficult times. Next, I would like to thank my siblings Sabine, Susanne, Kerstine and Ian for being themselves and of course all the rest of my family and friends; my grandparents, aunts and uncles, specifically Don Rocks, Janice Carter and Charlotte Puff who were always in close proximity in times of need.

I have been lucky in the course of my education to have been taught by exceptional teachers and scientists at every level of education. My high school chemistry teacher Wolfgang Kaspar gave me a basic chemistry background which provided all the fundamental knowledge I have needed to date. Dr. Philip McFadden, my undergraduate advisor, is an exceptional biochemist who had the patience to teach me protein chemistry and techniques of scientific investigation. Finally, my graduate mentor, Dr. Buddy Ullman, deserves the most credit for his tireless encouragement and tolerance in the past years. His scientific guidance and faith in his students make him the perfect mentor. It is

with great reluctance I leave his laboratory where I have learned much about the fascinating fields of protozoa and drug development. Not only was I fortunate with my choice of advisor, but the people in his laboratory are a motivated group of scientists who have been extremely supportive and deserve to be acknowledged: My good friend and aisle-mate John Jiang; The exceptional scientists Drs Armando Jardim and Nicola Carter; the lab manager Sarah Shih; Dan Scott and Erika Dahl who have greatly helped me; and all the rest of the Ullman lab!

Another group of people who were indispensable were my great collaborators, Dr. Maria Schumacher, an exceptional scientist and friend, Dr. Richard Brennan, who also volunteered for my advisory committee and Dr. David Roos and his laboratory - notably Mary Reynolds, Dr. Wolfgang Bohne and Dr. Robert Donald.

Last, but certainly not least I would like to thank the members of my committee for their scientific advice and willingness to participate in my graduate education: Drs Richard Brennan, Eric Barklis, and David Kabat.

Abstract

Toxoplasma gondii is an intracellular protozoan parasite that has gained considerable notoriety with the advent of the acquired immunodeficiency syndrome (AIDS). Additionally, congenital toxoplasmosis is a major problem in the United States and is the leading cause of neurological defects in infants, affecting about 1 in 1000 live births. Therapy for toxoplasmosis is far from optimal, as the commonly used antifolate combination of pyrimethamine-sulfadiazine can cause severe side effects, thereby necessitating discontinuation of treatment and provoking the generation of drug-resistant forms of the parasite. Thus, the need for new and more efficacious antitoxoplasmal agents is acute.

The phosphoribosyltransferases have been touted as attractive targets for rational inhibitor design. *T. gondii* relies heavily on this class of enzymes for purine and pyrimidine salvage suggesting that inhibitors of these enzymes may be potent anti-toxoplasmotic drugs. A biochemically rational approach to inhibitor design requires an intimate understanding of a protein. To this end, two phosphoribosyltransferases were studied; the purine salvage enzyme hypoxanthine-guanine-xanthine phosphoribosyltransferase (HGXPRT) and the pyrimidine salvage enzyme uracil phosphoribosyltransferase (UPRT).

The HGXPRT in *T. gondii* appears to be expressed as two separate isoforms which arise from a single transcript and differ by an insertion of 49 amino acids in the N-terminus of isoform II. The two isoforms were expressed in *E. coli* and purified by affinity chromatography. It was found that both isoforms are expressed in *Toxoplasma* and that these isoforms do not differ significantly in their kinetic properties or their intracellular stability. Further studies in collaboration with Dr. David Roos and Dr. Robert Donald indicate that the isoforms differ by their subcellular localization; isoform-I is cytosolic and isoform II is targeted to the plasma membrane.

Biochemical studies led to the development of a high-yield purification scheme for isoform-I which was used to generate large quantities of purified enzyme for further mechanistic and structural analysis. K_m^{APP} values of 66 μM , 18 μM , 1.0 μM , and 1.7 μM were determined for phosphorylribosepyrophosphate (PRPP), xanthine, guanine, and hypoxanthine respectively. Mechanistic studies intimate that the enzyme follows a compulsory ordered bi-bi mechanism in which PRPP binds first followed by the purine base. The reaction traverses the transition state and pyrophosphate is released followed by the nucleoside monophosphate. These steps are accompanied by conformational changes: An increase in hydrodynamic radius was observed upon binding of PRPP and a change in the secondary structure accompanied the binding of the nucleoside monophosphate product. The enzyme exists in a monomer-dimer equilibrium with a K_D of 38 μM . Two residues were studied by site-directed mutagenesis and found to be important in purine binding: Phe-178 of the *L. donovani* HGPRT which participates in base stacking and Asp-206 of the *T. gondii* HGXPRT which is involved in determining substrate specificity. Three classes of inhibitors were also discovered. Substrate analogs such as 8-azahypoxanthine, a mechanism-based inhibitor cycloPRPP, and two classes of structure-based inhibitors. The inhibitors had K_i values ranging from 700 nM to 400 μM .

The UPRT enzyme exists as a monomer in solution and binds its substrates PRPP and uracil with K_m^{APP} values of 243 μM and 3.5 μM respectively. The enzyme is responsible for the toxicity of 5-fluorouracil in *Toxoplasma* and converts this analog efficiently with a K_i of 25 μM . Chemical modifications with phenylglyoxal and tetranitromethane indicate that two residues types, tyrosyl and arginanyl, are important for UPRT catalysis. The enzyme is highly sensitive to oxygen due to numerous cysteine residues. Chemical modification experiments determined that these residues are not vital for catalysis. To stabilize the enzyme, the mutant C128V was generated by Erika Dahl. This mutant behaves kinetically very similarly to the wild type protein but is more resistant to oxidative inactivation. A high-yield expression and purification system was developed and large quantities of C128V UPRT were generated for initial kinetic and structural studies which are now underway.

I. Introduction

1. *Toxoplasma gondii*, an overview

1.1. History

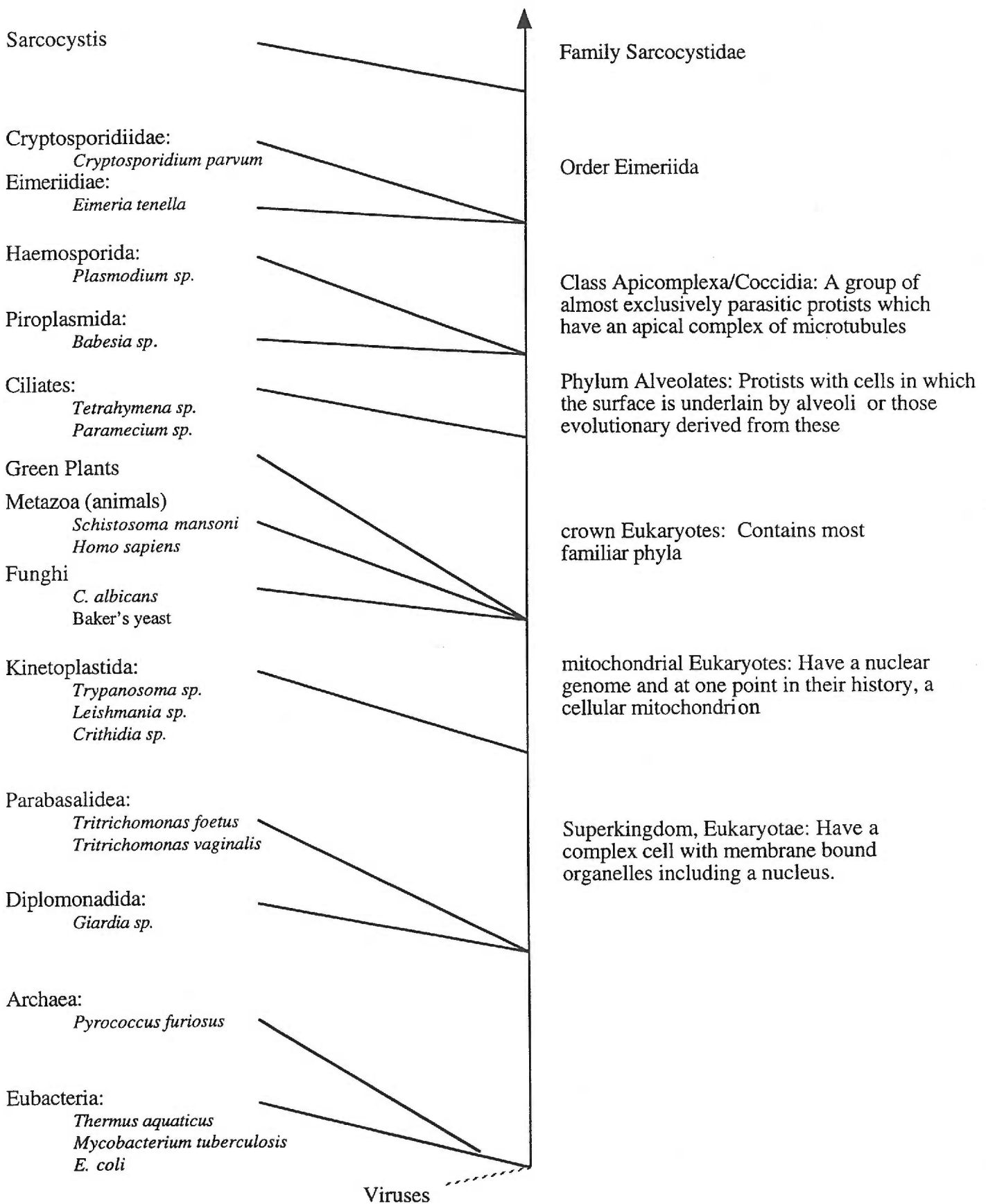
It is hypothesized that many billions of years ago the earth existed in a hot primordial state in which volcanic eruptions, earthquakes, and acid rains stirred the “Haldane Soup” which was to give rise to primitive life on this planet. The first progenitor cells which developed were probably little more than microscopic sacs of catalysts surrounded by a film or membrane to isolate them from their environment allowing for the creation of an internal chemical environment semi-autonomous from its local surroundings. The primitive cells slowly used up the supply of organic molecules which they had fermented in the early oxygen depleted atmosphere of the earth, and photosynthesis was developed to create an alternate method for energy production. The composition of free gases in the surroundings changed to an oxidizing environment which favored the development of respiration and the metabolism found in most eukaryotic cells [1]. Early in this process life forms branched into three major categories which compete with each other to this date: the *Archeobacteria*, which are found in high temperature and high pressure environments and have distinct metabolic pathways and ribosomal RNA sequences; the *Eubacteria*, which are characterized by their lack of complex organellar structure and nuclei and contain many familiar bacteria such as *Escherichia coli*, *Mycobacterium tuberculosis*, and *Thermus aquaticus* [2]; and the *Eukaryotes*, organisms containing a true nucleus and complex organelles such as

mitochondria and a Golgi apparatus.

The evolution of *Toxoplasma gondii* has been complex and even today is not completely understood. The presence of mitochondria together with the unique apicoplast has led to theories implying that *T. gondii* has undergone at least two lateral acquisitions of genes by engulfing a prokaryote which degenerated into the mitochondrion, and the incorporation of an algae-like cell which now presents itself as the apicoplast [3]. The mitochondrion participates in cellular respiration to supply the cell with an energy source, ATP, using an electron transport chain, while the function of the apicoplast remains elusive in these cells. Current hypotheses about the function of the apicoplast include storage and exchange of metabolites and a role in fatty acid metabolism similar to the role of the plastid organelles in plants [4]. Phylogenetic analyses of genomic sequences of *T. gondii* place it in the vicinity of the dinoflagellates while DNA sequences from the apicoplast have strong similarities to those found in the plastid organelles from plant organisms such as *Euglena*. Currently, *Toxoplasma spp.* have been placed in the order *Apicomplexa* with notorious organisms such as *Cryptosporidium*, *Plasmodium*, *Eimeria* and the family *Sarcocystidae*. (Figure 1).

Figure 1: Phylogenetic tree for *Toxoplasma gondii*

Toxoplasma gondii



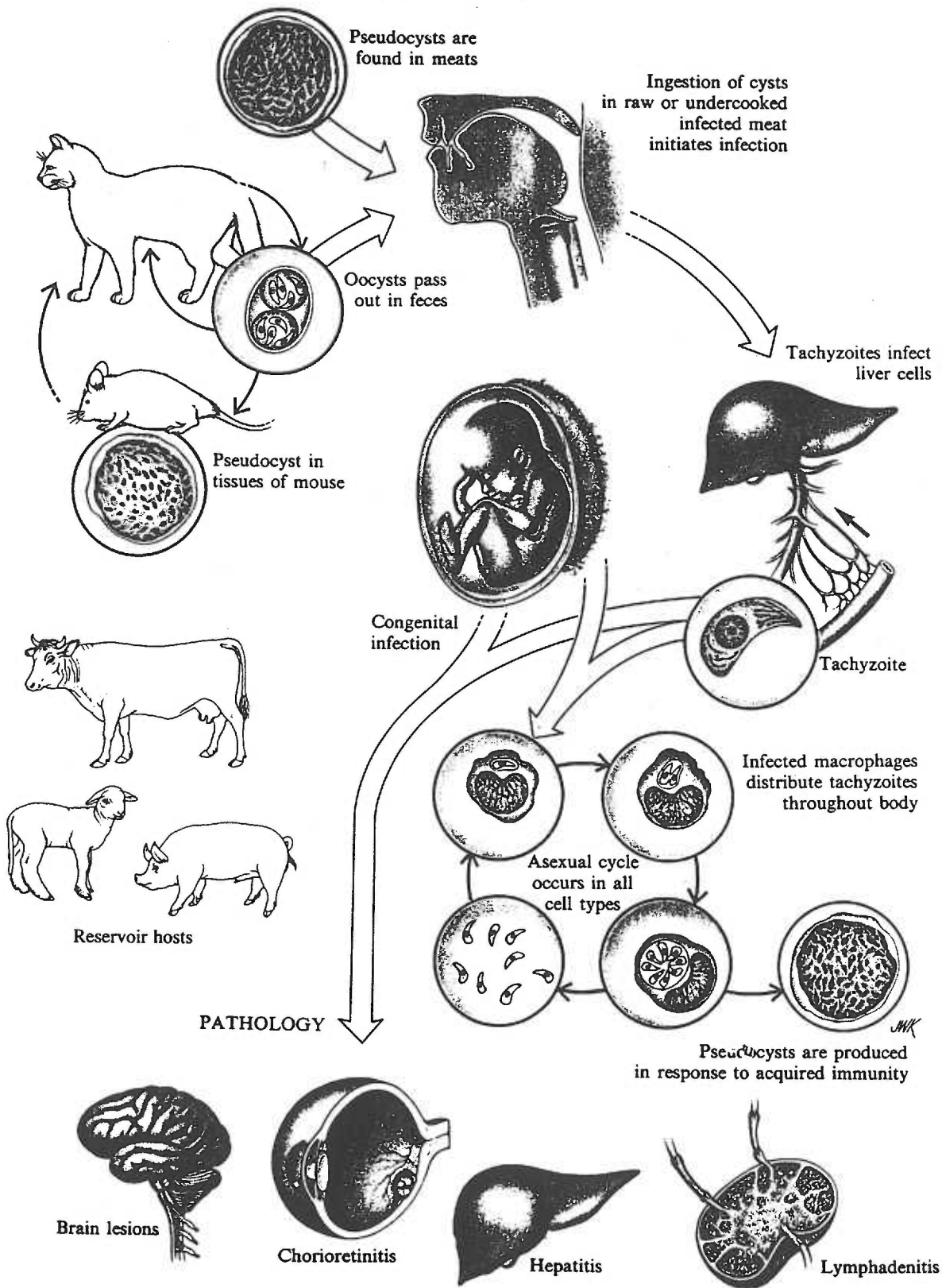
1.2. Life cycle

T. gondii was discovered in 1908 by Nicolle and Manceaux in the plasma of *Ctenodactylus gondi*, a gerbil-like animal which inhabits the North African desert. In 1923, the first cases of congenital toxoplasmosis were reported by Janku, and the organism was linked to this disease in 1939 by Wolf *et al.* Two years later, the “acquired form” of toxoplasmosis was recognized by Pinkerton, Henderson, and independently by Sabin. Fenkel *et al.* discovered the sexual stage of *T. gondii* and identified the organism as a coccidian parasite in 1970 [5]. The research of these and many other people has led to the model of the parasites life cycle as presented below. Protozoan parasites tend to have complex life cycles with a variety of morphological forms characteristic of each stage. *Toxoplasma* is no exception to this rule and has a variety of life-cycle stages as it passes from one host to another (Figure 2). Unlike many protozoan parasites, *T. gondii* does not utilize an insect vector for transmission from one host to another. The sexual stage of *T. gondii* initiates within the intestines of felines which are therefore considered the definitive host of *Toxoplasma*. When a cat ingests pseudocysts residing in the flesh and brain of infected animals, the pseudocyst walls are dissolved in the gut and the bradyzoite form of *T. gondii* emerges. These organisms infect gut epithelial cells and transform into merozoites which divide numerous times before rupturing the host cells and entering the feline intestinal lumen. Some of these merozoites perpetuate this cycle by infecting other intestinal epithelial cells while others transform into gametocytes which fuse to form oocysts. The oocysts are passed out with the stool and can remain viable outside the host for many months. These oocysts infect their next host by a fecal-oral route.

Figure 2: Life cycle of *Toxoplasma gondii*¹

¹ Figure from Katz M, Despommier DD, and Gwadz RW, Parasitic Diseases Second Edition *Springer-Verlag* (1988).

Toxoplasma gondii



Within the gastrointestinal tract, the wall of the oocyst is digested by the prospective host, and the parasite is released into the lumen of the gut where they penetrate the intestinal wall and are rapidly distributed throughout the body by circulating macrophages. These intracellular organisms are referred to as tachyzoites. Tachyzoites spread throughout the body and infect virtually every cell type they encounter. Proliferation of the parasite is soon checked by the immune system in immunocompetent hosts. Most of the tachyzoites are cleared by activated macrophages and the parasite lies dormant in the form of pseudocysts ready to reemerge should the host become immunocompromised or eaten by another host. The life-cycle is completed when a cat ingests pseudocysts from an infected animal.

1.3. Cell culture and biology

T. gondii tachyzoites can easily be cultured axenically. The RH-strain of *Toxoplasma*, the most commonly used laboratory strain, is usually grown at 37°C on human foreskin fibroblasts (HFFs), as these cells form a single monolayer with strong contact inhibition. The cultures are placed in a humidified CO₂ incubator in modified Eagle's medium with 1% heat-inactivated fetal bovine serum. Under these conditions, the tachyzoites divide in a parasitophorous vacuole by synchronous binary fission, doubling every 5-7 hours, and eventually lysing the cell monolayer. Released parasites remain viable with a half-life of about 10 hours. Cells grown in this manner can be purified on a cellulose column or by filtration through a polycarbonate filter with $\approx 3\mu\text{m}$ pore size [6]. RH tachyzoites cultured in this manner are highly virulent and can be used for infectivity studies in mice.

The ultrastructure of a tachyzoite is depicted in Figure 3. *Toxoplasma* exhibits a polarized morphology with the apical complex on the anterior side and polar posterior rings. The cell structure is maintained by a tubulin cytoskeleton consisting of 22 microtubules extending from the apical complex to the posterior end. The organelles in the anterior end are postulated to function in invasion into the host cell. Motility of the parasite is achieved by actin and myosin motors [7].

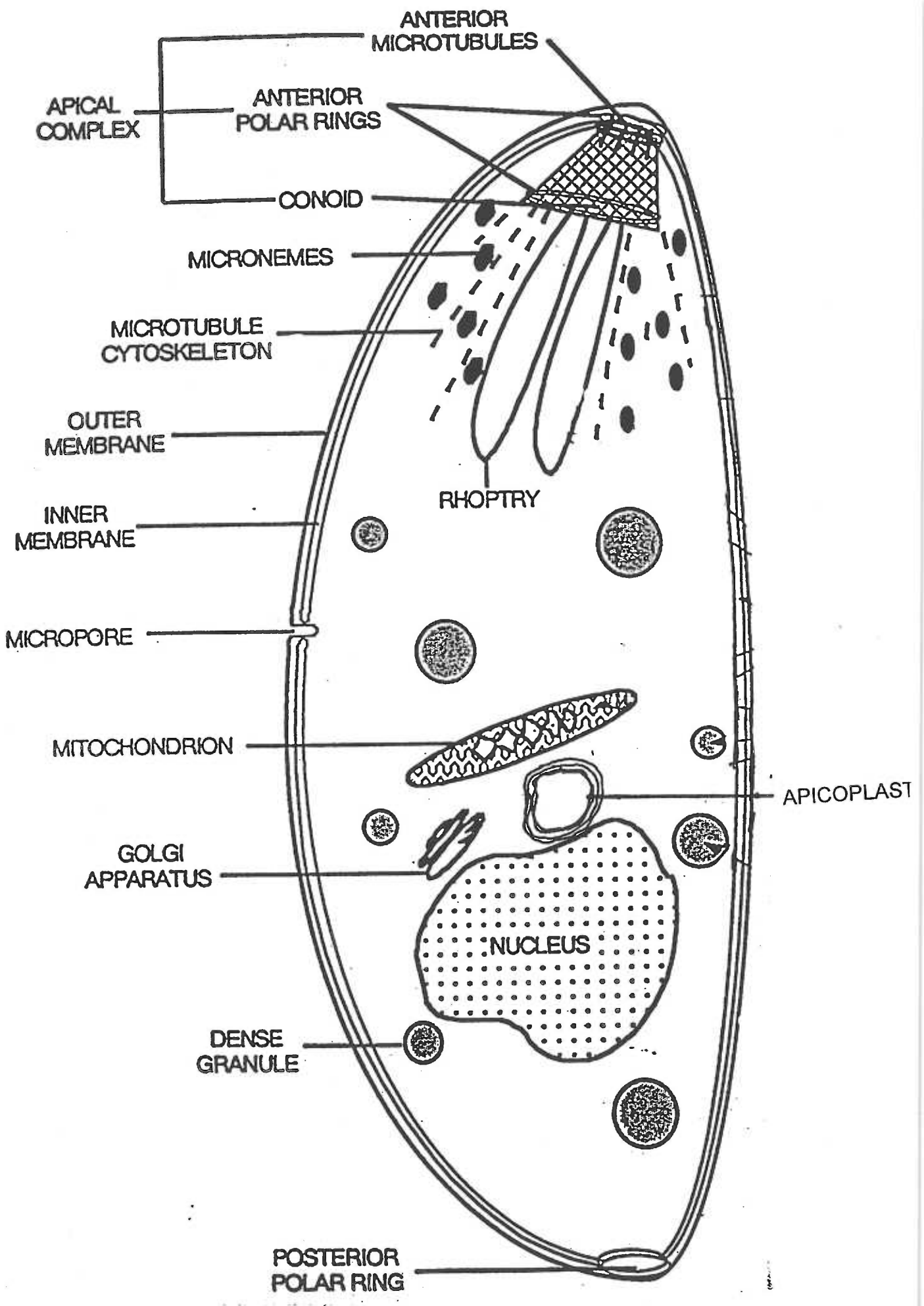
The parasite contains at least three genomes: the apicoplast DNA, a mitochondrial genome of about 36 kb [8], and the nuclear genome. *Toxoplasma* is a haploid organism during most of its life cycle and organizes its nuclear genome on at least 8 chromosomes which range from 2 to >10 million base pairs. The total genome size is estimated to be 8×10^7 bp with a GC content of 55% [9]. Not much is known about transcription and translation in *Toxoplasma*. The RNA polymerase enzymes of *T. gondii* have not been well characterized and of translation little is known other than its susceptibility to cycloheximide [10] and a 5' translation initiation consensus site which has been defined as [gNCAAa ATG g] [11].

1.4. Pathogenesis of Toxoplasmosis

T. gondii infections can be acquired by numerous routes. Probably the most common mechanism of transmission is by the ingestion of pseudocysts in raw, undercooked meat or eggs. Household cats are also a risk factor although excreted oocysts are not infective for 2 to 3 weeks. Laboratory infections and transmission through municipal water supplies have also been reported [12,13]. The parasite is distributed throughout the world and is implicated in congenital and clinical pathogenesis [14].

Figure 3. Tachyzoite ultrastructure²

² Figure adapted from McLeod R., Mack, D., Brown, C. *Toxoplasma gondii* - New Advances in Cellular and Molecular Biology Experimental Parasitology 72:109-121. (1991).



There are two major clinical presentations of toxoplasmosis, a congenital form which is transmitted from a sero-negative mother to the developing infant if the mother is infected during pregnancy and an acquired form which results from recrudescence of dormant parasites in immunocompromised patients and has recently gained much attention with the advent of the acquired immunodeficiency syndrome (AIDS) [15,16]. The congenital form of toxoplasmosis accounts for about 3,000 incidents per year in the United States alone [17]. Affected infants suffer from loss of vision and hearing and acute mental retardation arising from neurological deformities induced by a persistent parasitemia, which interferes with normal development. Treatment options include folate antagonist combinations such as pyrimethamine (1 mg/kg) and sulfadiazine (100 mg/kg). Adverse effects from the folate antagonists include headaches, anemia, and gastrointestinal distress. Alternatively, macrolide antibiotics can be prescribed for the treatment of congenital toxoplasmosis. Spiramycin (100 mg/kg) and clindamycin (300 mg/kg) are members of this class of drugs and have been shown to be equally effective against *Toxoplasma* as the antifolates. Drug toxicity here includes colitis, diarrhea and nausea [18].

Acquired toxoplasmosis has long been a problem in immunocompromised individuals, but only recently has this disease gained much attention as an AIDS opportunistic pathogen. It is the most common opportunistic infection of the nervous system in AIDS patients and is found in up to 40% of all AIDS cases [19]. Clinical toxoplasmosis is associated with headaches, confusion and fever and is invariably fatal if left untreated. Diagnosis is confirmed by characteristic focal brain lesions caused by nests of parasites in

the nervous system or by an immunofluorescence assay which screens for antitoxoplasma IgG in patients sera. Neither of these methods is conclusive however as up to 22% of the patients with clinical toxoplasmosis show no antitoxoplasma IgG [20] and brain lesions in AIDS patients can also stem from microsporidium infections [21]. Treatment options for clinical toxoplasmosis are similar to those in the congenital form, although generally much higher doses are prescribed with 4g sulfadiazine / 75 mg pyrimethamine per day or up to 4.3 g of clindamycin per day [22]. The efficacy of these treatment regimens is high and improvement is seen in 90% of the treated patients within 14 days. However, drug toxicity is very high and adverse reactions are seen in 65% of all patients treated [23]. Clearly better, more specific medications need to be discovered as the high rates of drug toxicity often lead to discontinuation of therapy and thus resistant parasites may be developing.

The significance of congenital toxoplasmosis worldwide can be estimated from the fact that 17.5% to 52.3 % of all women with abnormal pregnancies and abortions are seropositive for *Toxoplasma* compared to 7% to 51.3% for pregnant women without morbidity during pregnancy [24]. The continuous spreading of the human immunodeficiency virus (HIV) and the large number of congenital infections worldwide make it imperative that *T. gondii* should be studied to develop new and more effective treatment regimens.

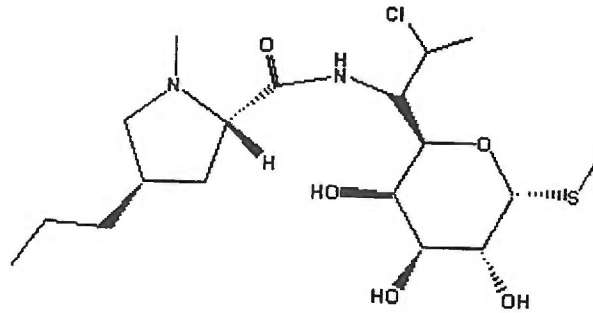
The targets for the antifolate drugs are well defined. Pyrimethamine (Figure 4) acts on the dihydrofolate reductase moiety of the bifunctional dihydrofolate reductase - thymidylate synthase enzyme (DHFR-TS). The *T. gondii* DHFR-TS has been cloned [25] and biochemically characterized [26]. It is a 610 amino acid polypeptide with a molecular mass of 69 kD which catalyzes both the formation of thymidylate and the NADPH-dependent

reduction of dihydrofolate to tetrahydrofolate. Pyrimethamine competes with dihydrofolate for binding to the active site of the DHFR moiety of this protein to which it binds with a K_i in the low nanomolar range and thus inhibits folate metabolism. Sulfadiazine (Figure 4) acts by inhibiting the dihydropteroate synthetase (DHPS) function of *T. gondii* which is also found on a bifunctional protein in the parasite, the hydroxymethyldihydropterin pyrophosphokinase-dihydropteroate synthase. This enzyme has recently been cloned and characterized by T. V. Pashley *et al.* [27] and is a 664 amino acid protein with a predicted molecular weight of 72 kD.

The mode of action of the macrolide antibiotics such as clindamycin (Figure 4) and spiromycin is not yet understood. This class of drugs has been postulated to inhibit protein synthesis. However, ribosomal sequence alignments would predict that the nuclear derived ribosomes should be resistant to macrolide antibiotics and protein labeling studies have shown that protein synthesis *in vitro* is virtually normal in parasites treated with these antibiotics [28]. The unconventional kinetics of parasite killing [29] and sequence alignments of apicoplast derived ribosomal subunits would indicate that the true target for this class of drugs is protein synthesis inside the apicoplast, an organelle which is not well understood to date.

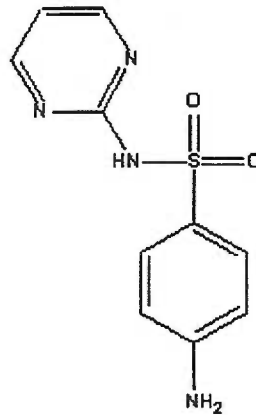
Figure 4: Commonly used drugs for toxoplasmosis

Clindamycin:



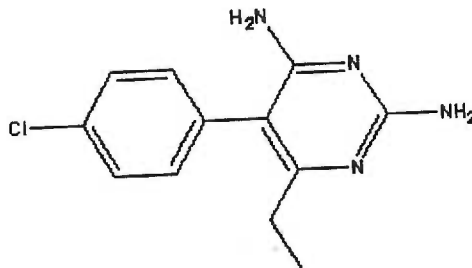
7-chloro-6,7,8-trideoxy-6-(1-methyl-trans-4-propyl-L-2-pyrrolidinecarboxamido)-1-thio-L-threo-α-D-galacto-octopyranoside
[C₁₈H₃₃ClN₂O₅S]; M.W. = 424.98 g/mol

Sulfadiazine:



4-amino-N-2-pyrimidinyl-sulfadiazine
[C₁₀H₁₀N₄O₂S]; M.W. = 250.27 g/mol

Pyrimethamine:



5-(p-chlorophenyl)-6-ethyl-2,4-diaminopyrimidine
[C₁₂H₁₃ClN₄]; M.W. = 248.71 g/mol

1.5. Purine and Pyrimidine Metabolism in *T. gondii*

1.5.1. Purine Metabolism

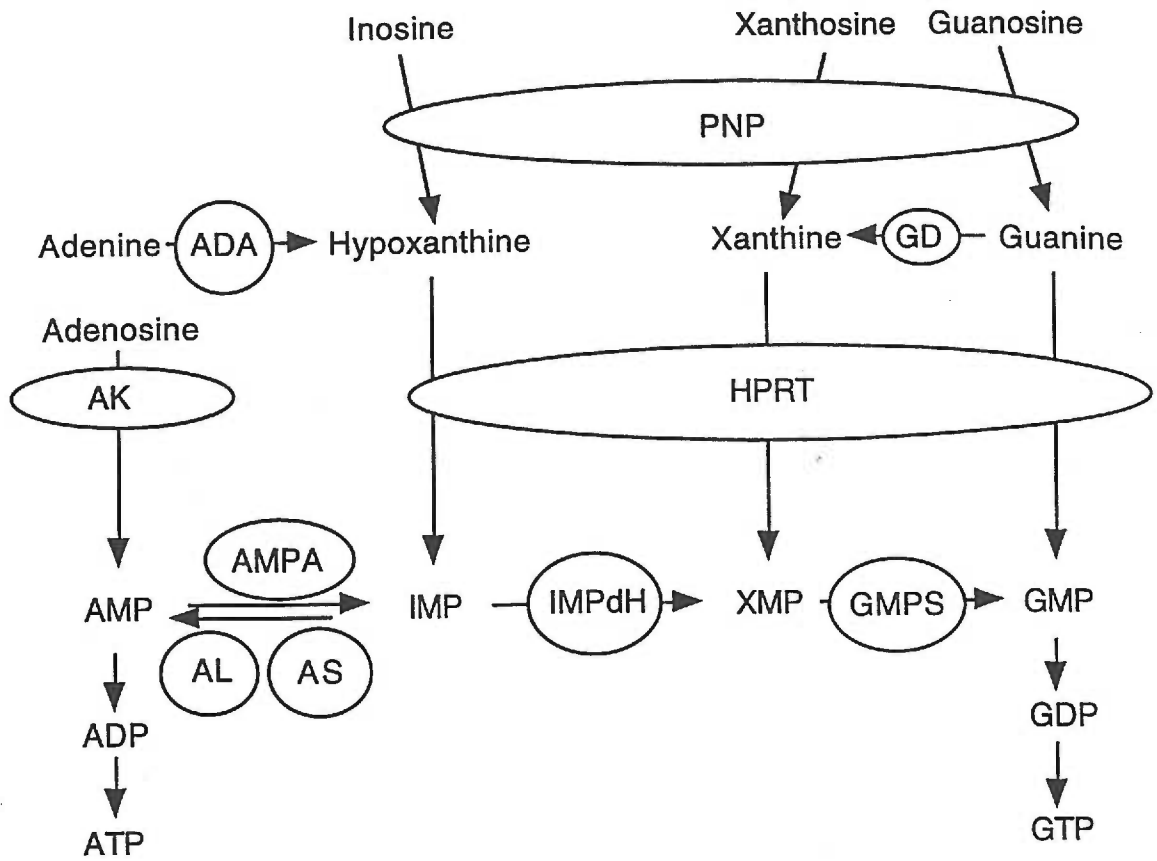
There are two major branches in purine biochemistry, the *de novo* synthesis of purines and the salvage and recycling of purine bases. Synthesis of purines begins with 5-phosphorylribose-1-pyrophosphate (PRPP) and ends with the formation of inosine monophosphate (IMP). This is an expensive process for a cell in that it requires ten enzymes and the use of numerous ATP and folate molecules [30]. Thus, it is not surprising that parasites which have been driven by evolutionary forces to streamline their genome have often lost the genes required for the *de novo* biosynthesis of purines. This is particularly true for the parasitic protozoans and all of the known organisms in this group cannot generate the purine ring *de novo* and are completely reliant on a functioning purine salvage pathway to generate adenylate and guanylate nucleotides [31]. Nucleotide formation by the salvage pathways occurs by three major routes: Phosphoribosyltransfer of the 5-phosphorylribose moiety of PRPP to preformed purine bases; Transfer of phosphate to nucleosides by nucleoside kinases, and the sequential action of purine nucleoside phosphorylases or hydrolases, yielding purine bases from purine nucleosides and phosphoribosyltransferases which then take the purine bases to the nucleotide level. *Toxoplasma gondii* cannot perform *de novo* synthesis of purines and relies on two major enzymes for purine salvage, the adenosine kinase (AK) and the hypoxanthine-xanthine-guanine phosphoribosyltransferase

(HGXPRT) [32]. Purine salvage must occur with the HGXPRT and AK synthesizing nucleotides followed by the actions of inosinate-monophosphate dehydrogenase (IMPDH) and guanosine monophosphate synthase (GMP synthase) to yield guanylate nucleotides; and the actions of either AK directly or adenylosuccinate synthase and adenylosuccinate lyase acting on IMP (Figure 5) to yield adenylate nucleotides [33]. Purine metabolism in *Toxoplasma* therefore relies heavily on these two enzymes which makes these pathways ideal targets for rational inhibitor design as inhibiting one of these enzymes should reduce the parasite's viability and without either of these protein functioning the organism should die. Indeed, no one to date has been able to create double knock outs in both of the genes for *AK* and *HGXPRT* [34], although each one can be deleted quite easily to yield the single knock-out.

1.5.2. Pyrimidine Metabolism

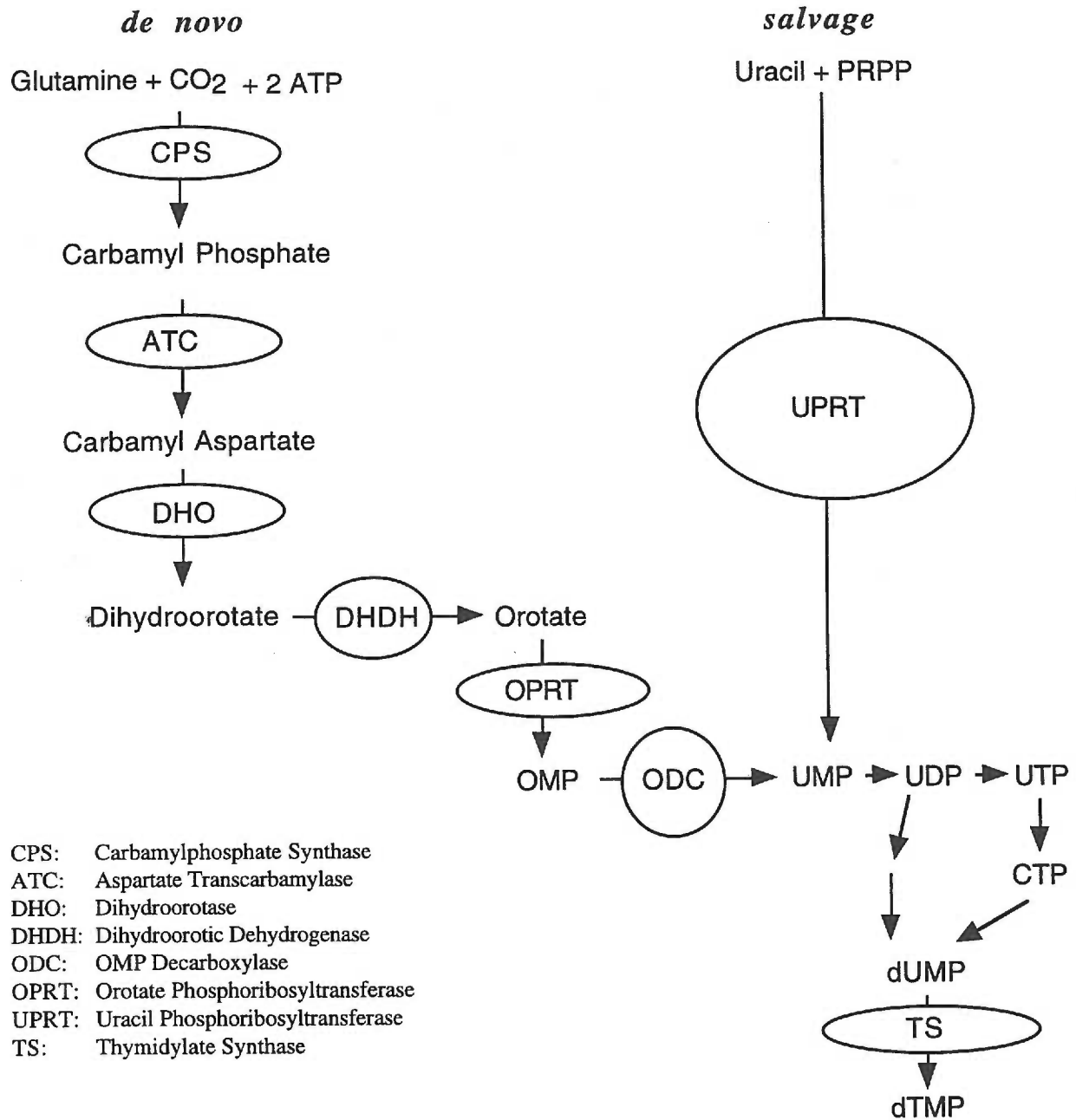
Unlike the purine metabolic pathways, the pyrimidine pathway has not been extensively characterized in *Toxoplasma*. Early studies noted that the parasite will incorporate radiolabeled precursors into pyrimidine nucleotides [35], and the existence of *de novo* pyrimidine synthesis is well established for *T. gondii*. In addition to the *de novo* synthesis, the parasite can perform pyrimidine salvage and is able to phosphoribosylate uracil using the enzyme uracil phosphoribosyltransferase (Figure 6) [36,37]. This activity is unique to the parasite and can be exploited by targeted subversive substrates such as 5-fluorouracil which is part of the therapeutic regimen for clinical toxoplasmosis [38] and has been shown to specifically target UPRT in the parasite, as *uprt* parasites are resistant to the drug [39].

Figure 5: Purine metabolism in *T. gondii*



- PNP: Purine Nucleoside Phosphorylase
 ADA: Adenine Deaminase
 GD: Guanine Deaminase
 AK: Adenosine Kinase
 HPRT: Hypoxanthine Guanine Xanthine Phosphoribosyltransferase
 AMPA: AMP Deaminase
 AS: Adenylosuccinate Synthase
 AL: Adenylosuccinate Lyase
 IMPdH: IMP Dehydrogenase
 GMPS: GMP Synthetase

Figure 6: Pyrimidine metabolism in *T. gondii*



2. Phosphoribosyltransferases

Phosphoribosyltransferases (PRTs) are a group of proteins which catalyze the transfer of the phosphoribosyl group of 5-phosphorylribose-1-pyrophosphate (PRPP) to other organic molecules. This reaction is dependent on a divalent cation and results in the release of pyrophosphate [40].

2.1. Phosphoribosyltransferases in metabolism

In metabolism, these enzymes are involved in numerous pathways [41] including amino acid, nucleotide, and cofactor biosynthesis (Table 1), however for the scope of this thesis, I will focus on the purine/pyrimidine PRTs.

Table 1. PRTs and their functions

Enzyme name	E.C. number	Metabolic pathway
adenine PRT	2.4.2.7	purine salvage / recycling
hypoxanthine PRT	2.4.2.8	purine salvage / recycling
uracil PRT	2.4.2.9	pyrimidine salvage / recycling
orotate PRT	2.4.2.10	pyrimidine biosynthesis
nicotinate PRT	2.4.2.11	biosynthesis of NAD
nicotinamide PRT	2.4.2.12	biosynthesis of NAD
amido PRT	2.4.2.14	biosynthesis of purines
ATP PRT	2.4.2.17	biosynthesis of histidine
anthranilate PRT	2.4.2.18	biosynthesis of tryptophan
quinolinic acid PRT	2.4.2.19	biosynthesis of NAD
dioxotetrahydropyrimidine PRT	2.4.2.20	biosynthesis / salvage of pyrimidines
nicotinate mononucleotide-5,6-dimethylbenzimidazole PRT	2.4.2.21	biosynthesis of cobalamin
guanine xanthine PRT	2.4.2.22	purine salvage / recycling

A number of purine and pyrimidine PRT enzymes have been identified to date. The purine PRTs function within the cell to either scavenge or recycle intracellular purine bases and form purine nucleoside-monophosphates (NMPs). IMP and XMP are further processed to either GMP or AMP. GMP or AMP is then converted by phosphokinases to form the nucleoside triphosphates (NTP). The NTPs can then be used in the cell as a source of energy; as building blocks of ribonucleic acid (RNA) and deoxyribonucleic acid (DNA); and in cellular signaling mechanisms. These functions of PRTs are key to the survival of protozoan parasites as these are completely reliant on PRTs for the formation of these important purine nucleotides, while mammals and most higher eukaryotes can form their own adenylate and guanylate nucleotides *de novo*. The central role of PRTs in protozoan survival may be reflected in the fact that these parasites have evolved an additional xanthine PRT enzyme which mammals lack and can thus metabolize xanthine directly to the nucleotide level. Similarly, the pyrimidine PRTs form vital precursors for RNA and DNA synthesis. However, the purine ring is synthesized directly on the ribose sugar and no purine PRT functions in the *de novo* biosynthesis of purines³. In contrast, the pyrimidine ring is synthesized alone and the OPRT enzyme attaches this ring to the ribose-monophosphate. Thus, of the two pyrimidine PRTs, the uracil PRT, which is present in protozoa but not found in humans, recycles and scavenges a pyrimidine, while the OPRT catalyzes a step in the *de novo* biosynthesis of pyrimidines [42].

³ However there is a PRT in the first step of purine biosynthesis, the amido PRT, as seen in table 1.

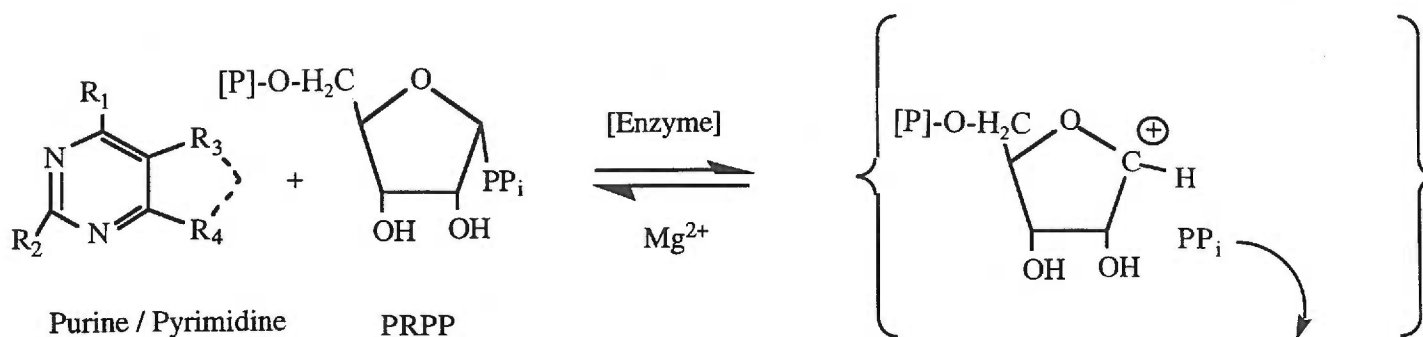
The metabolic importance of these enzymes is reflected in human hereditary diseases associated with PRT deficiencies. A deficiency in OPRT activity causes orotic aciduria which can result in mental retardation [43]. An APRT deficiency, which is linked to an autosomal recessive disorder resulting in the excretion of free adenine and 2,8-dihydroxyadenine - compounds which are poorly soluble in water - produces kidney stones and renal failure [44]. HGPRT deficiency causes Lesch-Nyhan Syndrome, an X-linked disorder characterized by self-mutilation, mental retardation, and acute gout. Partial loss of HGPRT activity is associated with a more mild form of the disease [45]. It is easily seen that the PRT enzymes are central enzymes in purine and pyrimidine metabolism and have thus been subject to extensive biochemical and structural analysis.

2.2. Biochemistry of phosphoribosyltransfer

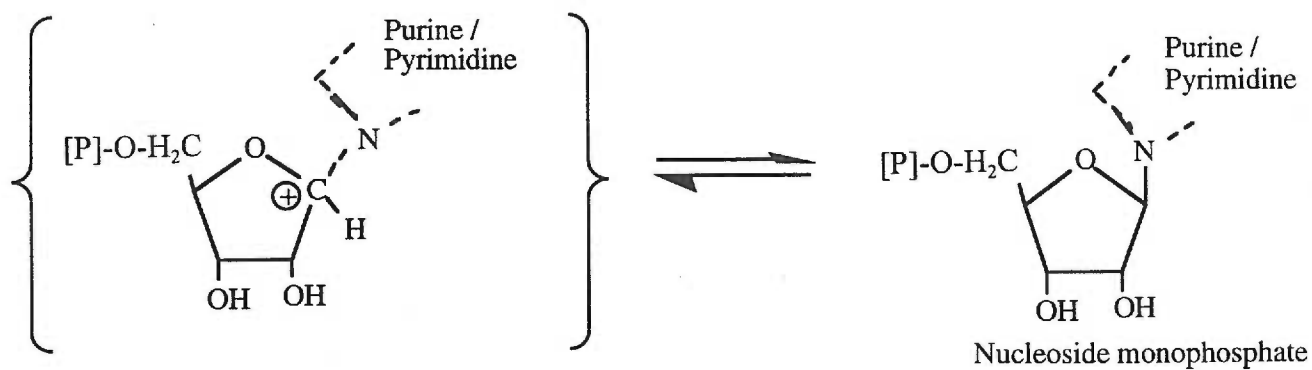
The purine/pyrimidine PRT enzymes all catalyze a condensation reaction in which an N-glycosidic bond is formed between the C1' atom in the ribose sugar ring of α -D-PRPP and the N-9 of a purine or the N-1 of a pyrimidine substrate. These reactions yield pyrophosphate and a nucleoside monophosphate. This reaction is Mg^{2+} dependent, however, other divalent cations such as Mn^{2+} and Co^{2+} can be alternate cofactors for this reaction [46]. The chemical mechanism is thought to be an S_N1 -type nucleophilic substitution with an oxocarbenium ion intermediate [47,48]. Although S_N1 mechanisms usually yield both stereoisomers [49], this enzymatically catalyzed reaction selects for β -glycosidic bonds and the reaction seems to occur with a complete inversion of configuration (Figure 7).

Figure 7: Chemistry of the purine / pyrimidine phosphoribosyltransferase reaction

I. Formation of the Oxycarbonium Ion

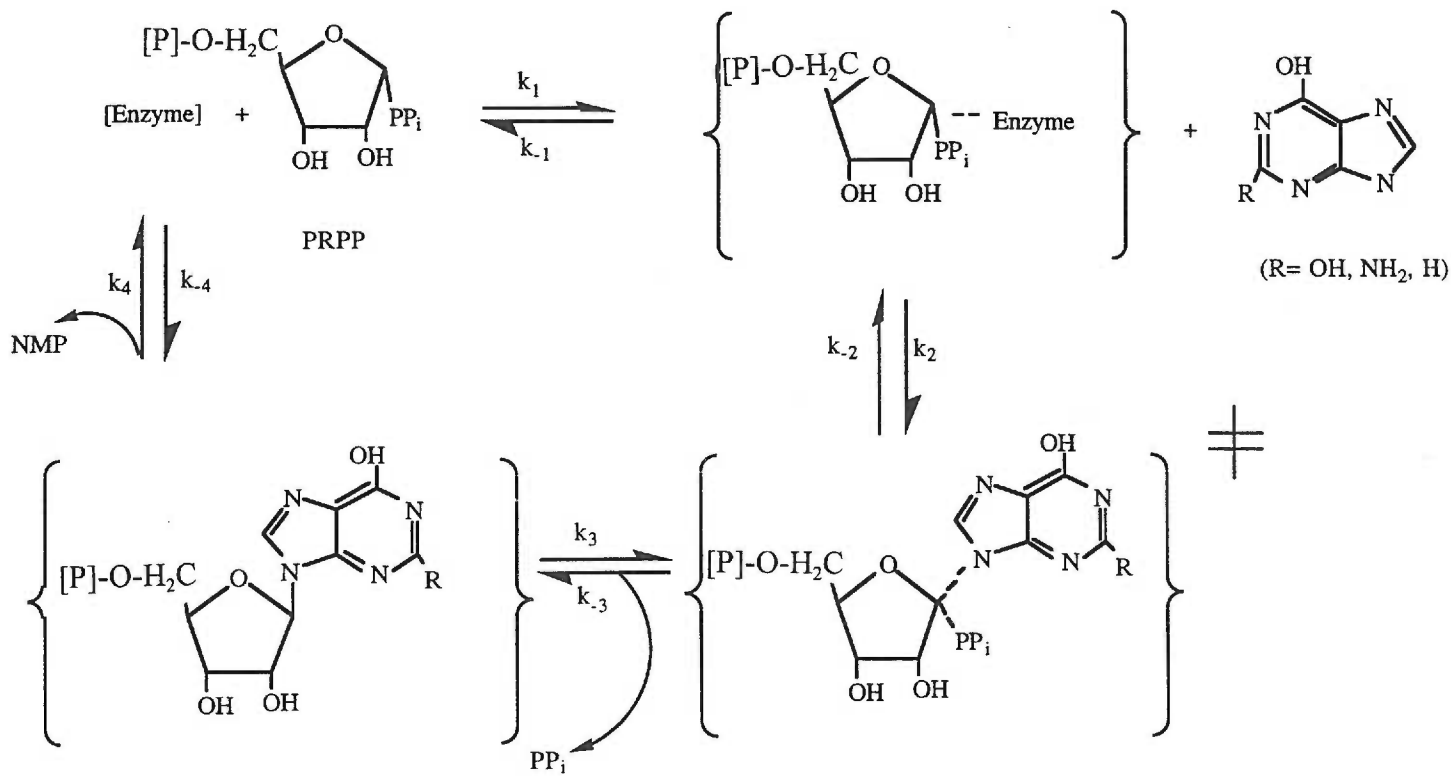


II. Nucleophilic Attack by Purine / Pyrimidine Nitrogen



Many different enzymatic mechanisms have been reported for these reactions. Although there have been debates about the exact mechanism, it seems that the hypoxanthine, guanine, and xanthine PRT enzymes follow a sequentially ordered bi-bi mechanism, in which magnesium-PRPP binds first followed by the purine base. The reaction proceeds rapidly and pyrophosphate is released followed by the nucleoside monophosphate [50,51,52]. The rate-limiting step in this transfer is the release of the NMP from the active site [53] (Figure 8). The kinetic mechanisms reported for uracil PRTs from *Giardia intestinalis* and *Acholeplasma laidlawii*, are a rapid-random equilibrium mechanism [54] or a ping-pong type mechanism [55], respectively, while orotate PRT from *Salmonella typhimurium* follows a random-sequential mechanism [56]. Mechanistic studies on the adenine PRT have indicated that this enzyme may follow a ping-pong type mechanism [57]. The variety of mechanisms reported may reflect the fact that many of these studies have been done in a cursory fashion and kinetic mechanisms reported based upon limited data. Careful studies such as those done for the human HGPRT may reveal that many of these enzymes follow similar kinetic mechanisms.

Figure 8: Kinetic mechanism of the hypoxanthine-(xanthine)-guanine phosphoribosyltransferases



2.3. Structural features of phosphoribosyltransferases

Several members of the purine/pyrimidine PRT family have been cloned, sequenced, and overexpressed from a variety of organisms [58]. Sequence alignment analyses of the different classes of PRTs show that these proteins share a common peptide sequence motif which is also found in the PRPP synthetase enzyme and has thus been implicated in PRPP binding. The motif consists of 13 amino acids:

1	2,3	4	5	6	7	8	9	10	11	12	13
[LIVMFYWCTA]	- 2x [LIVM]	- [LIVMF]	- [DE]	-D-	[LIVMS]	- [LIVM]	- [STAVD]	- [STAR]	- [GAC]	-x-	[STAR]

The acidic amino acids at position 5 and 6 are highly conserved in PRTs from phylogenetically diverse organisms and are thought to be involved in coordination of the divalent cation cofactor [59]. Other than the PRPP binding consensus sequence there is little primary sequence conservation within the classes of PRTs (Figures 9a-d). The crystal structures of a number of purine / pyrimidine PRTs have been solved. Interestingly, although these proteins share little primary sequence homology they are found to have a high degree of structural similarity. They all have two domains, a hood region involved in purine or pyrimidine binding, and a core region consisting of a β -sheet surrounded by a number of α -helices (Figure 10). The crystal structures of the HG(X)PRTs in the product bound forms indicate that the internal β -sheet of the core region is involved in contacting the ribose-5-phosphate moiety of the nucleotide ligand. The catalytic pocket is an invagination at the

interface between the hood and core regions. A flexible loop has been identified in the crystal structures of the purine / pyrimidine PRT proteins and has been conjectured to be involved in PRT catalysis in part by shielding the transition state oxocarbonium ion from side reactions with the solvent [51]. In addition, many PRT enzymes are rapidly inactivated by Tyr-modifying reagents [60] and Tyr residues found on the flexible loops have been implicated in PRT catalysis [61]. Binding of the pyrimidine and purine substrates is apparently achieved via aromatic-aromatic interactions with conserved aromatic side chains while the nucleobase specificity appears to be directed by hydrogen bonds from side chain and backbone atoms of residues forming the active site. The quaternary structures of the PRT enzymes are more diverse. The OPRT enzymes are obligate dimers as the active sites of these enzymes share residues from the polypeptide chains of their neighbors [62]. UPRT enzymes can be functional monomers [63], but are often found as multimers [64,65]. HG(X)PRT enzymes are usually found as dimers [66] or tetramers [67] but do not share catalytically active residues in their active sites and show no allostery. These enzymes can be active as monomers [68]. The APRT enzymes are found as monomers or dimers [69].

Figure 9a: Alignment of HG(X)PRT enzymes

HG(X)PRT

	1				50
PLASMODIUM	MPIPNNPGAG	ENAFDPVFK	DDDGYDLDSF	MIPAHYKKYL	TKVLVPNGVI
TOXOPLASMAMYIP	DNTFYNADDF	LVPFHCKPYI	DKILLPGGLV
HUMANMA	TRSPGVVSD	DEPGYDLDF	CIPNHYAEDL	ERVFIHGLI
T. FOETUS	MTETPMDDL	ERVLYNQDDI
L. DONOVANIMSN	SAKSPSPVPG	DEGRRNYPMS	AHTLVTQEQV
T. CRUZIMPREYEFA	EKILFTEEEI
	51				100
PLASMODIUM	KNRIEKLAYD	IKKVYNN...	EEFH
TOXOPLASMA	KDRVEKLAYD	IHRTYFG...	EELH
HUMAN	MDRTERLARD	VMKEMGG...	HHIV
T. FOETUS	QKRIRELAAE	LTEFYED...	KNPV.
L. DONOVANI	WAATAKCAKK	IAEDYRSFKL	TT.....	DNPLY
T. CRUZI	RTRIMEVAKR	IADYKKGGL	RP.....	YVNPLV
	101				150
PLASMODIUM	ILCLLKGSRG	FFTALLKHL	RIHNYSAVEM	SKPLFGEHYV	RVKSYCND.Q
TOXOPLASMA	IICILKGSRG	FFNLLIDYLA	TIQKYSGRES	SVPPFFEHYV	RLKSYQND.N
HUMAN	ALCVLKGGYK	FFADLLDYIK	ALNRNSDRSI	PMTV...DFI	RLKSYCND.Q
T. FOETUS	MICVLTGAVF	FYTDLLKHL.	..D.....	..FQLEPDI	ICSSY.SGTK
L. DONOVANI	LLCVLKGSFI	FTADLARFLA	DEG.....	..VPVKVEFI	CASSYGTGVE
T. CRUZI	LISVLKGSFM	FTADLCRALS	DFN.....	..VPVRMEFI	CVSSYGEVTV
	151				200
PLASMODIUM	STGTLEIV.S	EDLSCLKGK.	<u>HVLIVEDIID</u>	TGKTLVKFCE	YL..KKFEIK
TOXOPLASMA	STGQLTVL.S	DDLSIFRDK.	<u>HVLIVEDIVD</u>	TGFTLTEFGE	RL..KAVGPK
HUMAN	STGDIKVI	DDLSTLTGK.	<u>NVLIVEDIID</u>	TGKTMQTL	LV..RQYNPK
T. FOETUS	STGNLTISKD	LK.TNIEGR.	<u>HVLIVEDIID</u>	TGLTMYQLLN	NLQ.MR.KPA
L. DONOVANI	TSGQVRMLLD	VR.DSVENR.	<u>HILIVEDIVD</u>	SAITLOYLMR	FML.AK.KPA
T. CRUZI	SSGQVRMLLD	TR.HSIEGH.	<u>HVLIVEDIVD</u>	TALTLYLYH	MYF.TR.RPA
	201				250
PLASMODIUM	TVAIACLFIK	.RTPLWNGFK	ADFGVFSIPD	HVVGYSLDY	NEIFRDLHDC
TOXOPLASMA	SMRIATLVEK	.RTDRSNL	GDFVGFSD	VWVGGCYDF	NEMFRDFDHV
HUMAN	MVKVASLLVK	.RTPRSVGYK	PDFVGFEPD	KVVGYALDY	NEYFRDLNHV
T. FOETUS	SLKVCTLCDK	DIGKKAYDVP	IDYCGFVVEN	RYIIGYGDF	HNKYRNLVPI
L. DONOVANI	SLKTVVLLDK	.PSGRKVEVL	VDYPVITIPH	AFVIGYMDY	AESYRELRLDI
T. CRUZI	SLKTVVLLDK	.REGRRVPPS	ADYVVANIPN	AFVIGYGLDY	DDTYRELRLDI
	251				291
PLASMODIUM	..CLVNDEGK	KKYKATSL..
TOXOPLASMA	..AVLSDAAR	KKFEK.....
HUMAN	..CVISETGK	AKYKA.....
T. FOETUS	..GILKESVY	T.....
L. DONOVANI	..CVLKKEYY	EKPESKV...
T. CRUZI	..VVLRPEVY	AEREAARQK	QRAIGSADTD	RDAKREFH	SK Y

PURINE BINDING REGION IN BOLD-FACE
 PRPP BINDING REGION UNDERLINED

Figure 9b: Alignment of APRT enzymes

APRT

	1				50	
HUMANADSEL	QLVEQRIRSF	PDF..PTPGV	VFRDISPVLK	
MOUSEMSEPFL	KLVARIRVF	PDF..PIPGV	LFRDISPLLK	
ARABIDOPSIS	M ATEDVQDPRI	AKIASSIRVI	PDF..PKPGI	MFQDITLLL	
E. COLI	MTATAQQ..L	EYLKNSIKSI	QDY..PKPGI	LFRDVTSLLE	
YEASTMSISESYA	KEIKTAFRQF	TDF..PIEGE	QFEDFLPIIG	
L. DONOVANI		MPFKEVSPNS	FLLDDSHALS	QLLKKSYRWY	RFADVSSITE	
	51				100	
HUMAN		DPASFRAAIG	LLARHLKATH	GGR.IDYIAG	LDSRGFLFGP	SLAQELGLGC
MOUSE		DPDSFRASIR	LLASHLKSTH	SGK.IDYIAG	LDSRGFLFGP	SLAQELGVGC
ARABIDOPSIS		DTEAFKDTIA	LFVDRYK...	DKG.ISVVAG	VEARGFIFGP	PIALAIGAKF
E. COLI		DPKAYALSID	LLVERYK...	NAG.ITKVVG	TEARGFLFGA	PVALGLGVGF
YEAST		NPTLFQKLVH	TFKTHLEEKF	AKEKIDFIAG	IEARGLLFGP	SLALALGVGF
L. DONOVANI		SPETLKAIRD	FLVQYRAMS	PAP..THILG	FDARGFLFGP	MIAVELEIPF
	101				150	
HUMAN		VLIRKRGKLP	GPTL.WASYS	LEY...GKAE	LEIQKDALEP	<u>GQRVVVVDDL</u>
MOUSE		VLIRKQKLP	GPTV.SASYS	LEY...GKAE	LEIQKDALEP	<u>GQRVVIVDDL</u>
ARABIDOPSIS		VPMRKPKKLP	GKVI.SEEYS	LEY...GTDT	IEMHVGAVEP	<u>GERAIIDDL</u>
E. COLI		VPVRKPKKLP	RETI.SETYD	LEY...GTDQ	LEIHVDAIKP	<u>GDKVLLVDDL</u>
YEAST		VPIRRVGKLP	GECA.SITFT	KLD...HEEI	FEMQVEAIPF	<u>DSNVVVVDDV</u>
L. DONOVANI		VLMRKADKNA	GLLIRSEPYE	KEYKEAAPEV	MTIRYGSIGK	<u>GSRVVLIDDY</u>
	151				200	
HUMAN		<u>LATGGTMNAA</u>	CELLGRLQAE	VLECVSLV.E	LTSLKGREKL	APVPF..FSL
MOUSE		<u>LATGGTMFAA</u>	CDLLHQLRAE	VVECIVSLV.E	LTSLKGRERL	GPIPF..FSL
ARABIDOPSIS		<u>LATGGTLAAA</u>	IRLLERVGVK	IVECACVI.E	LPELKGKEKL	GETSL..FVL
E. COLI		<u>LATGGTIEAT</u>	VKLIRRLGGE	VADAAFII.N	LFDLGGEQRL	EKQGITSYSL
YEAST		<u>LATGGTAYAA</u>	GDLIRQVGAH	ILEYDFVLV.	LDSLHGEEKL	SAPIFSILHS
L. DONOVANI		<u>LATGGTALSG</u>	LQLVEASDAV	VVEMVSIL.S	IPFLKAAEKI	HSTANSRYKD
	201				240	
HUMAN		LQYE.....	
MOUSE		LQYD.....	
ARABIDOPSIS		VKSAA.....	
E. COLI		VPPFGH....	
YEAST		
L. DONOVANI		IKFISLLSDD	ALTEENCGDS	KNYTGPRVLS	CGDVLAEHPH	

PURINE BINDING REGION IN BOLD-FACE
 PRPP BINDING REGION UNDERLINED

Figure 9c: Alignment of OPRT enzymes

OPRT

	1				50
E. COLIMKP	YQRQFIEFAL	SKQVLKFGF
SALMONELLAMKP	YQRQFIEFAL	NKQVLKFGF
YEAST	MSASTTSLEE	YQKTFLELGL	ECKALRFGSF
	51				100
E. COLI	TLKSGRKSPY	FFTAGLFNTG	RDLALLGRFY	AEALVDSGIE	FDLLFGPAYK
SALMONELLA	TLKSGRKSPY	FFNAGLFNTG	RDLALLGRFY	AEALVDSGIE	FDLLFGPAYK
YEAST	KLNSGRQSPY	FFNLSLFNSG	KLLANLATAY	ATAIIQSELK	FDVIFGPAYK
	101				150
E. COLI	GIPIATTTAV	ALAE...HHD	LDLPYCFNRK	EAKDHGEGGN	LVGSALQG.R
SALMONELLA	GIPIATTTAV	ALAE...HHD	KDLPYCFNRK	EAKDHGEGGS	LVGSALQG.R
YEAST	GIPLAAIVCV	KLAEIGGTKF	QGIQYAFNRK	KVKDHGEGGI	IVGASLEDKR
	151				200
E. COLI	<u>VMLVDDVITA</u>	<u>GTA</u> .RESMEI	IQANGATLAG	LLISLDRQ..	..ERGRGEIS
SALMONELLA	<u>VMLVDDVITA</u>	<u>GTA</u> IRESMEI	IQAHGATLAG	VLISLDRQ..	..ERGRGEIS
YEAST	<u>VLIIDDVMTA</u>	<u>GTA</u> INEAFEI	ISIAQGRVVG	CIVALDRQEV	IHESDPERTS
	201				248
E. COLI	AIQEVERDYN	CKVISIITLK	DLIAYLEERL	EMAEHLAAVK	AYREEFGV
SALMONELLA	AIQEVERDYG	CKVISIITLK	DLIAYLEEKP	DMAEHLAAVR	AYREEFGV
YEAST	ATQSVSKRYN	VPVLSIVSLT	QVVQFMGNRL	S.PEQKSAIE	NYRKAYGI

PRPP BINDING REGION UNDERLINED

Figure 9d: Alignment of UPRT enzymes

UPRT

	1				50
B. SUBTILISMG
STREPTOCOCCUSMG
E. COLIM
TOXOPLASMAMAQV	PASGKLLVDP	RYSTNDQEEES	ILQDIITRFP
YEAST	MNPLFFLASP	FLYLTYLIYY	PNKGSFVSKP	R...NLQKMSSEPFK

	51				100
B. SUBTILIS	KVYVFDHP.L	IQHKLTYIRN	ENTGTKDFRE	LVDEVATLMA	FEITRDLPLE
STREPTOCOCCUS	KFQVISHP.L	IQHKLSILRR	EDTSTKDFRE	LVNEIAMLMG	YEVSRDLPLE
E. COLI	KIVEVKHP.L	VKHKLGLMRE	QDISTKRFRE	LASEVGSLLT	YEATADLETE
TOXOPLASMA	NVVLKQTAQ	LRAMMTIIRD	KETPKKEEFVF	YADRLIRLLI	EEALNELPFE
YEAST	NVYLLPQTNQ	LLGLYTIIRN	KNTTRPDFIF	YSDRIIRLLV	EEGLNHLPVQ

	101				150
B. SUBTILIS	EVDINTPVQA	AKSKVISGKK	LGVVPILRAG	LGMVDGILKL	IPAAKVGHVQ
STREPTOCOCCUS	EVEIQTPITK	TVQKQLSGKK	LAIVPILRAG	IGMVDGFSL	VPAKVGHHIG
E. COLI	KVTIEGWNGP	VEIQIKGKK	ITVVPILRAG	LGMMDGVLEN	VPSARISVVG
TOXOPLASMA	KKEVTTPLDV	SYHGVSFYSK	ICGVSIVRAG	ESMESGLRAV	CRGCRIGKIL
YEAST	KQIVETDTNE	NFEGVSFMGK	ICGVSIVRAG	ESMEQGLRDC	CRSVRIGKIL

	151				200
B. SUBTILIS	LYRDPETLKP	VEYYVKLPSD	<u>VEEREFIVVD</u>	<u>PMLATGGSAV</u>	EAIHSLKKRG
STREPTOCOCCUS	MYRDEETLEP	VEYLVKLPED	<u>IDQRQIFVVD</u>	<u>PMLATGGSAI</u>	LAVDSLKKRG
E. COLI	MYRNEETLEP	VPYFQKLVSN	<u>IDERMALIVD</u>	<u>PMLATGGSVI</u>	ATIDLLKKAG
TOXOPLASMA	IQRDETTAEP	KLIYEKLPAD	<u>IRDRWMLLD</u>	<u>PMCATAGSVC</u>	KAIEVLLRLG
YEAST	IQRDEETALP	KLFYEKLPED	<u>ISERYVFLLD</u>	<u>PMLATGGSAI</u>	MATEVLIKRG

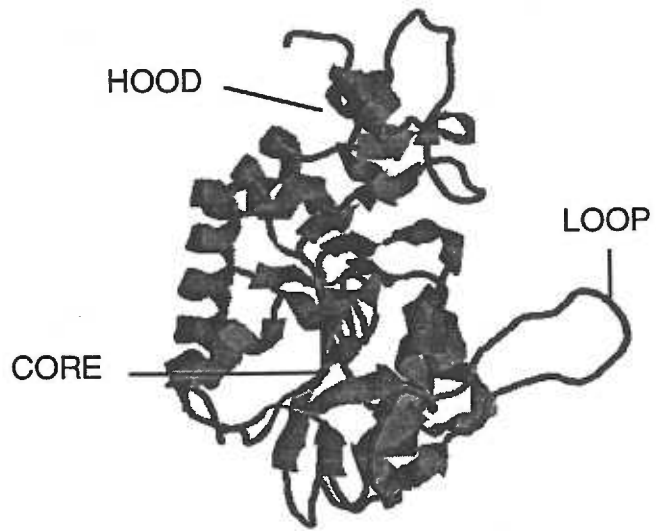
	201				250
B. SUBTILIS	AKN..IRFMC	LVAAPEGVVEE	LQKHSDVDI	YIAALDEKLN	EKGYIVPGLG
STREPTOCOCCUS	AAN..IKFVC	LVAAPEGVKK	LQDAHPDIDI	YTASLDEKLN	ENGYIVPGLG
E. COLI	CSS..IKVLV	LVAAPEGIAA	LEKAHPDVEL	YTASIDQGLN	EHGYIIPGLG
TOXOPLASMA	VKEERIIFVN	ILAAPQGIER	VFKEYPKVRM	VTAAVDICLN	SRYIVPGIG
YEAST	VKPERIYFLN	LICSKEGIEK	YHAAPPEVRI	VTGALDRGLD	ENKYLVPGLG

	251
B. SUBTILIS	DAGDRMFGTK
STREPTOCOCCUS	DAGDRLFGTK
E. COLI	DAGDKIFGTK
TOXOPLASMA	DFGDRYFGTM
YEAST	DFGDRYYCV.

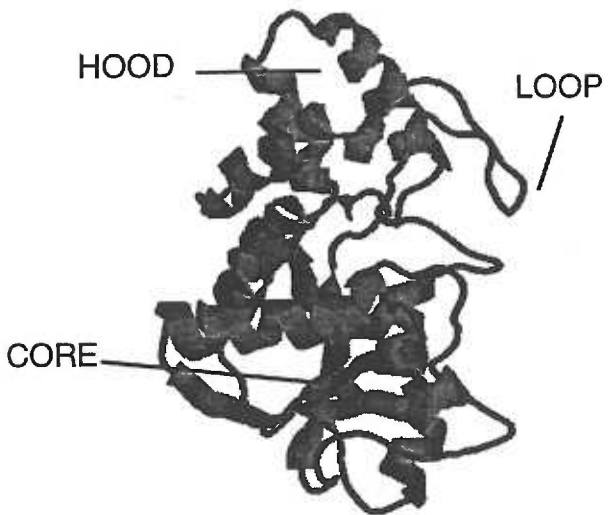
PRPP BINDING REGION UNDERLINED
 PYRIMIDINE BINDING REGION UNKNOWN

Figure 10: Structural conservation among phosphoribosyltransferases

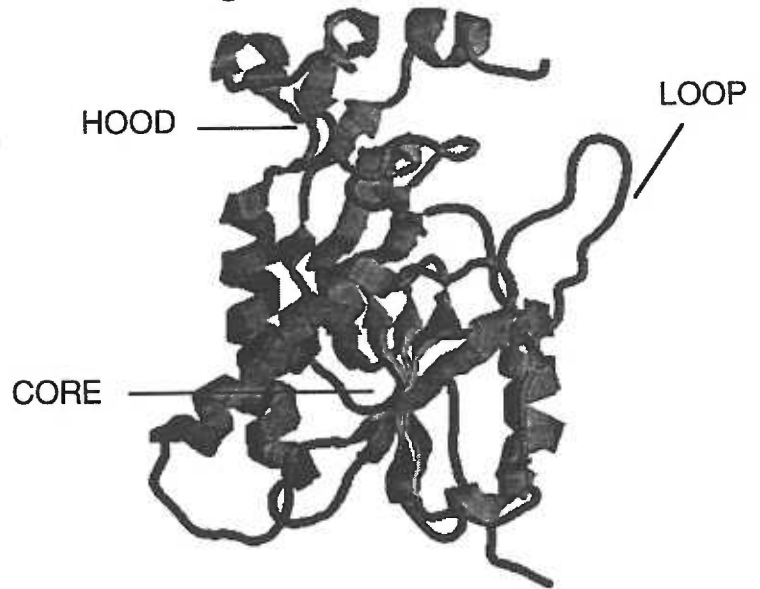
L. donovani APRT



S. typhimurium OPRT



T. gondii HGXPRT



2.4. Phosphoribosyltransferases as drug targets

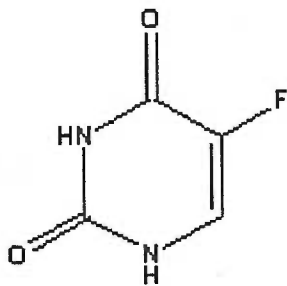
The phosphoribosyltransferases have been highly touted as targets for rational inhibitor design [70] and are already known to be important in the metabolism of drugs used to treat protozoal and other diseases. The action of the PRTs is to convert prodrug forms of “subversive” substrates into active metabolites which then inhibit down-stream enzymes or are incorporated into the nucleotide pool forming unstable nucleic acids which leads to cell death. Therapeutically relevant molecules which are activated by the purine / pyrimidine PRTs are allopurinol, a chemical commonly used to treat gout in humans [71], 5-fluorouracil, an antineoplastic agent [72], and 6-mercaptopurine, an antileukemic drug.

Allopurinol is a pyrazolopyrimidine that differs from its naturally occurring analog, hypoxanthine, by the nitrogen atom at position 7 which in allopurinol is a carbon, and by the presence of a nitrogen in the 8-position of the purine ring (Figure 11). In humans, allopurinol is a suicide inhibitor of the enzyme xanthine oxidase and is commonly used to control hyperuricemia. In contrast, allopurinol can be metabolized to the RNA level in many of the pathogenic hemoflagellates and causes cell death by destabilizing nucleic acids [73].

Allopurinol can be trapped and concentrated intracellularly by the action of the hypoxanthine - guanine PRT enzymes. The allopurinol ribonucleotide is then transaminated to form an aminopyrazolopyrimidine ribonucleotide which is phosphorylated to the triphosphate level and exerts its cytotoxic effects by mimicking ATP and being incorporated into RNA messages. The low toxicity of allopurinol to mammalian cells coupled with its potent antiparasitic effects have lead to the clinical application of allopurinol not only for the treatment of veterinary leishmaniasis,

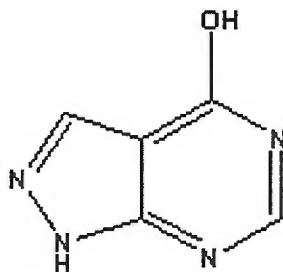
Figure 11: Subversive substrates of phosphoribosyltransferases

5-Fluorouracil:



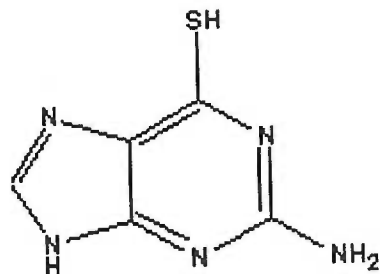
5-fluoro-2,4(1H,3H)-Pyrimidinedione
[C₄H₃FN₂O₂]; M.W. = 130.08 g/mol

Allopurinol:



4-hydroxy-1H-pyrazolo(3,4-d)pyrimidine
[C₅H₄N₄O]; M.W. = 136.11 g/mol

Thioguanine:



2-Amino-6-mercaptopurine
[C₅H₅N₅S]; M.W. = 167.19 g/mol

but also for treatment of cutaneous Leishmaniasis and Chagas' disease in humans [74,75].

5-fluorouracil, a subversive substrate of a pyrimidine PRT, is converted to 5-fluorouridine monophosphate and exerts its cytotoxic effect by inhibiting thymidylate synthase [76]. Unlike allopurinol, this compound can make its way into the polynucleotides of mammals and is highly toxic to dividing cells. In human cells, 5-fluorouracil is a subversive substrate of a PRT enzyme [77] in humans and is used as an antineoplastic agent in the chemotherapy of leukemia and a wide variety of other cancers [78,79]. 5-fluorouracil also inhibits growth of *Toxoplasma*, an effect mediated by the UPRT enzyme found in this parasite. Although this subversive substrate is not utilized as a first line drug in the treatment of *Toxoplasma* infections due to its low selectivity for the parasite and the resulting toxicity, it is prescribed to AIDS patients presenting with clinical toxoplasmosis [80].

A number of other cytotoxic, subversive substrates of PRT enzymes are known and each purine / pyrimidine PRT is a target for at least one of these analogs (Figure 11). These compounds are commonly used in cell culture as selectable markers for transformation, cell growth, and gene knockout experiments, and have been invaluable tools for the study of parasites [81,82]. The importance of further understanding the biological, chemical and structural mechanisms by which these therapeutically promising compounds exert their effects cannot be overemphasized as drugs which target PRTs may well become prominent players in the therapy of cancer, malaria, and the opportunistic pathogens of AIDS.

3. Rational Inhibitor Design

Many drugs are known to cause adverse reactions in patients leading to discomfort and discontinuation of therapy. The premature termination of treatment can lead to the development of drug resistant pathogens and loss of drug efficacy. Harmful side effects of treatment are largely due to lack of specificity of the therapeutic agent for the pathogen versus the patient. This can partially be attributed to the method by which many drugs have been developed, random screening of potential inhibitory compounds. Pathogens are grown on a convenient medium and chemicals are added to the culture at random. Those classes of compounds which show cytostatic effects are further tested until leads are found which potently inhibit cell growth of the pathogen. Next, these lead compounds are tested in animal models for effectivity and toxicity *in vivo*. Finally, after extensive testing, human trials are initiated to assess how effective and toxic the new drug is in humans [83]. This approach to drug design has been successful in the past in finding useful medications for a variety of diseases, but as it does not target the pathogen specifically, toxicity to the patient is common. Another drawback to this method is that while industrial drug companies have enormous capacities for drug testing, academic laboratories usually cannot muster the resources required for high throughput random screening and must therefore find a more focussed method for drug discovery.

Recently, more direct methods of drug discovery are being employed which

specifically target a metabolic pathway in the pathogen. Inhibitors, designed against proteins which are vital for the pathogens survival, are being developed as potential drugs for a variety of diseases. These inhibitors can be of two classes: the first are analogs which are modified versions of the enzyme's natural substrate and either inhibit an important enzyme directly, or are converted from a prodrug form to an active compound. Examples for the first class of drugs are allopurinol, which, with its metabolite oxypurinol, are suicide inhibitors of xanthine oxidase used in the treatment of gout [84], and 3'-azido-3'-deoxythymidine (AZT) which is activated by thymidylate kinase [85] and is a commonly prescribed drug for HIV infections. The second class of compounds are not usually related to an enzyme's natural substrate and are discovered by rational inhibitor design.

This form of inhibitor design is an emerging technique for the discovery of new potential drugs. The first step of this process of rational drug design is the identification of a target and validation of this target. Targets may include receptor sites on the cell surface for intracellular pathogens, vital metabolic pathways, DNA and RNA replication and transcription, and any other process which is vital for the pathogen to complete for its survival and propagation. After the target has been rationally defined, it must be proven that interference with the function of this target will lead to death of the pathogen or inhibition of its propagation. This can be done by showing that gene knockouts in the targeted locus are lethal, or by using known agents which interfere with the targets function. Once it is established that impeding the target will lead to death of the pathogen, the target needs to be characterized. This is done by cloning the gene encoding the protein, overexpressing it in a recombinant system, purifying the protein and doing extensive biochemical and structural

studies to understand as much as possible about the target. Next, one attempts the determination of a three dimensional structure of the target and uses the generated coordinates to screen a small molecule database for compounds which may bind to active sites on the target.

A commonly utilized program, DOCK, uses three dimensional coordinates to create a model of the active site which it fills with spheres of defined size. It then uses this sphere model for geometric matching with the atoms of compounds in small molecule databases. Compounds which are very similar in their three dimensional shape to the sphere model can then be matched chemically to hydrogen bond donors and acceptors, and matched by electrostatic potential to an electrochemical grid created inside the active site of the protein (Figure 12). The program collects descriptions of a number of the top compounds which can be obtained and screened for inhibitory effects biochemically and *in vivo* on the pathogen. Over 500,000 compounds can be computationally screened in a day and the number of biochemically active compounds discovered can be raised from 0.02% discovered in random screens to between 2-20% . Once an active compound has been identified, its mode of binding can be determined and more and more potent compounds can be discovered by iterative structure determination of the compound bound the target and chemical modification of the lead molecule (Figure 13). This strategy has been successfully employed for the discovery of numerous inhibitors of a variety of proteins such as the HIV protease [86,87], the malarial and schistosomal cysteine proteases [88], and thymidylate synthase [89]. Ligands of a variety of molecules, such as DNA [90] and cytochrome P450 [91], and inhibitors of virus fusion [92] have also been studied using this method. The wide range of

problems which can be addressed with structure based ligand and inhibitor design and its application to rational drug discovery will open exciting new avenues in computational biochemistry and should allow for the rapid discovery of new and specific inhibitors for proteins from a wide range of organisms and with a number of different functions. However, as these techniques are just now emerging, further development of new program suites and increased computational power, coupled with advances in the biochemical understanding of receptor-ligand interactions will be required before structure-based inhibitor and drug design is widely accepted and used.

The following dissertation is a study of PRT enzymes in *T. gondii* which have been touted as targets for the type of inhibitor discovery mentioned above. The uracil PRT and the hypoxanthine-guanine-xanthine PRT of this parasite were overexpressed and studied using a variety of approaches to answer questions pertaining to the structure, function, and cell biology of these enzymes. The new classes of inhibitors discovered by these methods may prove to be viable lead compounds for the development of new, effective drugs for toxoplasmosis.

Figure 12: The DOCK suite of programs

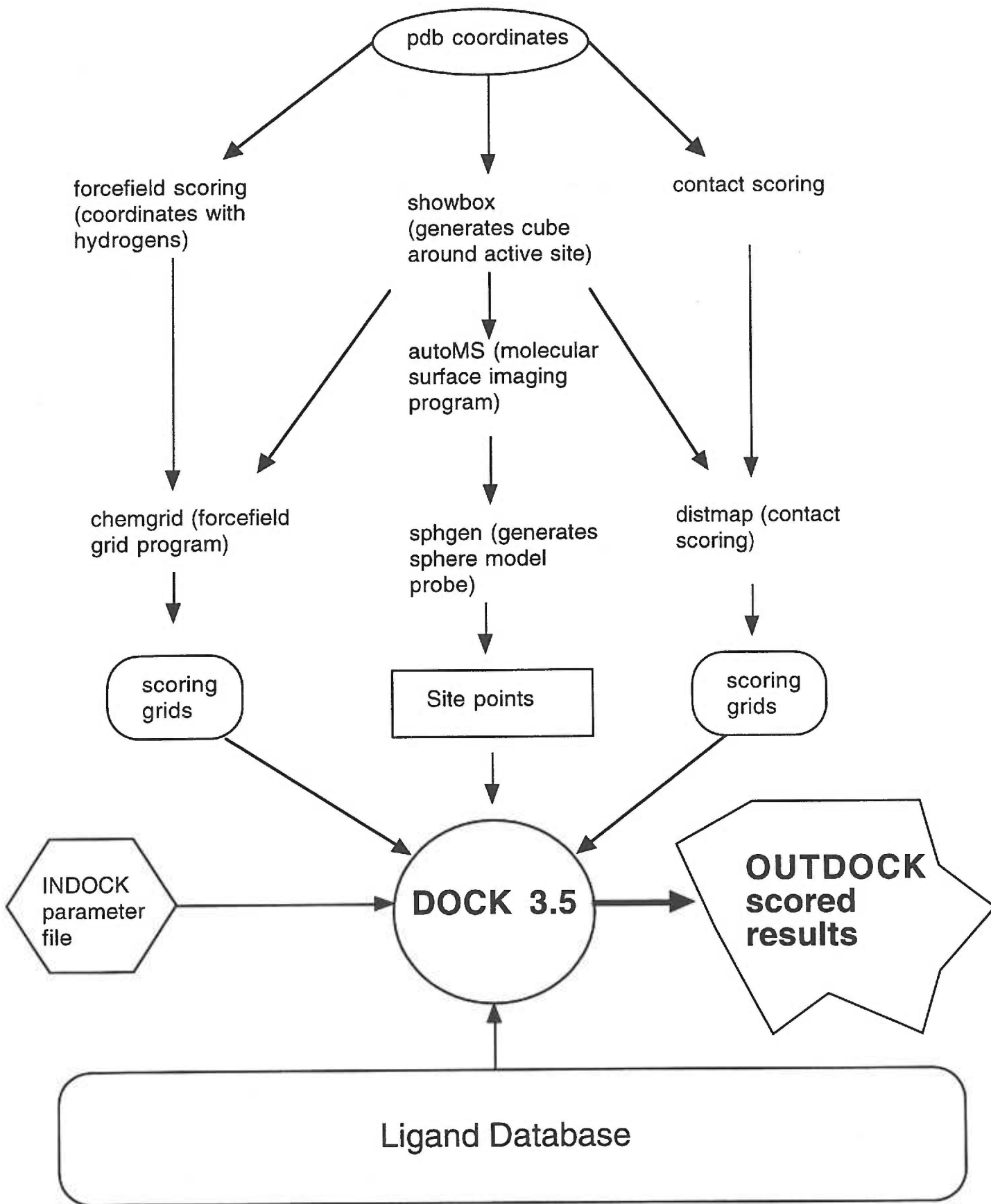


Figure 13: Iterative structure determination and inhibitor testing for the discovery of tight binding inhibitors

Determine crystal structure of target



Discover new class of inhibitors using DOCK 3.5



Determine inhibition constants of new inhibitor

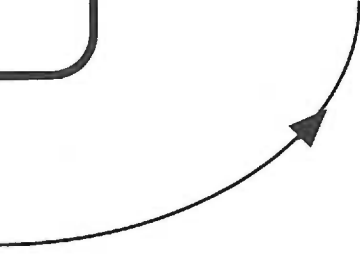


tight-binding Inhibitor

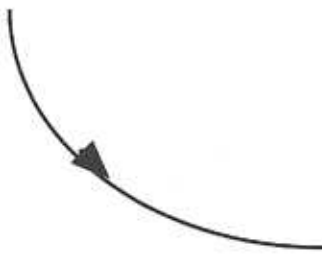
Synthesize new compound



Predict sites to modify for better inhibitor based on structure



Cocrystallize inhibitor with target



4. Literature Cited

1. Dickerson RE, and Geis I "Chemie" VCH Verlags GMBH Revision
3. Pg. 628-645 (1990).
2. Campbell NA "Biology" Benjamin/Cummings Publishing Co., Inc
Fourth Edition. 507-509 (1996).
3. Kohler S, Delwiche CF, Denny PW, Tilney LG, Webster P,
Wilson RJ, Palmer JD, Roos DS "A plastid of probable green
algal origin in Apicomplexan parasites" *Science*
275(5305):1485-1489 (1997).
4. David Roos, personal communication.
5. Katz M, Despommier DD, and Gwadz RW, "Parasitic Diseases"
Second Edition Springer-Verlag (1988).
6. Roos, DS., Donald, GK., Morrisette, NS., and Moulton, ALC
"Molecular Tools for Genetic Dissection of the Protozoan
Parasite *Toxoplasma gondii*" *Methods in Cell Biology* Vol. 45
Academic Press Inc. 25-61 (1994).
7. McLeod R., Mack, D., Brown, C. "*Toxoplasma gondii* - New
Advances in Cellular and Molecular Biology" *Experimental
Parasitology* 72:109-121 (1991).
8. Borst P., Overdulve, JP., Weijers, PJ., Fasefowler, F. and
Vandenberg, M. "DNA Circles with Cruziforms from *Isospora
Toxoplasma Gondii*" *Biochimica Biophysica Acta* 781:100 (1984).
9. Cornelissen, AWCA., Overdulve JP., and Van der Ploeg M.
"Determination of Nuclear DNA of Five Eucoccidian Parasites,
Isospora (Toxoplasma) gondii, *Sarcocystis cruzi*, *Eimeria
tenella* *E. acervulina*, and *Plasmodium berghei* with special
reference to gametogony and meiosis in *I. (T.) gondii*"
Parasitology 88:531-553 (1984).
10. Beckers CJM, Roos DS, Donald RGK, Luft BJ, Schwab JC, Cao
Y and Joiner KA, "Inhibition of Cytoplasmic and Organellar
Protein Synthesis in *Toxoplasma gondii* - Implications for the
target of Macrolide Antibiotics" *J. Clin. Invest.* 95 (1995).

11. Seeber F, "Consensus sequence of translational initiation sites from *Toxoplasma gondii* genes" *Parasitology Research* 83:309-311 (1997).
12. Herwaldt BL, Juranek DD, "Laboratory-Acquired Malaria, Leishmaniasis, Trypanosomiasis and Toxoplasmosis" *Am. J. Trop. Med. Hyg.* 48,3:313-323 (1993).
13. "The Quality of Drinking Water not Strain'd" *The Lancet* 350,9072 (1997).
14. Zuber P, and Jacquier P "Epidemiology of Toxoplasmosis: Worldwide Status." *Schweiz Med. Wochenschr. Suppl.* 65:19S-22S (1995).
15. Kovar, IZ. "Neonatal and Pediatric Infections" *Curr. Opin. Infect. Dis.* 3:479-500 (1990).
16. Luft, BJ. and Remington, JS., "Toxoplasmic Encephalitis in AIDS" *Clin. Infect. Dis.* 15:211-222 (1992).
17. Joiner K., and Dubremetz, JF. "Toxoplasma gondii: a Protozoan for the Nineties" *Infection and Immunity* 1169-1172 (1993)
18. Katz, M, Despommier, DD., and Gwadz, RW., "Parasitic Diseases" Second Edition *Springer-Verlag* (1988)
19. Luft, B., and Remington, JS. "AIDS commentary: toxoplasmic encephalitis" *J. Infect. Dis.* 157:1-6 (1988).
20. Porter, SB., and Sande MA. "Toxoplasmosis of the Central Nervous System in the Acquired Immunodeficiency Syndrome" *New Eng. J. Med.* 327,23:1643-1648 (1992).
21. NCDDG-OI Meeting, Abstract (1997).
22. Dannemann, B., McCutchan JA., Israelski D. et al. "Treatment of toxoplasmic encephalitis in patients with AIDS: a randomized trial comparing pyrimethamine plus clindamycin to pyrimethamine plus sulfadiazine" *Ann. Intern. Med.* 116:33-43 (1992).

23. Porter, SB., and Sande MA. "Toxoplasmosis of the Central Nervous System in the Acquired Immunodeficiency Syndrome" *New Eng. J. Med.* 327,23:1643-1648 (1992).
24. Galvan RML, Soto MJL, Velasco CO, Perez, MR "Incidence of anti-Toxoplasma Antibodies in Women with High Risk Pregnancy and Habitual Abortion" *Rev. Soc. Bras. Med. Trop.* 28,4:333-337 (1995).
25. Roos DS, "Primary structure of the dihydrofolate reductase-thymidylate synthase gene from *Toxoplasma gondii*" *J Biol Chem* 268(9):6269-6280 (1993).
26. Trujillo M, Donald RG, Roos DS, Greene PJ, and Santi DV "Heterologous expression and characterization of the bifunctional dihydrofolate reductase-thymidylate synthase enzyme of *Toxoplasma gondii*" *Biochemistry* 35(20):6366-6374 (1996).
27. Pashley TV, Volpe F, Pudney M, Hyde JE, Sims PF, and Delves CJ "Isolation and molecular characterization of the bifunctional hydroxymethyldihydropterin pyrophosphokinase-dihydropteroate synthase gene from *Toxoplasma gondii*" *Mol Biochem Parasitol* 86(1):37-47 (1997).
28. Beckers CJ, Roos DS, Donald RG, Luft BJ, Schwab JC, Cao Y, Joiner KA "Inhibition of cytoplasmic and organellar protein synthesis in *Toxoplasma gondii*. Implications for the target of macrolide antibiotics" *J Clin Invest* 95(1):367-376 (1995).
29. Fichera ME, Bhopale MK, and Roos DS "In vitro assays elucidate peculiar kinetics of clindamycin action against *Toxoplasma gondii*" *Antimicrob Agents Chemother* 39(7):1530-1537 (1995).
30. Lehninger, AL. "Biochemistry" *Worth Publishers* Second Edition (1981).
31. Ullman, B. and Carter, D. "Hypoxanthine-Guanine Phosphoribosyltransferase as a Therapeutic Target in Protozoal Infections" *Infectious Agents and Disease* 4:29-40 (1995).

32. Schwartzman, JD., and Pfefferkorn, ER "Toxoplasma gondii: Purine Salvage in Mutant Host Cells and Parasites" *Experimental Parasitology* 53:77-86 (1982).
33. Krug, EC., Marr, JJ., and Berens, RL. "Purine Metabolism in *T. gondii*" *J. Bio. Chem.* 264,18:10601-10607 (1989).
34. Roos, DS. and Pfefferkorn ER. personal communication
35. Schwartzman, JD., and Pfefferkorn, ER "Pyrimidine Synthesis by Intracellular *Toxoplasma gondii*" *J. Parasitology* 67:150-156 (1982).
36. Pfefferkorn, ER., and Pfefferkorn, LC. "Toxoplasma gondii: Characterization of a mutant resistant to 5-fluorodeoxyuridine" *Experimental Parasitology* 42:44-55 (1977).
37. Pfefferkorn, ER. "Toxoplasma gondii: the Enzymatic Defect of a Mutant Resistant to 5-fluorodeoxyuridine" *Experimental Parasitology* 44:26-35 (1978).
38. Fung, HB and Kirschbaum, HL. "Treatment regimens for patients with toxoplasmic encephalitis" *Clinical Therapies* 18(6):1037-1056 (1996).
39. Donald, RGK., and Rood, DS "Insertional Mutagenesis and Marker Rescue in a Protozoan Parasite: Cloning of the Uracil Phosphoribosyltransferase Locus from *Toxoplasma gondii*" *Proc. Natl. Acad. Sci. USA* 92:5749-5753 (1995).
40. Scapin G, Grubmeyer C, Sacchettini JC "Crystal Structure of Orotate Phosphoribosyltransferase" *Biochemistry* 33(6):1287-1294 (1994).
41. Musick WD, "Structural features of the phosphoribosyltransferases and their relationship to the human deficiency disorders of purine and pyrimidine metabolism" *CRC Crit Rev Biochem* 11(1):1-34 (1981).
42. Matthews CK, van Holde K "Biochemistry".
43. Suttle DP, Bugg BY, Winkler JK, Kasalas JJ, "The metabolic Basis of Inherited Disease" *McGraw Hill*, New York 6th Ed. 1195-1226 (1989).

44. Simmonds HA, Sahota AS, VanAcker KJ, "The Metabolic and Molecular Basis of Inherited Disease" McGraw Hill, New York 1707-1724 (1995).
45. Nyhan WL, "Clinical features of the Lesch-Nyhan syndrome" *Arch Intern Med* 130(2):186-192 (1972).
46. Carter D, Donald RG, Roos D, Ullman B "Expression, purification, and characterization of uracil phosphoribosyltransferase from *Toxoplasma gondii*" *Mol Biochem Parasitol* 87(2):137-144 (1997).
47. Tao W, Grubmeyer C, Blanchard JS "Transition state structure of *Salmonella typhimurium* orotate phosphoribosyltransferase" *Biochemistry* 35(1):14-21 (1996).
48. Goitein RK, Chelsky D, Parsons SM "Primary 14C and alpha secondary 3H substrate kinetic isotope effects for some phosphoribosyltransferases" *J Biol Chem* 253(9):2963-2971 (1978).
49. Ege SN "Organic Chemistry" Second Edition D.C. Health and Company (1989).
50. Carter D, and Ullman B unpublished observation.
51. Wang CC, personal communication.
52. Yuan L, Craig SP 3d, McKerrow JH, Wang CC "Steady-state kinetics of the schistosomal hypoxanthine-guanine phosphoribosyltransferase" *Biochemistry* 31(3):806-810 (1992).
53. Xu Y, Eads J, Sacchettini JC, Grubmeyer C "Kinetic mechanism of human hypoxanthine-guanine phosphoribosyltransferase: rapid phosphoribosyl transfer chemistry" *Biochemistry* 36(12):3700-3712 (1997).
54. Dai YP, Lee CS, O'Sullivan WJ "Properties of uracil phosphoribosyltransferase from *Giardia intestinalis*" *Int J Parasitol* 25(2):207-214 (1995).
55. McIvor RS, Wohlhueter RM, Plagemann PGW, "Uracil phosphoribosyltransferase for *Acholeplasma laidlawii*: Partial Purification and Kinetic Properties" *J. Bacteriology* 156(1):192-197 (1983).

56. Bhatia MB, Vinitzky A, Grubmeyer C "Kinetic mechanism of orotate phosphoribosyltransferase from *Salmonella typhimurium*" *Biochemistry* 29(46):10480-10487 (1990).
57. Hori M, and Henderson JF, "Kinetic studies of adenine phosphoribosyltransferase" *J. Biol. Chem.* 241:3404 (1966).
58. Genbank query: "hypoxanthine phosphoribosyltransferase".
59. Schumacher MA, Carter D, Roos DS, Ullman B, and Brennan RG "Crystal Structure of *Toxoplasma gondii* HGXPRTase reveal the catalytic role of a long flexible loop" *Nature Structural Biology* 3(10):881-887 (1996).
60. Jardim A, and Carter D, unpublished observations
61. Jardim A, and Ullman B, "The Conserved Serine-Tyrosine Dipeptide in *Leishmania donovani* Hypoxanthine-guanine Phosphoribosyltransferase is Essential for Catalytic Activity" *J. Biol. Chem.* 272(14):8967-8973 (1997).
62. Henriksen A, Aghajari N, Jensen KF, and Gajhede M, "A flexible loop at the Dimer Interface is a Part of the Active Site of the Adjacent Monomer of *Escherichia coli* Orotate Phosphoribosyltransferase" *Biochemistry* 35:3803-3809 (1996).
63. Carter D, Donald RG, Roos D, Ullman B "Expression, purification, and characterization of uracil phosphoribosyltransferase from *Toxoplasma gondii*" *Mol Biochem Parasitol* 87(2):137-144 (1997).
64. Rasmussen UB, Mygind B, and Nygaard P, "Purification and some properties of uracil phosphoribosyltransferase from *Escherichia coli* K12" *Biochim. Biophys Acta* 881:268-275 (1986).
65. Natalini P, Ruggieri S, Santarelli I, Vita Al, and Magni G "Baker's yeast UMP:pyrophosphate phosphoribosyltransferase. Purification, enzymatic and kinetic properties". *J. Biol. Chem.* 254:1558-1563 (1979).
66. Allen TE, and Ullman B, "Molecular Characterization and Overexpression of the HG Phosphoribosyltransferase gene from *T. cruzi*" *Mol. Biochem. Parasit.* 65:233-245 (1994).

67. Yuan L, Craig SP, McKerrow JH, and Wang CC, "The Hypoxanthine-guanine phosphoribosyltransferase of *Schistosoma mansoni*" *J. Biol. Chem.* 265:13528-13532 (1990).
68. Carter, D unpublished observations
69. Allen T, Henschel EV, Coons T, Cross L, Conley J, and Ullman B "Purification and characterization of the adenine phosphoribosyltransferase and hypoxanthine-guanine phosphoribosyltransferase activities from *Leishmania donovani*" *Mol. Biochem. Parasit.* 33:273-282 (1989).
70. Ullman B, and Carter D. "Molecular and Biochemical Studies on the Hypoxanthine-guanine phosphoribosyltransferases of the Pathogenic Haemoflagellates" *Int. J. Parasit.* 27(2):203-213 (1997).
71. Gonzalez EB, Miller SB, Agudelo CA "Optimal management of gout in older patients" *Drugs Aging* 4(2):128-134 (1994).
72. Levi F, Zidani R, Misset JL "Randomized multicentre trial of chronotherapy with oxaliplatin, fluorouracil, and folinic acid in metastatic colorectal cancer" *Lancet* 350(9079):681-686 (1997).
73. Looker DL, Marr JJ, Berens RL "Mechanisms of action of pyrazolopyrimidines in *Leishmania donovani*" *J Biol Chem* 261(20):9412-9415 (1986).
74. Gallerano RH, Marr JJ, Sosa RR "Therapeutic efficacy of allopurinol in patients with chronic Chagas' disease" *Am J Trop Med Hyg* 43(2):159-166 (1990).
75. Martinez S, Marr JJ "Allopurinol in the treatment of American cutaneous leishmaniasis" *N Engl J Med* 326(11):741-744 (1992).
76. Jackman AL "Inhibition of thymidylate synthase: biochemical pharmacology of drugs with activity in colorectal cancer" *Tumori* 83(1 Suppl):S65-S66 (1997).

77. Ahmed NK, Haggitt RC, Welch AD "Enzymes of salvage and de novo pathways of synthesis of pyrimidine nucleotides in human colorectal adenocarcinomas" *Biochem Pharmacol* 31(15):2485-2488 (1982).

78. Vokes EE, "Intravenous 6-thioguanine or cisplatin, fluorouracil and leucovorin for advanced non-small cell lung cancer: a randomized phase II study of the cancer and leukemia group B" *Ann Oncol* 3(9), 727-732 (1992).

79. Goto M "Experience with 5-fluorouracil in malignant skin tumors" *Gan No Rinsho* 13(11), 992-997 (1967).

80. Fung HB and Kirschenbaum HL "Treatment regimens for patients with toxoplasmic encephalitis" *Clin Ther* 18(6), 1037-1056 (1996).

81. Bohne W and Roos DS "Stage-specific expression of a selectable marker in *Toxoplasma gondii* permits selective inhibition of either tachyzoites or bradyzoites" *Mol Biochem Parasitol* 88(1-2), 115-126 (1997).

82. Hwang HY, Gilberts T, Jardim A, Shih S, Ullman B "Creation of homozygous mutants of *Leishmania donovani* with single targeting constructs" *J Biol Chem* 271(48), 30840-30846 (1996).

83. Hamner CE, "Drug Development" 2nd Edition *CRC Press* 40-57 (1990).

84. Dunky A, Nitsche V, Eberl R "Therapeutic efficacy of slow-release allopurinol in gout and hyperuricaemia" *Wien Klin Wochenschr* 93(2):65-68 (1981).

85. Lavie A, Vetter IR, Konrad M, Goody RS, Reinstein J, Schlichting I "Structure of thymidylate kinase reveals the cause behind the limiting step in AZT activation" *Nat Struct Biol* 4(8):601-604 (1997).

86. Rutenber, E., Fauman, E.B., Keenan, R.J., Fong, S., Furth, P.S., Demontellano, P.R.O., Meng, E., Kuntz, I.D., Decamp, D.L., Salto, R., Rose, J.R., Craik, C.S. and Stroud, R.M., "Structure of a non-peptide inhibitor complexed with HIV-1 Protease - developing a cycle of structure-based drug design", *J. Biol. Chem.* 268, 15343-15346 (1993).

87. DesJarlais, R.L., Seibel, G.L., Kuntz, I.D., Furth, P.S., Alvarez, J.C., Ortiz de Montellano, P.R., DeCamp, D.L., Babe, L.M. and Craik, C.S. "Structure-based design of nonpeptide inhibitors specific for the human immunodeficiency virus 1 protease", *PNAS* 87, 6644-6648 (1990).

88. Ring, C.S. Sun, E., McKerrow, J.H., Lee, G.K., Rosenthal, P.J., Kuntz, I.D., and Cohen, F.E., "Structure-based inhibitor design by using protein models for the development of antiparasitic agents", *PNAS* 90, 3583-3587 (1993).

89. Shoichet, B.K., Stroud, R.M., Santi, D.V., Kuntz, I.D., and Perry, K.M. "Structure-based discovery of inhibitors of thymidylate synthase ", *Science* 259, 1445-1450 (1993).

90. Grootenhuis, P.D.J., Roe, D.C., Kollman, P.A., and Kuntz, I.D., "Finding potential DNA-binding compounds by using molecular shape", *J. Comput-Aided Molec. Des.* 8, 731-750 (1994).

91. DeVoss, J. and Demontellano, P.R.O., "Computer-Assisted, Structure-Based Prediction of Substrates for Cytochrome P450 (CAM)", *J. Am. Chem. Soc.*, 117, 4185-4186 (1995).

92. Bodian, D.L., Yamasaki, R.B., Buswell, R.L., Stearns, J.F., White, J.M., and Kuntz, I.D., "Inhibition of the fusion-inducing conformational change of influenza hemagglutinin by benzoquinones and hydroquinones", *Biochemistry* 32, 2967-78 (1993).

1. Overexpression and Characterization of HGXPRT isoforms

Darrick Carter, David Roos, Robert Donald, and Buddy Ullman

1. Introduction

The importance of the HGXPRT from *Toxoplasma gondii* in purine metabolism and as a target for structure-based inhibitor design has been outlined in the introductory chapters of this thesis. The genomic locus of *hgxpirt* was identified by insertional mutagenesis and selection for resistance to 6-thioxanthine. Two classes of cDNA were isolated, which apparently arise from alternate splicing of a single RNA transcript to yield two potential protein coding regions. These regions differ by the presence of an additional inserted sequence in the N-terminal region of the conceptually translated protein sequences (Figure 1.). The shorter of the two sequences was more abundant in cDNA libraries and termed *hgxpirt-I*, while the second, longer sequence was *hgxpirt-II*. Mutant parasite cells which were knocked-out in *hgxpirt* exhibited no detectable hypoxanthine, guanine, or xanthine PRT activity strengthening the hypothesis that both cDNA transcripts arise from a single genomic locus. HGXPRT activity could be restored by transfecting minigenes encoding either *hgxpirt-I* or *hgxpirt-II* into mutant *T. gondii* cells [1]. Whether or not both isoforms are expressed *in vivo* in *T. gondii* cells, or why the parasite would have two isoforms was not clear. This study reports the expression of both two isoforms in wildtype parasites and studies on the possible functions for the two proteins.

Figure 1: Alignment of HGXPRT-I and HGXPRT-II

```

1 maskpie..... 7
  |||||
1 maskpieesrsqkrsafsdifccctpnegaivpsdpmvstsapartsapa 50
  .
8 .....dygkgkgriegmyipdntfynaddflvpphckpyidkillpggl 51
  |||||
51 rssalqdygkgkgriegmyipdntfynaddflvpphckpyidkillpggl 100
  .
52 vkdrveklaydihrtyfgeelhiicilkgsergffnllidylatiqkysgr 101
  |||||
101 vkdrveklaydihrtyfgeelhiicilkgsergffnllidylatiqkysgr 150
  .
102 essvppffehyvrlksyqndnstgqltvlsddlsifrdkhvlivedivdt 151
  |||||
151 essvppffehyvrlksyqndnstgqltvlsddlsifrdkhvlivedivdt 200
  .
152 gftltefgerlkavgpksmriatlvekrtdrsnsikgdfvgfsiedvwiv 201
  |||||
201 gftltefgerlkavgpksmriatlvekrtdrsnsikgdfvgfsiedvwiv 250
  .
202 gccydfnemfrdfdvhavlsdaarkkfek 230
  |||||
251 gccydfnemfrdfdvhavlsdaarkkfek 279

```

Molecular mass (HGXPRT-I) = 26387 Da

Molecular mass (HGXPRT-II) = 31486 Da

2. Materials and Methods

2.1. HGXPRT-I and HGXPRT-II expression: Constructs containing the coding sequences for either *hgxpirt-I* or *hgxpirt-II* with an N-terminal NdeI site in pKS (-) were generously provided by Dr. David Roos. The constructs were digested with NdeI and ligated into an NdeI digested, Calf intestinal alkaline phosphatase treated pBAce vector [2]. Ligation reactions were transformed into XL1-blue cells and minicultures were screened for the correct insert. Positive cultures were maxipreped with the Qiagen maxiprep kit and DNAs further mapped by restriction digest. The pBAce constructs were then transformed into the *hgxpirt* deficient SΦ606 cell line and cultures were induced in low phosphate induction medium as described [3].

2.2. Purification of HGXPRT-I and HGXPRT-II: Recombinant proteins were purified by GTP-agarose affinity chromatography and elution with 1mM PRPP as described [4]. Additionally, HGXPRT-I was purified by standard biochemical means as reported in chapter 3 of this thesis.

2.3. SDS-PAGE: Proteins were fractionated on 15% polyacrylamide minigels at 220V constant voltage [5].

2.4. Kinetic Studies on HGXPRT isoforms: Assays were performed at 37°C in 50 mM Tris (pH=7.6), 5 mM MgCl₂, and 1 mM dithiothreitol buffer (TMD50) containing various

concentrations of [^{14}C] hypoxanthine, [^{14}C] xanthine, or [^{14}C] guanine and PRPP as indicated. Radiometric measurements were terminated by spotting onto Whatman DE81 filter paper, and the filters were washed 3 times with H_2O followed by a single wash with 95% ethanol. Filters were dried at 60°C and bound radiolabel quantified by liquid scintillation. The K_m^{app} values for PRPP, hypoxanthine, xanthine, and guanine were determined by Hanes analysis [6].

2.5. Antibody production and Western blotting: Antibodies against purified HGXPRT-I were generated by Cocalico Biologicals Inc. (Reamstown, PA). Parasite lysates were fractionated by SDS-PAGE and Western blotted.

2.6. Protein degradation studies: 50 ml cultures of *T. gondii* RH-strain parasites on human foreskin fibroblasts were purified from the host cells by passage through a 26 gauge needle and filtering through a $0.3\ \mu\text{m}$ Nalgene filter yielding 3.6×10^6 purified cells per ml. Cycloheximide was added in 20% ethanol to a final concentration of $22\ \mu\text{M}$ to inhibit protein synthesis [7] and aliquots containing 1.4×10^7 cells were removed at various time intervals. Protein extracts from 2×10^6 cells were fractionated on SDS-PAGE and Western blotted as described above and the resulting blots scanned and quantified using the NIH image software package provided by the National Institute of Health.

3. Results

3.1. Protein expression and purification: Both isoforms of HGXPRT were highly expressed in *E. coli* SΦ606 cells and were purified by affinity chromatography (Figure 2.) The purification yielded active HGXPRT proteins albeit at low levels. Purification of HGXPRT-I by standard biochemical means yielded large and replenishable quantities of highly active protein. *3.2. Western blot analysis of lysates from RH-strain Toxoplasma gondii:* Wildtype cells of the RH-strain of *T. gondii* express two proteins which are recognized by the polyclonal anti-HGXPRT antibody (Figure 3, Lane A). Deletion of the single genomic locus for *hgxprt* results in parasites which do not express either form of HGXPRT (Figure 3, Lane B) indicating that both proteins arise from a single genomic transcript. The identities of the two proteins are verified by the presence of bands corresponding to either HGXPRT-I or HGXPRT-II in the knock-out parasites which were transfected with the relevant minigene constructs (Figure 3, Lanes D and E).

3.3. Kinetic characterization: HGXPRT isoforms I and II did not differ significantly in their ability to recognize and phosphoribosylate their purine substrates (Table 1.) The slightly lower k_{cat} values determined for isoform II are probably not functionally significant as these values tend to scatter between experiments depending on the protein assay used and the freshness of the protein preparation.

Figure 2: Expression and affinity purification of recombinant HGXPRT isoforms. Lane A: crude lysate from *E. coli* transformed with vector alone. Lane B: crude lysate from *E. coli* transformed with *pBAce-hgxprt-I*. Lane C: affinity purified HGXPRT-I. Lane D: crude lysate from *E. coli* transformed with *pBAce-hgxprt-II*. Lane E: affinity purified HGXPRT-II.

A B C D E

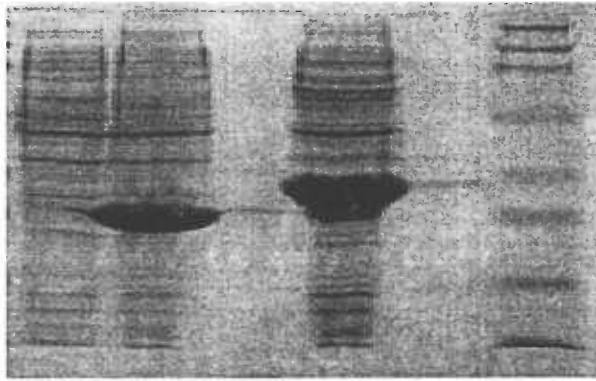


Figure 3: Western blot of *T. gondii* lysates. Wildtype, *hgxpri* deficient, and minigene-transfected RH-strain parasites were lysed and fractionated on SDS-PAGE. Proteins were blotted and blots probed with anti-HGXPRT antibodies. Lane A: wildtype RH-strain *T. gondii* tachyzoite lysate. Lane B: Δ *hgxpri* RH-strain *T. gondii* tachyzoite lysate. Lane C: wildtype RH-strain *T. gondii* tachyzoite lysate. Lanes D: Δ *hgxpri* RH-strain *T. gondii* tachyzoites transfected with the minigene for *hgxpri*-II. Lanes E: Δ *hgxpri* RH-strain *T. gondii* tachyzoites transfected with the minigene for *hgxpri*-I.

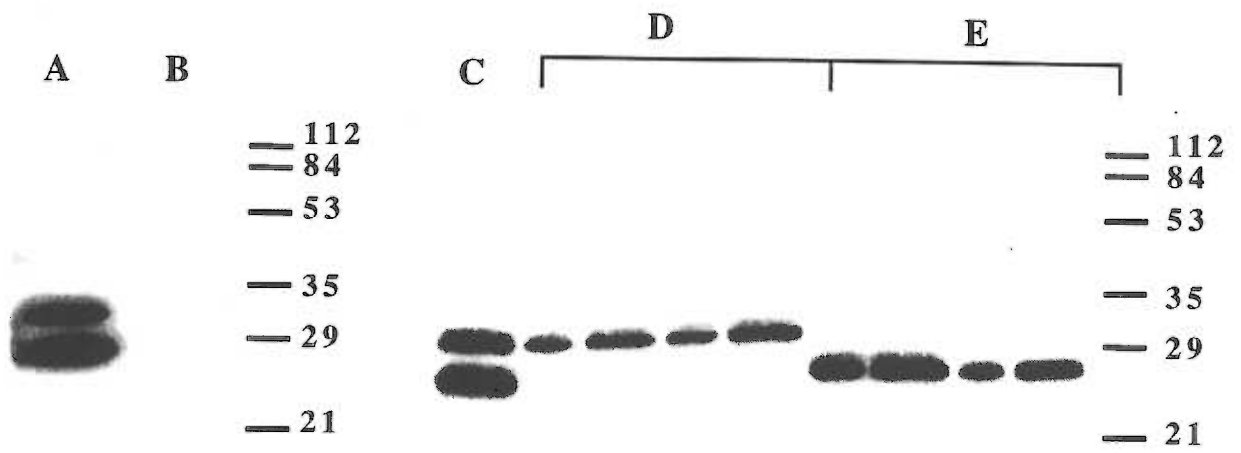


Table 1: Kinetic parameters for recombinant *T. gondii* HGXPRT isoforms

Parameter	Isoform	Substrate		
		Hypoxanthine	Xanthine	Guanine
K_m (μM)	I	1.7	18	1.0
	II	1.5	19	2.3
k_{cat} (s^{-1})	I	6.5	24	6.5
	II	2.3	14	3.1

3.4. Degradation of HGXPRT Isoforms

Time dependent degradation studies on HGXPRTs I and II reveal that isoform II is degraded slightly faster than isoform I (Figures 4A and B).

4. Discussion

The presence of two HGXPRT isoforms in *T. gondii* was postulated based on the sequences of two classes of *hgxpirt* cDNAs found in libraries from the parasite [8]. A polyclonal antibody which specifically recognizes HGXPRT in *T. gondii* lysates was generated and used to verify the presence of these isoforms in crude cell extracts. This finding is unique in that no other organism has been reported to express two forms of this enzyme [9,10,11,12,13]. To explain this atypical expression pattern, a number of hypotheses were tested relating to enzyme function, degradation, expression and localization. The kinetic evaluations reported above indicate that the two enzymes do not provide the cell with two discrete catalytic capacities as both proteins are virtually identical kinetically. Similarly

using densitometric analyses to study protein degradation (Figures 4A and B) no pronounced difference was found in the intracellular stability between HGXPRT isoforms I and II, indicating that regulation of enzyme levels is not the primary function of the two HGXPRTs. In collaboration with our laboratory, Dr. David Roos' laboratory has examined the enzyme's stage specific expression and localization. No difference in stage specific expression was found, however it was determined that the longer HGXPRT isoform, HGXPRT-II, was membrane associated. This membrane association is due to the 49 amino acid N-terminal insert which is sufficient for targeting of other proteins to the membrane and is likely to be driven by palmitoylation of the cysteine triplet found within this sequence (Figure 1.) [14]. The reason for such membrane association of one of the HGXPRT isoforms may lie in the parasite's requirement for purine scavenging [15]. Isoform II, which is localized to the plasma membrane, may function to trap purines intracellularly as they cross the parasites membrane, while isoform I salvages purine bases during metabolism within the cell.

Figure 4A: Densitometric analyses of fractionated RH strain *Toxoplasma* lysates. Protein synthesis in *Toxoplasma* was inhibited with cycloheximide. Crude lysates of parasites treated for various times were fractionated on SDS-PAGE and Western blotted with an anti-HGXPRT antibody.

22 hours



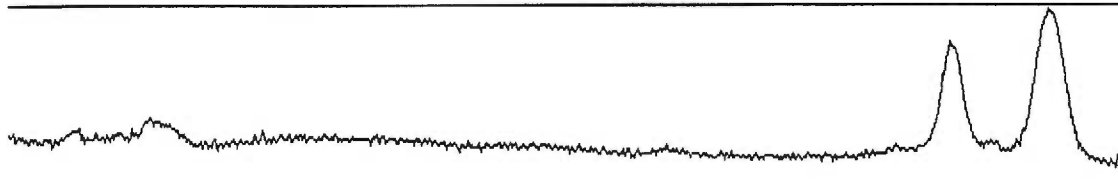
9.5 hours



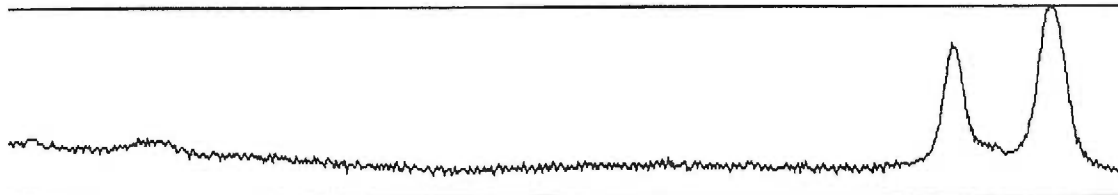
6 hours



4 hours



2 hours

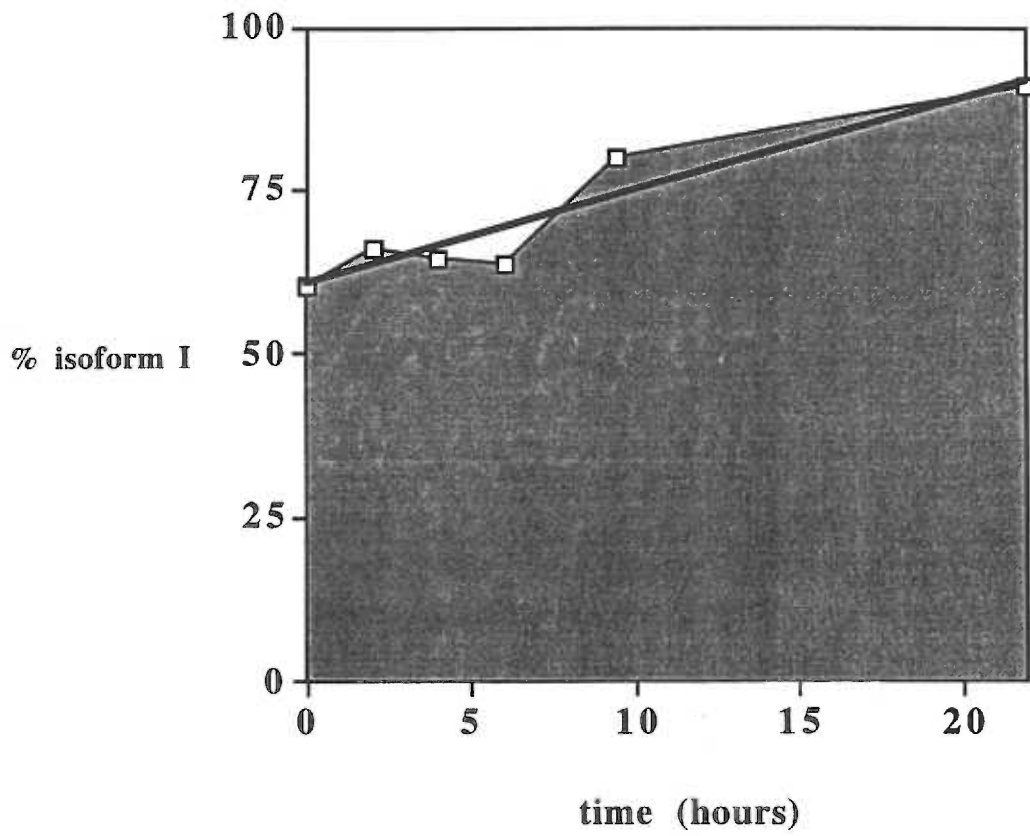


0 hours



▲ iso-II ▲ iso-I

Figure 4B: The areas of the peaks from Figure 4A were determined with the NIH-image software package and the ratios of HGXPRT-I to total HGXPRT protein calculated and plotted.



1. Donald, RGK, Carter, D, Ullman, B, and Roos, DS (1996) *J. Biol. Chem.* **271:24**, 14010-14019.
2. Craig SP, Yuan L, Kuntz DA, McKerrow JH and Wang CC (1991) *Proc. Natl. Acad. Sci. U.S.A.* **88**, 2500-2504.
3. Allen, T, Ullman B, (1994) *Mol. Biochem. Parasit.* **65**, 233-245.
4. Allen, T, Henschel, TC, Cross, L, Conley, J, and Ullman, B (1989) *Mol. Biochem. Parasit.* **33**, 273-282.
5. Laemmli, UK (1970) *Nature* **227**, 680-685.
6. Cornish-Bowden A. (1995) *Fundamentals of Enzyme Kinetics*. Portland Press London, U.K.
7. Beckers, CJM, Roos, DS, Donald, RGK, Luft, BJ, Schwab, JC, Cao, Y, and Joiner, K, (1995) *J. Clin. Invest.* **95**,
8. Donald, RGK, Carter, D, Ullman, B, and Roos, DS (1996) *J. Biol. Chem.* **271:24**, 14010-14019.
9. Craig, SP, McKerrow, JH, Newport, GR, and Wang CC (1988) *Nucleic Acids Res.* **16**, 7087-7101.
10. Tuttle, JV, and Krenitsky, TA (1980) *J. Biol. Chem.* **255:3**, 909-916.
11. Ullman B, and Shih, S; personal communication.
12. Ali, LZ, and Sloan, D (1982) *J. Biol. Chem.* **257:3**, 1149-1155.
13. King, A, and Melton, DW (1987) *Nucleic Acids Res.* **15:24**, 10469-10481.
14. Roos, DS, and Donald, RGK, personal communication.
15. Ullman B, and Carter D (1995) *Infect. Agents Dis.* **4**, 29-40.

2. Characterization of HGXPRT isoform I

2.1. Expression, purification, and biochemical properties of the *T. gondii* HGXPRT-I enzyme

Darrick Carter and Buddy Ullman

1. Introduction

The phosphoribosyltransferases (PRTs) involved in purine salvage are key enzymes in the purine metabolism of many protozoan parasites [1]. The hypoxanthine-guanine-xanthine PRT of *T. gondii* provides a key function in purine scavenging for this organism and is thus an attractive target for inhibitor design. Biochemically rational inhibitor design requires extensive understanding of an enzyme, including structural and biochemical features which allow a protein to drive catalysis. A basis for performing extensive studies on an enzyme which will provide such information is generating large quantities of this protein in homogeneous form and understanding of the environments required for efficient catalysis and stability. Thus, the focus of this section is the creation of a high-yield expression construct, the purification of this enzyme, and the initiation of general biochemical studies which provide the foundation for further biochemical and structural analyses.

2. Materials and Methods

2.1. HGXPRT-I expression: An *hgxpirt-I* construct with an N-terminal NdeI site in pKS (-) was generously provided by Dr. David Roos. The construct was digested with NdeI and ligated into an NdeI digested, Calf intestinal alkaline phosphatase treated pBAce vector. Ligation reactions were transformed into XL1-blue cells and minicultures were screened for the correct insert. Positive cultures were maxiprepped with the Qiagen maxiprep kit and DNAs further mapped by restriction digest. The pBAce-*hgxpirt-I* construct was then transformed into the *hgxpirt* deficient SØ606 cell line and cultures were induced in low phosphate induction medium as described [2].

2.2. PRTase activity: Assay cocktails contained a [C-14] labeled purine base at saturating concentrations and 2mM 5-phosphorylribosepyrophosphate in 50mM Tris, pH=7.5; 5mM MgCl₂ and 2mM dithiothreitol (TMD50 buffer). Reactions were initiated by addition of enzyme to the cocktail at 37°C and time points were taken by spotting aliquots on DE-81 paper (Whatman). Free purine base was then removed by washing twice with water and once with 70% ethanol. Filters were dried in a 80°C oven and bound radioactive isotopes quantified with a Beckman scintillation counter in the presence of aqueous fluor.

2.3. Purification of HGXPRT:

Crude extracts: 1 to 4 liters of bacterial cultures were induced as described above and harvested by centrifugation in an RC-3 centrifuge at 4,500 rpm. Cell pellets were resuspended in TMD50 buffer. The suspension was passed through a French pressure cell at 16,000 psi and extracts were clarified by centrifugation at 30,000 x g for 30 min.

DEAE cellulose chromatography: DEAE-cellulose columns were prepared by preswelling DEAE cellulose (Sigma D-8382) in 6M urea and washing the columns with 2M NaCl. 50ml columns were then equilibrated in TMD-50 buffer and crude extracts were loaded. A salt gradient from 0 to 500 mM NaCl in TMD50 was run and A_{280} monitored. Fractions containing GPRT activity were found in the flow through and pooled.

Ammonium sulfate precipitation: Ammonium sulfate was added to the DEAE chromatography pools at 65% saturation and precipitated protein was pelleted by centrifugation at 30,000 x g for 30 min. Pelleted protein was redissolved in TMD50 with 10% glycerol.

Gel permeation chromatography: Redissolved protein from the ammonium sulfate cut was chromatographed over a 100 ml Sephadex G-100 column (Pharmacia Biotech Inc.) and protein elution monitored at 280nm. Fractions with GPRT activity were pooled for analysis by SDS-PAGE.

2.4. *SDS-PAGE*: Proteins were fractionated on 15% polyacrylamide minigels at 220V [³].

2.5. *Isoelectric point determination*: Purified HGXPRT-I was loaded on a isoelectric focussing gel and isoelectric focussing was performed against known standards.

2.6. *Divalent cation specificity*: Divalent cations were added to reaction mixes to 10 mM final concentration and HPRT activity was monitored with the radiolabelled assay described above. HPRT activity was then normalized as a percentage of the activity found in the presence of magnesium chloride.

2.7. *Inhibition by sulfhydryl reactive reagents*: Mercuric chloride, Ellman's reagent, parahydroxy-mercurobenzoate or iodoacetamide were added to HGXPRT-I protein (10 mg/ml) to a final concentration of 0.2 mM. Reactions proceeded for 30 min at ambient temperatures in the absence of DTT. Residual activity was assayed as described above and compared to mock-treated HGXPRT-I.

2.8. *Inactivation by GMP-dialdehyde*: HGXPRT-I protein (10 mg/ml) was treated with GMP-dialdehyde at 0.1 mM. Reactions were allowed to proceed on ice for 0, 30, 60, or 120 min and stopped by addition of excess sodium borohydride. Schiff's bases were then reduced for 20 min with sodium borohydride and HPRT activity was assayed as described above and compared to GMP treated proteins.

2.9. *Specificity of HGXPRT*: PRT assays were performed as described above in the presence of [C-14]-guanine, [C-14]-hypoxanthine, [C-14]-xanthine, [C-14]-adenine and [H-3]-allopurinol (Moravek Biochemicals).

2.10. *Temperature dependence of HGXPRT*: HPRT assays were performed in triplicate at temperatures ranging from 20°C to 100°C and rates were plotted on an Arrhenius plot.

2.11. *pH profile*: HPRT activity was quantified at various pHs ranging from pH=4 to 9.

3. Results and Discussion

3.1. *Subcloning and expression*: A 702 b.p. NdeI fragment containing the entire HGXPRT-I coding region was subcloned into the pBAce expression vector [4] (Figure 1.) and high levels of expression were achieved after induction in low phosphate induction medium (Figure 5., Lane B). The protein partitioned largely in the soluble fraction of the crude extract and was highly active (data not shown)

3.2. *Purification*: HGXPRT-I eluted in the unbound fractions of the DEAE chromatography run under the conditions employed (Figure 2.). In conditions of low magnesium in the buffer, HGXPRT-I binds weakly to the DEAE-cellulose matrix indicating that the presence of 5mM to 10mM Mg²⁺ is sufficient to bar HGXPRT-I from binding. At 65% ammonium sulfate, virtually all HGXPRT-I is precipitated from solution after 2 hours (Figure 3.) and

found in the protein pellet after high speed centrifugation. Redissolved HGXPRT-I from this fraction behaves as an oligomer in gel permeation chromatography as it elutes near or at the void volume of the columns employed (Figure 4.). SDS-PAGE on pooled fractions (Figure 5.) indicates that the HGXPRT-I protein is homogenous at the end of this purification procedure.

3.3. General biochemical properties: As expected, the HGXPRT recognizes hypoxanthine, xanthine, and guanine efficiently and converts these purines rapidly to nucleotides. The protein converts allopurinol poorly and does not recognize adenine at all (Data not shown). Purified HGXPRT-I migrates as a 27 kD protein on SDS-PAGE gels in agreement with the predicted molecular weight of 26.4 kD based on the conceptually translated cDNA sequence. The enzyme exhibits a pI value of approximately 5.5 as determined by migration on an isoelectric focussing gel and comparison to standards of known isoelectric point. Similarly to other purine PRT proteins, enzymatic activity increases as the pH increases and no pH optimum was determined within the pH range tested. The protein can utilize Zn^{2+} , Mn^{2+} , Ca^{2+} and Co^{2+} as alternate metal cofactors, but not Fe^{3+} , Cd^{2+} , or Pb^{2+} (Figure 6). HGXPRT-I is resistant to temperatures of up to 65° C and begins irreversibly unfolding at higher temperatures. At temperatures lower than 65 degrees Celcius, the activity increases in accordance with Arrhenius' law and extrapolation from an Arrhenius plot reveals an overall activation energy of about 73 kJ/mol (Figure 7)

3.4. Chemical modification of HGXPRT: The enzyme is sensitive to the tyrosyl-modifying

reagent tetranitromethane as are many of the known PRTases [5]. This sensitivity is likely to be due to the presence of an important Tyr-residue at position 118 in a long flexible loop which is critical for catalysis [6]. Additionally, the enzyme is susceptible to many of the Cys-modifying reagents such as Ellman's reagent, HgCl_2 , and para-aminomercurobenzoate (Figure 8). Inhibition of enzymatic activity by sulfhydryl-modifiers is proportional to the bulk of the chemical indicating that Cys-residues may be proximal to the active site, but not directly involved in catalysis. These findings are consistent with the reported crystal structure of the HGXPRT-I [7] in which there is a Cys dyad proximal to the active site which is not directly involved in catalysis. Exposure of the protein to GMP-dialdehyde efficiently inactivates HGXPRT-I (Figure 9) indicating both that GMP can bind to the free enzyme and that there is a candidate amine group proximal to the ribose ring with which the aldehyde can form a Schiff's base.

Figure 1: Map of the pBAce-HGXPRT I construct

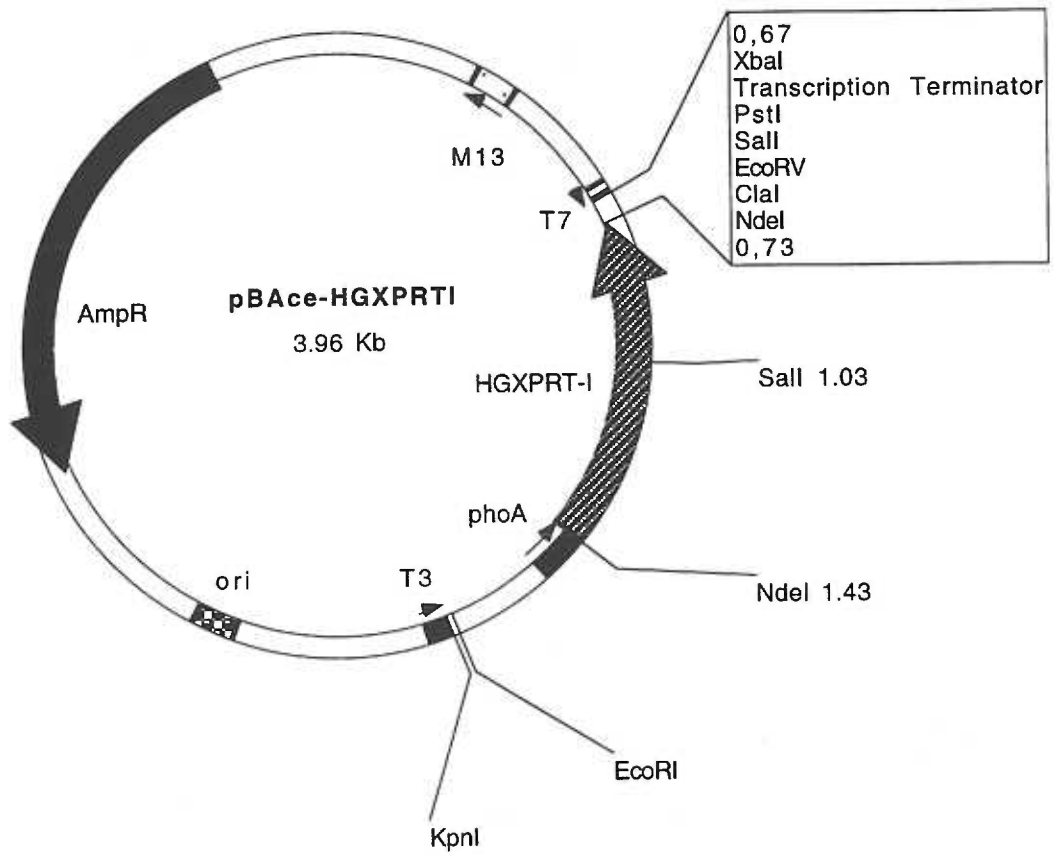


Figure 2: DEAE Chromatography of HGXPRT-I

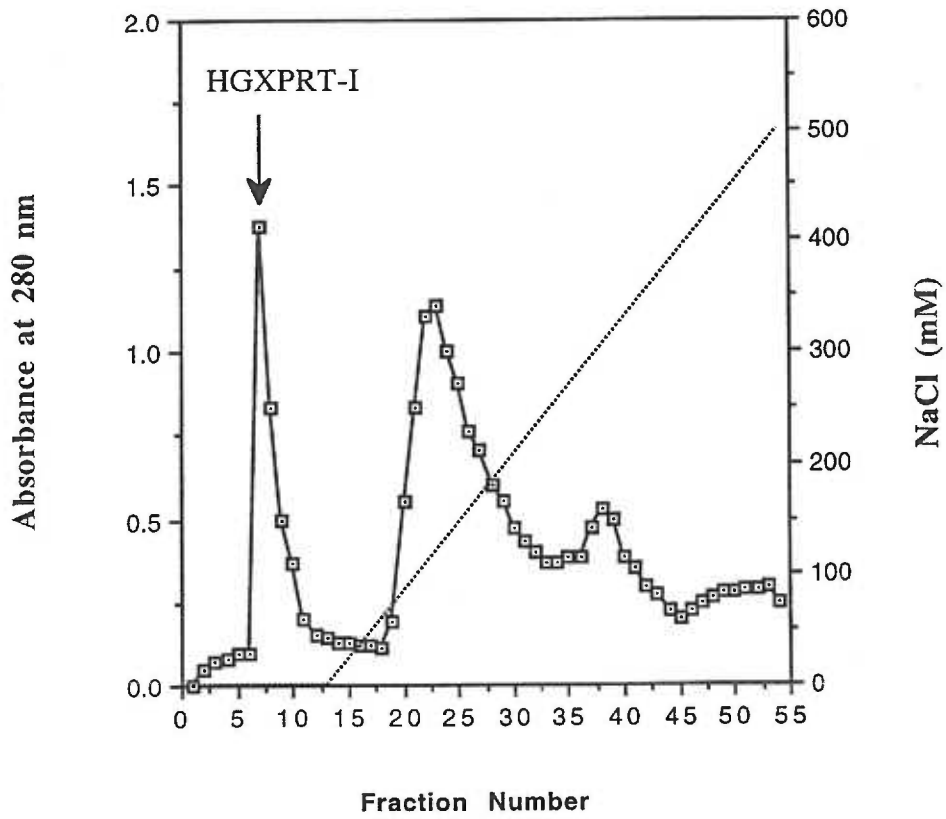


Figure 3: Ammonium sulfate precipitation of HGXPRT-I

HPRT activity

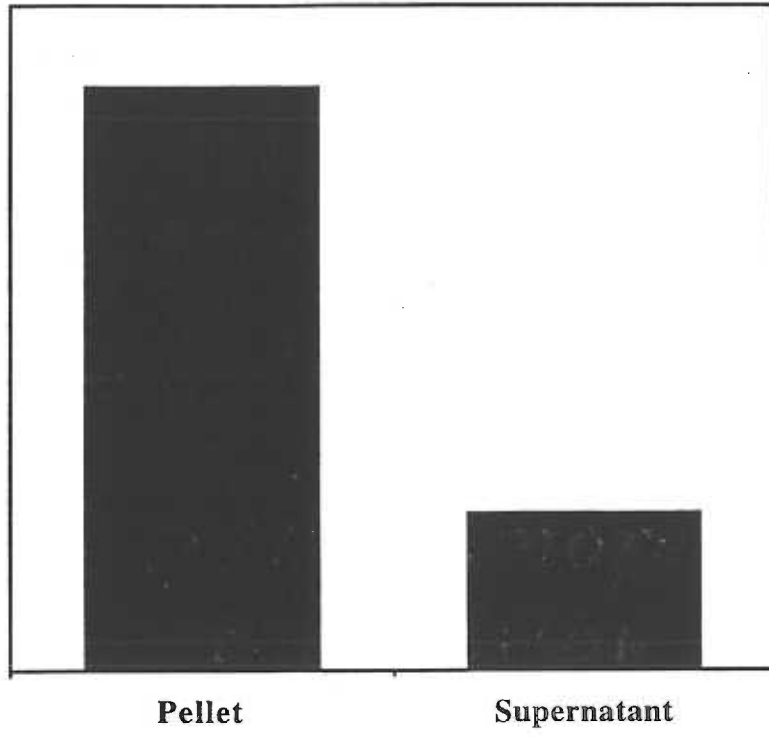


Figure 4: Gel permeation chromatography of HGXPRT-1

Absorbance at 280 nm

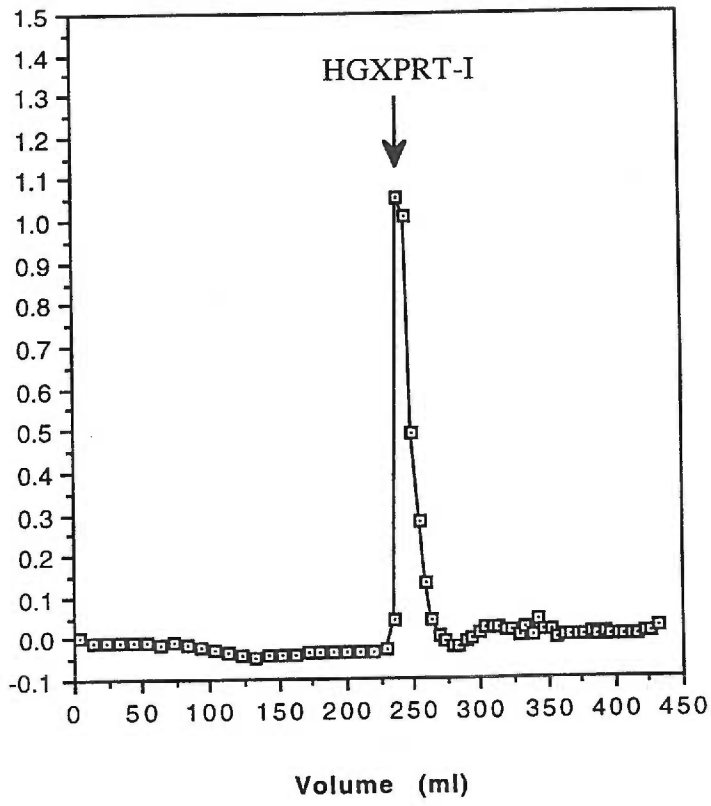


Figure 5: Purification of HGXPRT-I. 5-10 μg of protein were loaded on each lane and fractionated by SDS-PAGE. Proteins were visualized by staining with Coomassie brilliant blue. Lane A: Crude lysate of *E. coli* transformed with vector alone. Lane B: Crude lysate of *E. coli* transformed with pBAce-hgxprt-I expression construct. Lane C: unbound protein from DEAE-cellulose chromatography. Lane D: ammonium sulfate precipitated proteins. Lane E: pooled fractions from gel permeation chromatography.

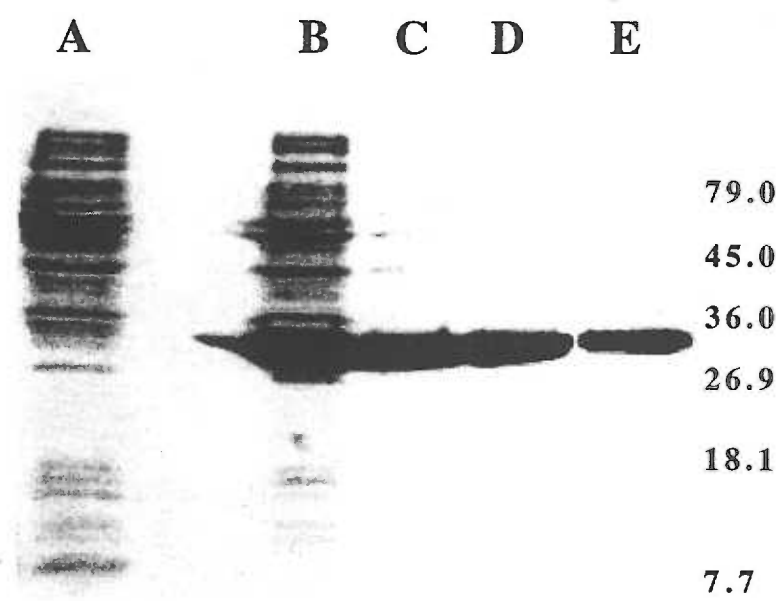


Figure 6: Divalent Cation usage by HGXPRT-I

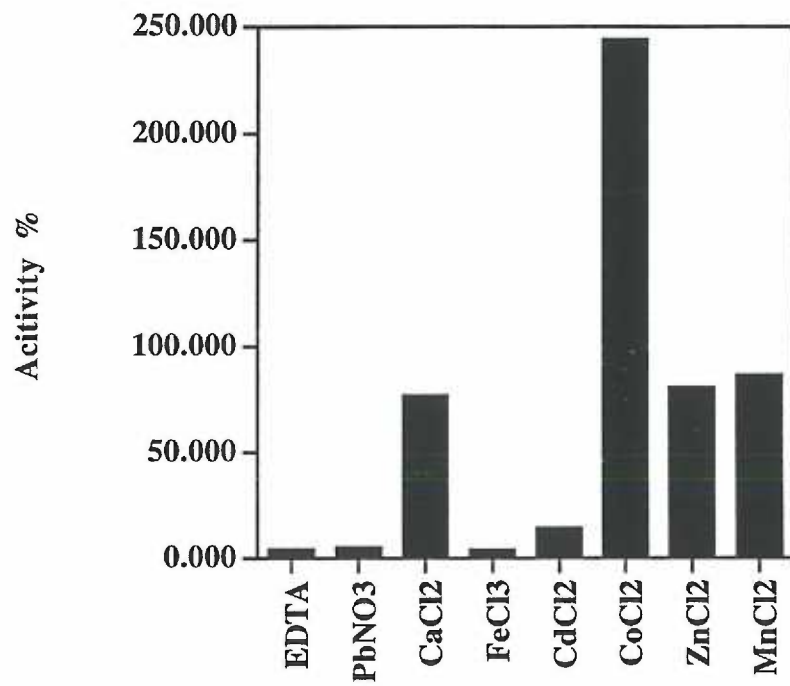


Figure 7: Arrhenius plot of reaction rates for HGXPRT-I

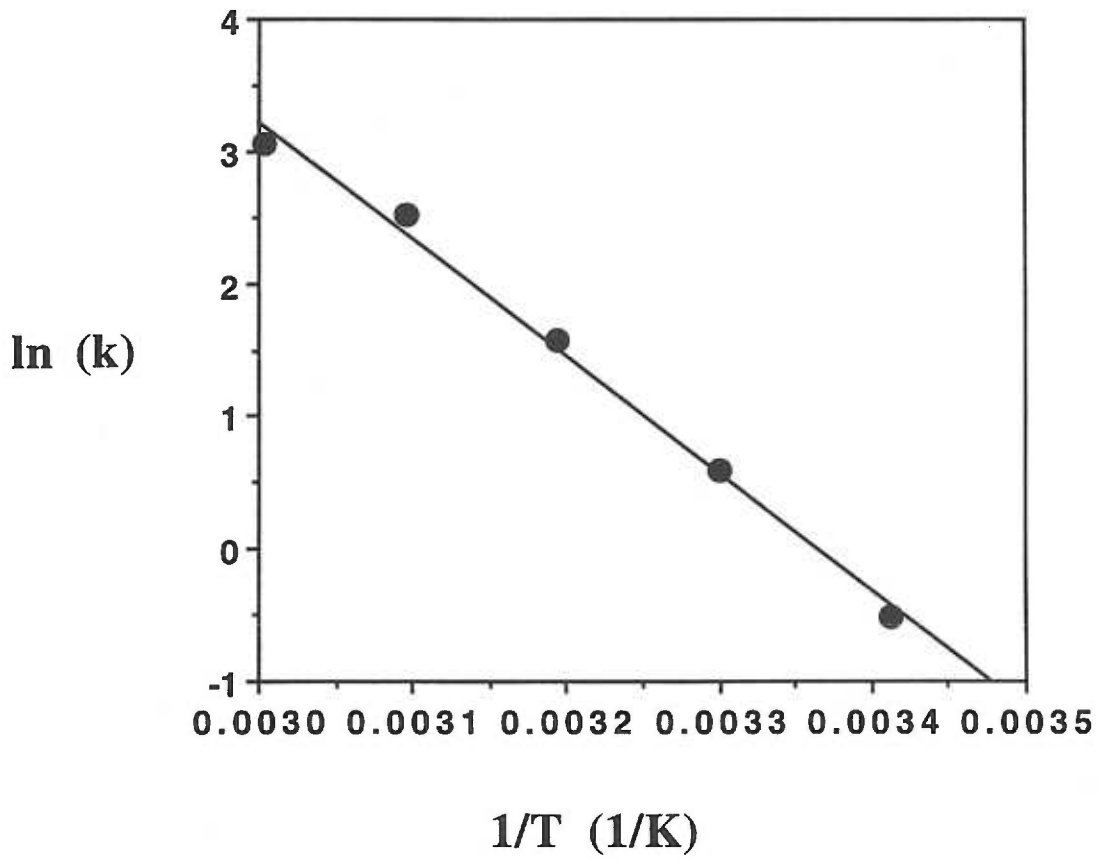


Figure 8: Effect of Cysteine modifying reagents on HGXPRT-I

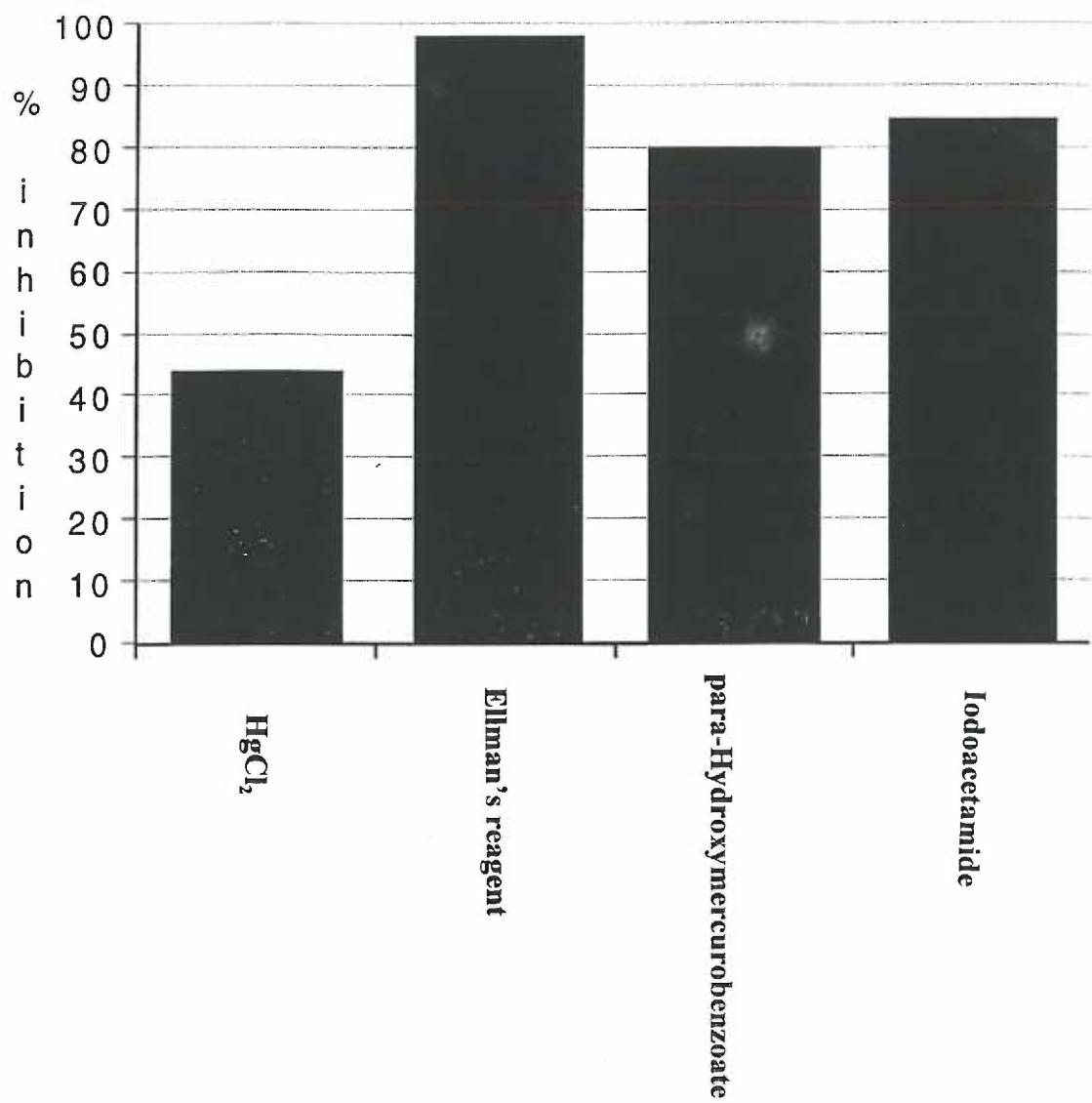
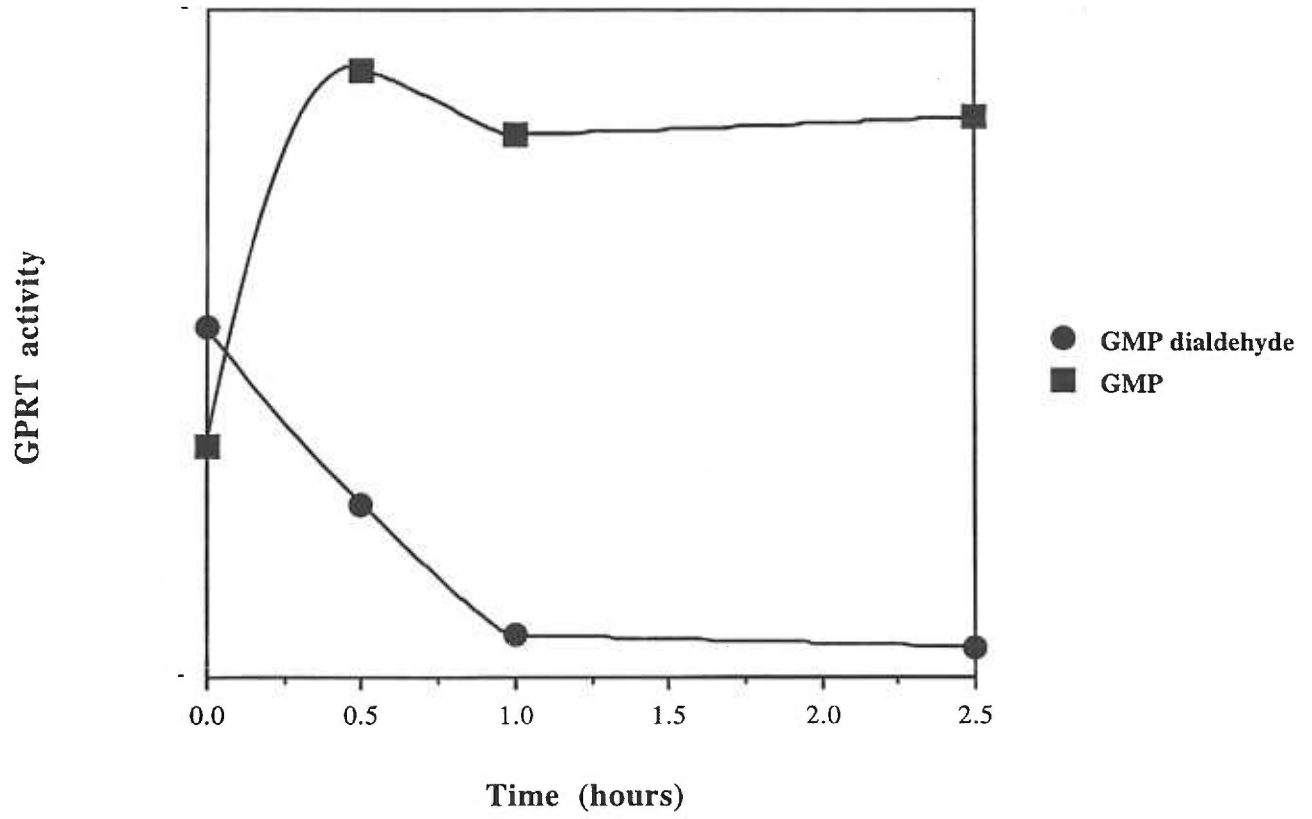


Figure 9: GMP dialdehyde dependent inactivation of HGXPRT-I



- 1 . Ullman, B. and Carter, D. (1995) *Infectious Agents and Disease* 4:29-40.
- 2 . Allen, T, Ullman B, (1994) *Mol. Biochem. Parasit.* 65, 233-245.
- 3 . Laemmli, UK (1970) *Nature* 227, 680-685.
- 4 . Craig SP, Yuan L, Kuntz DA, McKerrow JH and Wang CC (1991) *Proc. Natl. Acad. Sci. U.S.A.* 88, 2500-2504 .
- 5 . Armando Jardim, Darrick Carter and Buddy Ullman, unpublished observation.
- 6 . Jardim A, and Ullman B (1997) *J. Biol. Chem.* 272(14):8967-8973.
- 7 . Schumacher MA, Carter D, Roos DS, Ullman B, and Brennan RG (1996) *Nature Structural Biology* 3(10):881-887.

2.2. Structural Studies on the *T. gondii* HGXPRT-I enzyme

Darrick Carter and Buddy Ullman

1. Introduction

The hypoxanthine - guanine - (xanthine) phosphoribosyltransferase (HG(X)PRT) enzymes are attractive targets for rational inhibitor design and for the discovery of new leads for antiparasitic drugs [1,2]. Structures have been determined for a number of these proteins and exhibit a common fold consisting of a hood and a core domain [3,4,5]. However, as most of these structures are of either apo-enzyme forms or product-bound forms of the PRTs, little or no structural information is known about the conformational changes occurring during catalysis. The kinetic mechanism of the enzyme is sequentially ordered with the phosphorylribosepyrophosphate (PRPP) binding first to the active site followed by the purine base [6]. The enzyme then moves through a transition state in which an oxocarbenium ion is formed on the ribose sugar. After a nucleophilic attack of the N-9 of the purine base on this ion, an N-glycosidic bond is formed and the pyrophosphate product is released followed by the nucleoside monophosphate. Intimate knowledge of the structure - function relationships in the enzyme's architecture as it moves through this catalytic procedure is necessary for biochemically rational inhibitor design. Thus, thorough understanding of the enzyme's structure and intermediate conformations will be vital for the discovery of new lead compounds for drug development targeting the HG(X)PRT enzymes.

2. Materials and Methods

2.1. HGXPRT-I expression and purification: The pBAce-*hgxpirt-I* construct was transformed into the *hgxpirt* deficient SΦ606 cell line and cultures were induced in low phosphate induction medium and purified as described in chapter 2.1.

2.2. PRTase activity: Assay cocktails contained a [C-14] labeled purine base and 2mM 5-phosphorylribosepyrophosphate in TMD50 buffer. Reactions were initiated by addition of enzyme to the cocktail at 37°C and time points were taken by spotting aliquots on DE-81 paper (Whatman). Free purine base was then removed by washing twice with water and once with 70% ethanol. Filters were dried in a 80°C oven and bound radioactive isotopes quantified with a Beckman scintillation counter in the presence of aqueous fluor.

2.3. Seleno-methionine derivative for X-ray crystallographic studies: BL41 cells were transformed with the pBAce-HGXPRT-I construct previously described . Modified low phosphate induction medium (LPI) [7] was prepared as follows: Casamino acids were substituted at 7 g/l with an amino acid mixture of: 5g L-alanine, 4g L-arginine, 4g L-aspartate, 4g L-glutamate, 6.5g L-glutamine, 5.5g glycine, 1g L-histidine, 2.3g L-isoleucine, 4.2g L-lysine, 1.3g L-phenylalanine, 1g L-proline, 21g L-serine, 2.3g L-threonine, 1.7g L-tyrosine, 2.3g L-valine, 4g L-asparagine, 0.3g L-cysteine, 0.3g L-tryptophan, and 2.3g L-leucine. The LPI was also supplemented with 0.3 g thymine, 1 g uracil, 1 g adenine, and 1 g guanosine. D-glucose was increased to 10 g/l. 50 ml of an overnight culture of BL-41 cells

transformed with the HGXPRT-I expression construct was diluted into 500 ml LB broth containing 500 mg/l ampicillin and grown at 37°C for 1 hour. The cells were then harvested by centrifugation and LB broth was carefully removed. This culture was resuspended in 2 l LPI as prepared above and grown in the dark at 37°C for 2 days. Cultures were harvested and expressed protein was purified as described above.

2.4. Oligomeric state of the HGXPRT-I: Purified HGXPRT-I protein was chromatographed by high pressure liquid chromatography over a Protein-Pak 125 gel permeation chromatography column equilibrated in 30 mM Tris pH 7.5, 10 mM MgCl₂, 5 mM Dithiothreitol (DTT), 100 mM NaCl, and 0.05 % sodium azide. The retention times of the protein were compared to those determined for molecular weight markers, bovine serum albumin (66.2 kD), carbonic anhydrase (29 kD) and cytochrome C (12.4 kD). To verify the retention times of the putative dimeric state of the enzyme, protein was co-injected with bovine serum albumin and fractions were collected, acetone precipitated, and fractionated on SDS-PAGE [8]. To determine the active form of the enzyme, fractions corresponding to either the dimer or the monomer were collected and assayed for HGXPRT activity. Activities were normalized to the peak areas and specific activities compared.

2.5. Dissociation constant for the monomer - dimer equilibrium: The dissociation constant was determined by serially diluting the protein in 50 mM Tris pH 7.5, 5 mM MgCl₂, 2 mM DTT buffer (TMD50) in a range from 0.01 mg / ml to 10 mg / ml. The protein was allowed

to equilibrate for 1 h at 37°C and then injected and fractionated on the HPLC as described above. The peak areas were measured for the monomer and the dimer and plotted versus the protein concentration.

2.6. Effect of PRPP on the protein's conformation: Purified HGXPRT-I was run in the presence and absence of 1mM PRPP over the HPLC column described above and retention times were determined. Additionally, the protein was subjected to dynamic light scattering analysis on a DynaPro-801. Collected data were analyzed bimodally and Stoke's radii were determined for both the monomeric and dimeric states of the enzyme in the presence and absence of 1 mM PRPP.

2.7. Circular Dichroism on various states of the HGXPRT-I: HGXPRT-I was dialyzed overnight against 20 mM sodium phosphate buffer pH 7.5. Either 5mM PRPP-Mg²⁺, 5mM xanthosine monophosphate, or 0.1 mM hypoxanthine were added to the enzyme and CD-spectra were gathered on each sample.

3. Results

Selenomethionine derivative of HGXPRT-I: Protein was successfully expressed and purified from metC deficient *E. coli*. The enzyme was highly active and could be used to generate crystals similarly to the wild-type HGXPRT-I. This protein had incorporated L-Se-methionine in place of the naturally occurring L-methionine and was successfully used as a heavy atom derivative for phase determination.

Oligomeric state of HGXPRT-I: The HGXPRT-I protein exists in a monomer-dimer equilibrium. The protein in the dimer peak, when fractionated on SDS-PAGE, runs concomitantly with the protein in the monomeric peak indicating that both peaks are HGXPRT-I. The dimer peak also elutes slightly after bovine serum albumin (66 kD), consistent with the predicted molecular mass of the dimer (53 kD) (Figure 1.). Both forms of the protein exhibit similar specific activities (data not shown).

Dissociation constant for the monomer - dimer equilibrium: HGXPRT-I could be dissociated into monomers at physiologically relevant concentrations of the enzyme (Figure 2.). The dissociation constant calculated from the graph is 38 μM .

PRPP binding to HGXPRT-I: HPLC traces in the presence and absence of PRPP indicate that a change in the protein's hydrodynamic radius occurs upon binding of this substrate as the retention time for the dimer peak increases by 0.77 minutes in the presence of PRPP. A similar effect is observed using dynamic light scattering (Table 1.)

Table 1. Changes in calculated Stoke's radii with PRPP

Oligomeric State of HGXPRT-I	without PRPP	with 10 mM PRPP
monomer	1.48	1.98
dimer	4.11	4.85

Circular Dichroism of HGXPRT-I with various ligands: Circular dichroism indicated no readily observable change in the amount of secondary structures with either PRPP or purine base present. Adding product, IMP, to the protein did give a noticeable shift at 240 nm, indicating a decrease in the α -helical content of the protein (Figure 3.). This finding is consistent with the known product-bound structures which have been determined for HG(X)PRT enzymes.

4. Discussion

The HGXPRT-I protein exists in a monomer-dimer equilibrium and undergoes conformational changes as it is bound to various ligands. Although the intracellular concentrations of the enzyme are not known, reports of co-purification of isoform I and isoform II [9] would indicate that the protein exists at least partially as a dimer inside the parasite cell. The function of this association is not known as the protein is active in both states. The dissociation constant is also relatively high indicating that this association is not vital for the protein. Oligomerization of these proteins may be an evolutionary artifact remaining from PRT enzymes which are obligate dimers and share residues in their active sites [10]. Binding of PRPP to the *T. gondii* HGXPRT induces a conformational change in the enzyme which increases the apparent hydrodynamic radius of the protein. This change in diameter is seen both on size exclusion chromatography and with dynamic light scattering. As this conformational change does not include a dramatic change in the amounts of secondary structures present in the protein as determined by circular dichroism, it is tempting to speculate that the change is associated with a movement of a flexible loop in the active site which is poised to shield the oxycarbonium ion from bulk solvent [11]. Movement of this loop outward allows for the purine base to enter the active site which likely causes a second shift in conformation. After the enzyme has catalyzed its reaction, another structural change occurs which folds out the shielding flexible loop and which is accompanied by a change in the protein's secondary structure which can be detected by circular dichroism in solution and can be seen in the crystal structure of an XMP bound form of the enzyme.

Figure 1: HPLC size exclusion chromatography of HGXPRT-I

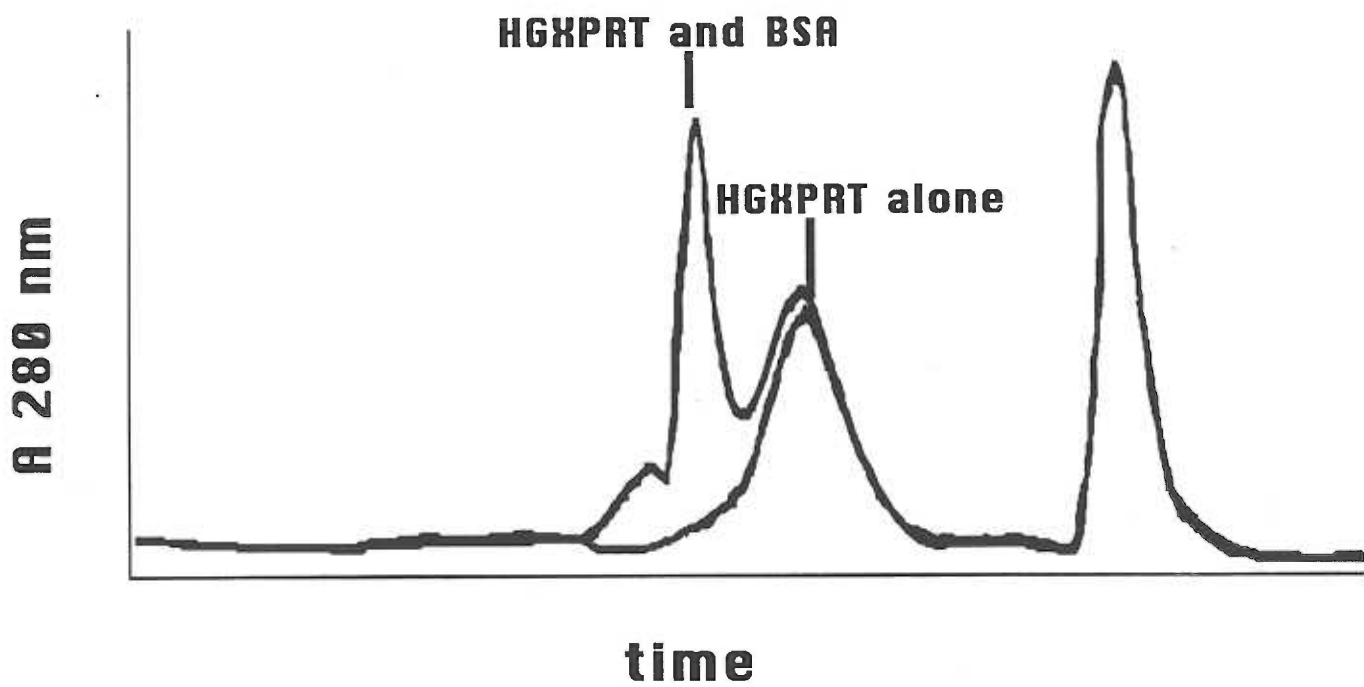


Figure 2: Dissociation of HGXPRT-I as a function of concentration

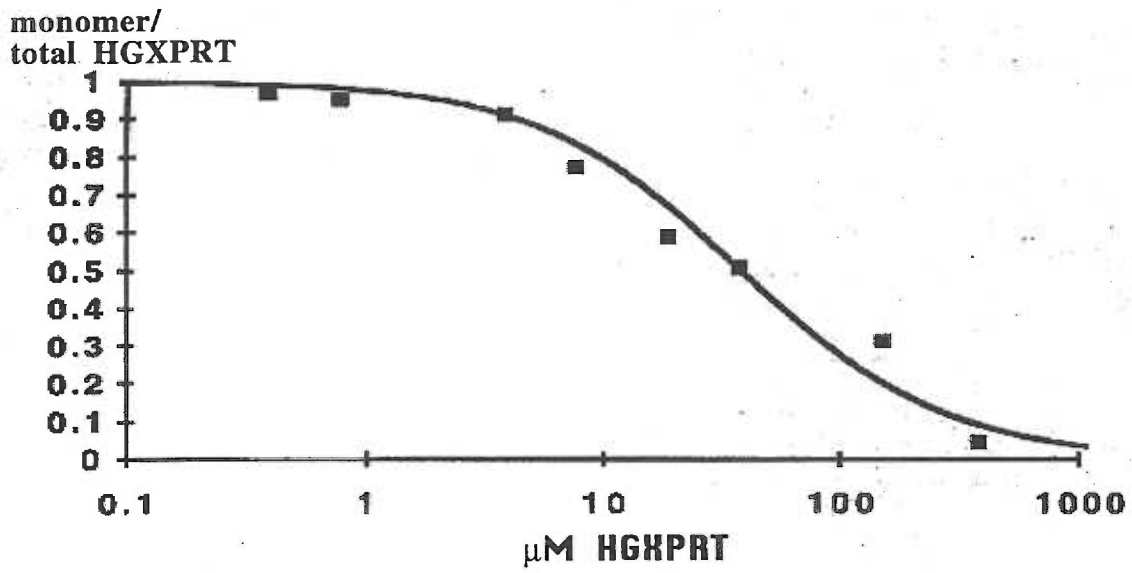
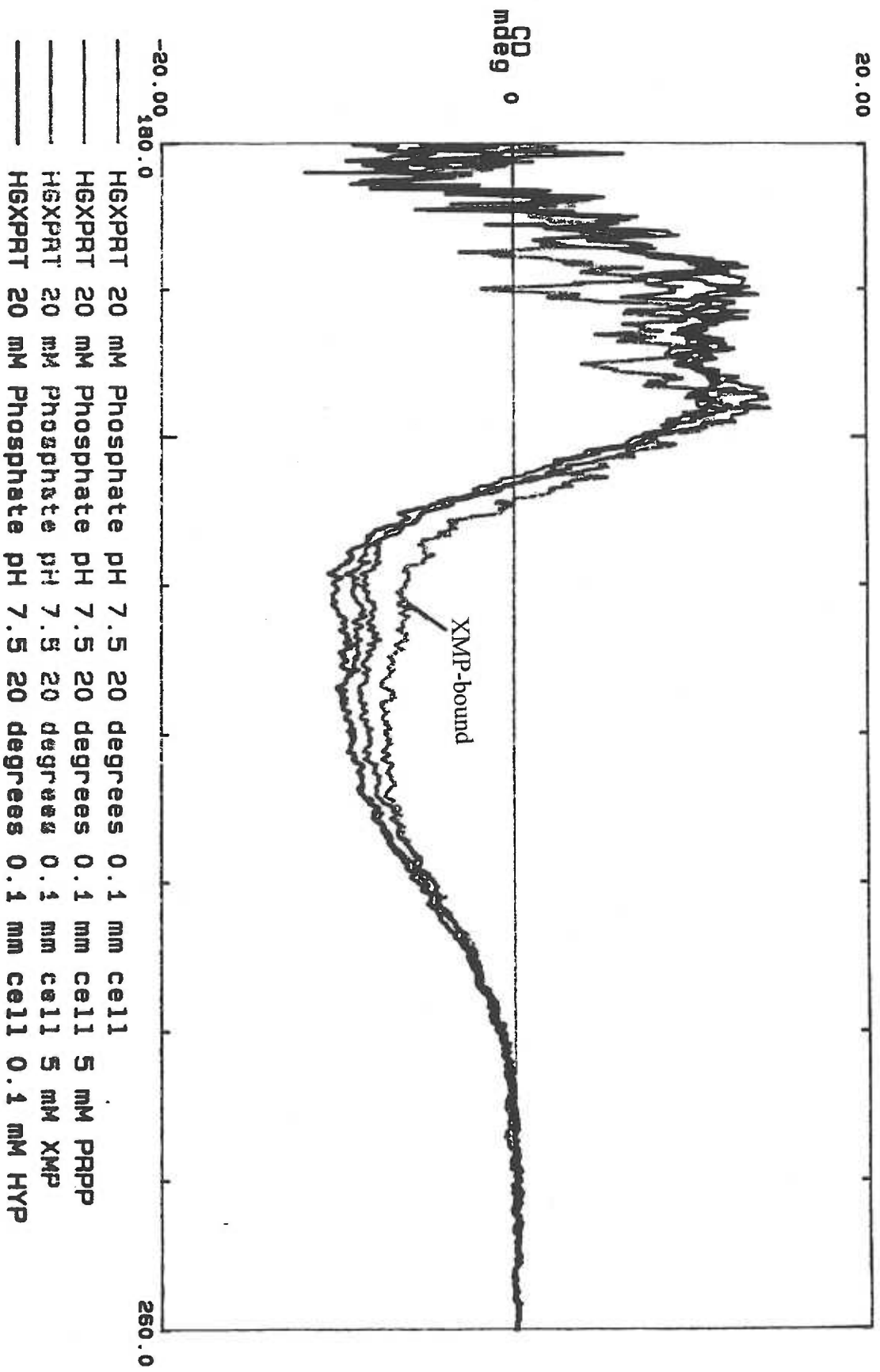


Figure 3: Circular dichroism studies on HGXPRT-I



1. Ullman B, and Carter D. (1997) *Int. J. Parasit.* **27(2)**:203-213.
2. Ullman, B. and Carter, D. (1995) *Infectious Agents and Disease* **4**:29-40.
3. Schumacher MA, Carter D, Roos DS, Ullman B, and Brennan RG (1996) *Nature Structural Biology* **3(10)**:881-887.
4. Eads JC, Scapin G, Xu Y, Grubmeyer C, Sacchettini JC. (1994) *Cell* **78**:325-334.
5. Somoza JR, Chin MS, Focia PJ, Wang CC, Fletterick RJ. (1996) *Biochemistry* **35**:7032-7040.
6. Xu Y, Eads J, Sacchettini JC, Grubmeyer C (1997) *Biochemistry* **36(12)**:3700-3712.
7. Allen TE, Hwang H-Y, Jardim A, Olafson R, Ullman B. (1995) *Mol Biochem Parasitol* **73**:133-145.
8. Laemmli UK. (1970) *Nature* **227**:680-685.
9. Robert Donald, personal communication.
10. Henriksen A, Aghajari N, Jensen KF, and Gajhede M, (1996) *Biochemistry* **35**:3803-3809.
11. Jardim A, Ullman B. (1997) *J Biol Chem* **271**:30840-30846.

2.3. Kinetic Studies on the *T. gondii* HGXPRT-I enzyme

Darrick Carter and Buddy Ullman

1. Introduction

The kinetic properties and mechanism of the HGXPRT protein are important to know for the design of new types of subversive substrates and for efficient analysis of inhibition data gathered in the presence of newly discovered inhibitors. Understanding the kinetic properties of an enzyme is also important for determining its true substrates and metabolic functions, information which is vital for target validation. Structure-based inhibitor design can be performed against numerous conformations of an enzyme as it undergoes catalysis and mechanistic studies provide the information needed for determining structures of catalytically important states of a protein. Additionally, transition-state analogs are usually highly effective inhibitors and mechanistic studies can provide information on the enzyme in its transition state. A thorough understanding of an enzyme's substrate preferences and catalytic turnover numbers is a prerequisite for biochemically rational inhibitor design.

2. Materials and Methods

2.1. HGXPRT-I expression and purification: The pBAce-hgxpirt-I construct was transformed into the hgxpirt deficient SΦ606 cell line and cultures were induced in low phosphate induction medium and purified as described .

2.2. PRTase activity: Assay cocktails contained a [C-14] labeled purine base and 2mM 5-phosphorylribosepyrophosphate in TMD50 buffer. Reactions were initiated by addition of enzyme to the cocktail at 37°C and time points were taken by spotting aliquots on DE-81 paper (Whatman). Free purine base was then removed by washing twice with water and once with 70% ethanol. Filters were dried in a 80°C oven and bound radioactive isotopes quantified with a Beckman scintillation counter in the presence of aqueous fluor.

Alternatively, for kinetic studies leading to secondary plots [1] a spectrophotometric assay was employed as described [2].

2.3. Steady State Kinetic Measurements for the Forward Reaction: Steady state kinetic parameters were determined by saturating the enzyme with one substrate and varying the concentration of the second substrate. Kinetic parameters for PRPP were determined by measuring rates at 50 μM hypoxanthine with PRPP-Mg concentrations ranging from 25 μM to 10 mM. For the purine base kinetics, rates were measured at 2 mM PRPP and base concentrations were varied from 1 μM to 110 μM. Kinetic data were plotted and analyzed by the method of Hanes.

2.4. Steady State Kinetic Measurements for the Reverse Reaction. For kinetic analysis of

the reverse reaction, the formation of hypoxanthine from IMP and PP_i was monitored in a xanthine oxidase coupled reaction as described [3]. Pyrophosphate concentrations were varied from 10 μ M to 0.5 mM at a constant IMP concentration of 500 μ M. For IMP kinetics, concentrations ranged from 5 μ M to 500 μ M at a constant PP_i concentration of 0.5 mM.

2.5. Sub-saturating kinetics to determine kinetic parameters: To verify the accuracy of the kinetic parameters determined above and to initiate mechanistic studies, subsaturating kinetic studies were performed with hypoxanthine and PRPP. PRPP concentrations and hypoxanthine concentrations were varied simultaneously, with PRPP ranging from 25 to 500 μ M and hypoxanthine concentrations ranging from 5 to 100 μ M. Results were analyzed by the method of Hanes, and the kinetic parameters replotted on a secondary plot as described .

2.6. Magnesium inhibition: Magnesium dependent inhibition of HGXPRT-I was determined by measuring activities at saturating concentrations of PRPP and hypoxanthine with divalent magnesium concentrations ranging from 5 μ M to 1M. The results were plotted by the method of Hanes, and substrate inhibition was observed by deviations from linear kinetics.

2.7. Product inhibition by IMP or pyrophosphate: 100 μ M IMP or pyrophosphate were added to saturating assay cocktails as described above and activity assays were performed in the presence or absence of these products. Rates with product were compared to those determined in the absence of product.

3. Results

3.1. Inhibition studies with products or Mg^{2+} : Both products inosine monophosphate and pyrophosphate inhibited the forward reaction of the HGXPRT-I. Magnesium ions begin to inhibit the enzyme at 100 mM and exhibit “substrate” inhibition kinetics (Figure 1.).

3.2. Steady-state kinetic measurements in the forward direction: As seen in figure 2., steady-state kinetic values were determined for all of the three purine base substrates. K_m values of 66, 1.7, 1.0 and 18 μM were determined for PRPP, hypoxanthine, guanine, and xanthine respectively. v_{max} values of 6.2, 15, 15, and 54 $\mu\text{mol}/\text{min}/\text{mg}(\text{protein})$ were also determined for PRPP, hypoxanthine, guanine, and xanthine from the plots shown.

3.3. Steady-state kinetics In the reverse direction: Figure 3. indicates the behavior observed for the enzyme in the reverse direction. From this figure, K_m values of 9.2 μM and 24 μM could be determined for the binding of IMP and PP_i respectively. The maximum velocity for this reaction was 4.5 $\text{nmol}/\text{min}/\text{mg}(\text{HGXPRT-I})$, approximately 1,000 times less than that for the forward reaction.

3.4. Subsaturating kinetics: Extensive kinetic studies were performed with hypoxanthine and PRPP to determine exact K_m values using secondary plots for both hypoxanthine and PRPP. Plots of $[\text{Substrate}] / v_{\text{max}}^{\text{APP}}$ versus $[\text{Substrate}]$ were linear and revealed K_m values of 59 μM for PRPP and 1.63 μM for hypoxanthine, in close agreement with the values

determined from steady state kinetics with one substrate saturated as discussed above.

Replots of v versus $v / [\text{PRPP}]$

were linear with intersections in the first quadrant, consistent with an ordered mechanism in which PRPP binds first to the enzyme.

4. Discussion

The enzyme, HGXPRT-I, catalyzes the conversion of the three purine bases hypoxanthine, guanine, and xanthine to their nucleoside monophosphate forms. The K_m and v_{\max} values determined for this enzyme are comparable to those values determined for other HG(X)PRT enzymes [4]. Unlike mammalian cells, which have only an HGPRT function, the *T. gondii* enzyme recognizes xanthine as well, albeit with a K_m value which is more than 10 times higher than the other two purines. This may be reasonable as *T. gondii* is an intracellular parasite of mammals and utilizes the PRT enzymes to scavenge purine bases from the host [5]. There would be less competition for xanthine, as the host lacks XPRT activity, and thus, less evolutionary pressure to build an enzyme which recognizes xanthine in the low micromolar range. Alternatively, it may be difficult for an enzyme to recognize both guanine and xanthine with high efficiency as one has a hydrogen bond donor at the 2 position, and one is a hydrogen bond acceptor. The HPRT reaction is reversible, and hypoxanthine and PRPP can be formed by the action of the HGXPRT enzyme on IMP and PP_i . This reaction is less efficient than the forward reaction exemplifying the principle of an enzyme which “drags its heels” in the direction which is metabolically unfavorable to allow

for other, downstream, metabolic machinery to accept the product of the reaction before thermodynamic equilibria are reached. Inhibition studies and further kinetic studies on the HGXPRT-I are consistent with the reported compulsory-ordered bi-bi mechanism for HG(X)PRT enzymes [6]. However, although inhibition by pyrophosphate is accounted for in this model, a more simple explanation of the inhibition data observed here is that both IMP and PP_i can bind to the apo-enzyme and thus the product-release step may be random. The replot of the kinetic data with PRPP and other observations such as structural shifts in the presence of PRPP alone on HPLC, dynamic light scattering, and crystal set-ups [7], while no such behavior is observed with purine base alone, indicate that the substrate binding step is truly compulsory ordered with PRPP binding first followed by the purine base. The inhibition results obtained at numerous concentration of magnesium are more difficult to interpret. A simple explanation may be that magnesium is a cofactor which needs to bind to the enzyme for catalysis to occur, but as magnesium concentrations increase, the cation interferes with some part of the enzymatic mechanism. However, it has been reported that the species which binds to PRT enzymes is not magnesium, but the PRPP-magnesium complex [8], and that magnesium binding to the active site alone may inhibit the formation of product in the active site, as active sites of other HG(X)PRTs containing product do not have magnesium bound [9,10]. Thus, the inhibition data could be interpreted as binding of magnesium to PRPP in the low micromolar range, which allows for the formation of more and more true substrate, explaining the early rise in activity as Mg^{2+} increases. Next, at about 100 mM magnesium starts to bind to the active site in the absence of PRPP and competes with the binding of the Mg^{2+} -PRPP complex, or with the formation of the enzymes post-

catalytic state. Similar coordination of other divalents to the active site, such as zinc or nickel ions, which inhibit the enzyme [11], may be the reason these ions inhibit the PRT enzymes as they may bind to the enzyme at much lower concentrations than those required for their formation of the PRPP complex.

Figure 1: Magnesium dependent rates of the HGXPRT-I; Arrow indicates concentration at which substrate inhibition begins to occur. Dotted line indicates extrapolated kinetics in the absence of substrate inhibition.

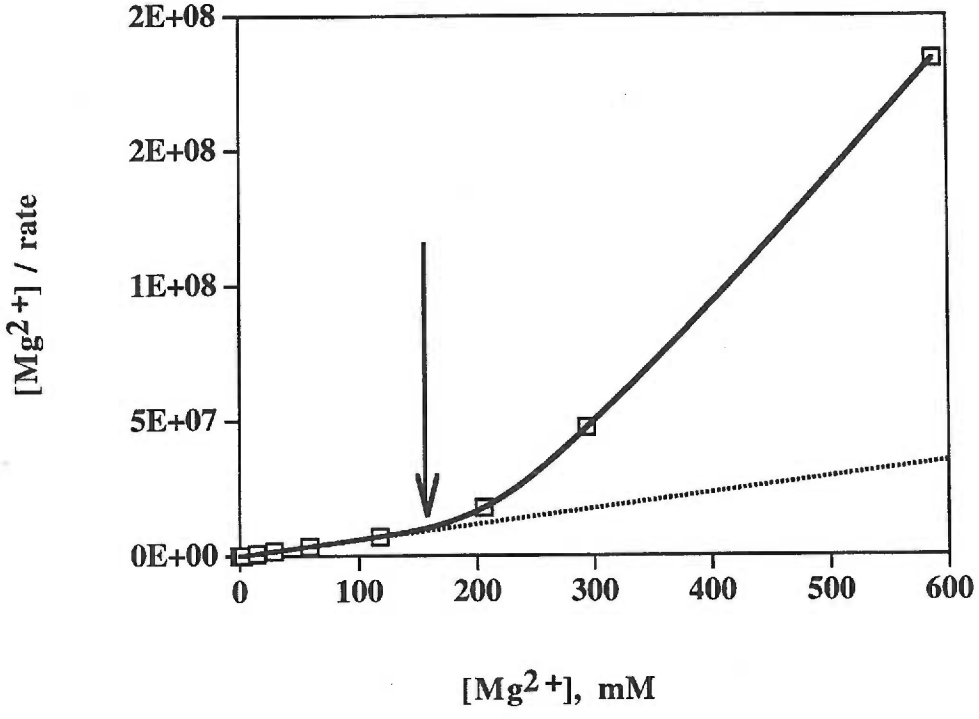


Figure 2: Steady state kinetics of the HGXPRT-I in the forward direction

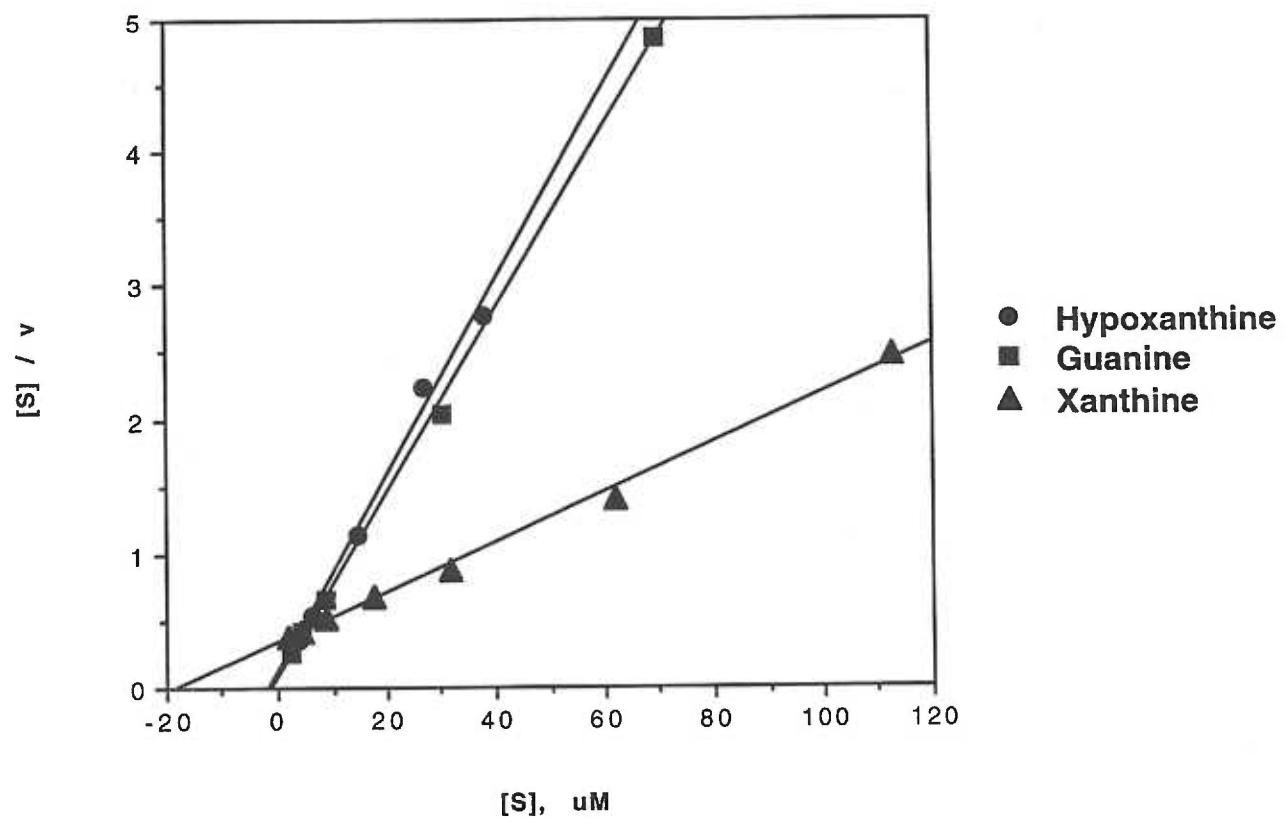


Figure 3: Steady state kinetic of the HGXPRT-I in the reverse direction

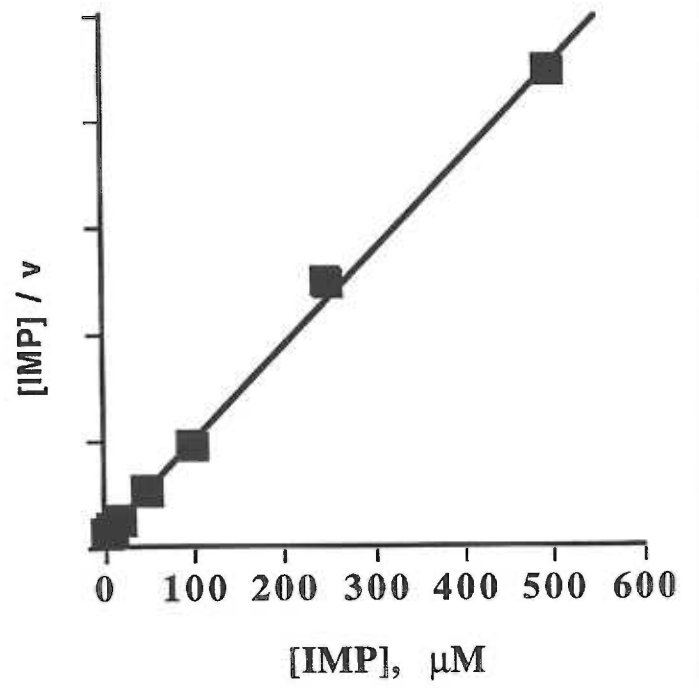
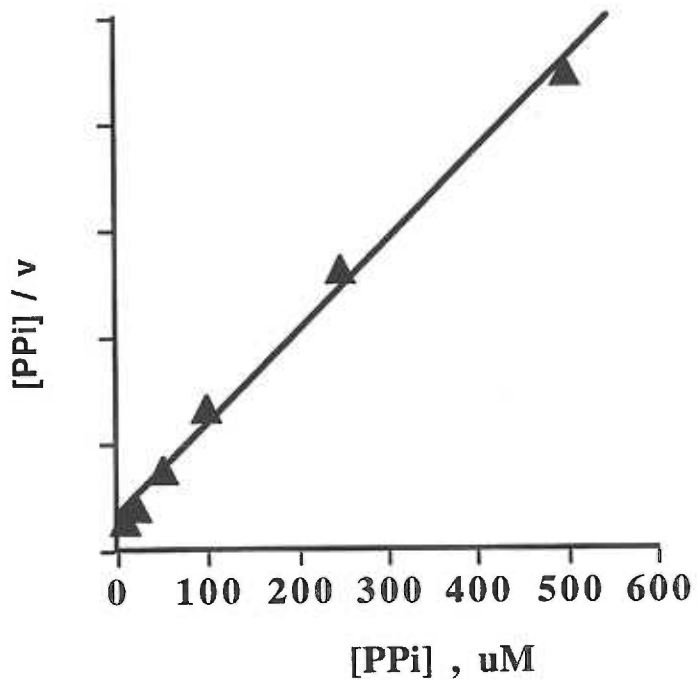
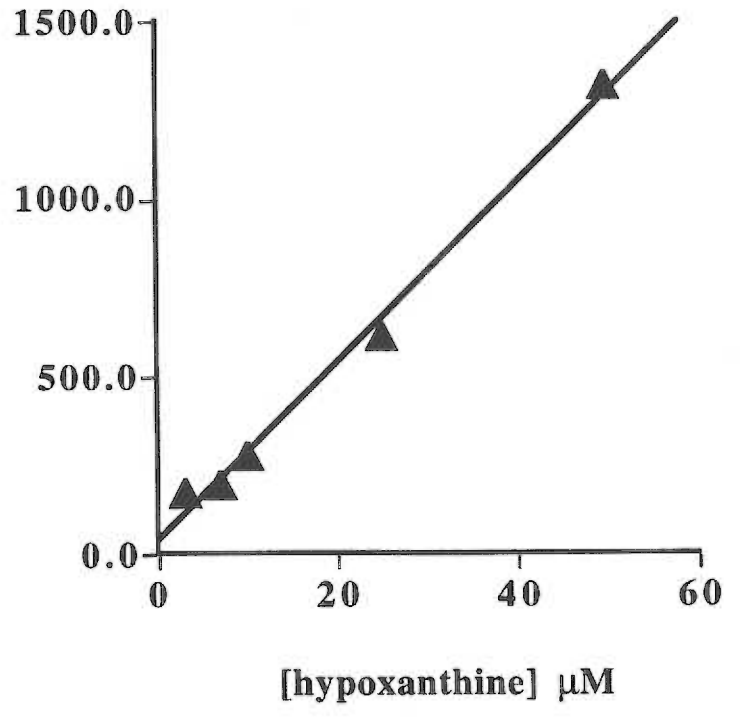
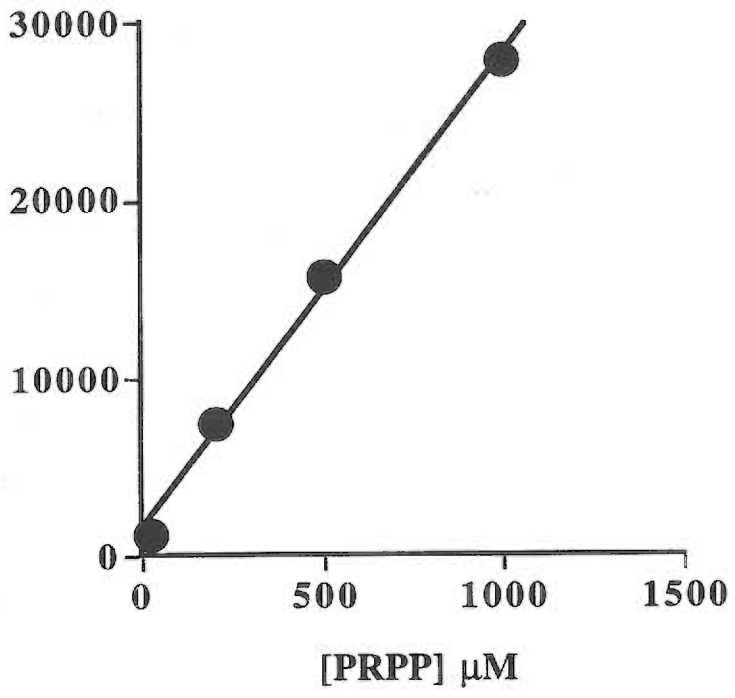


Figure 4: Secondary plot of hypoxanthine and PRPP kinetics. y-axis units are

$$[\text{Substrate}]/V_{\max}^{\text{APP}}$$



1. Cornish-Bowden A. (1995) *Fundamentals of Enzyme Kinetics*. London: Portland Press.
2. Jardim A, Ullman B. (1997) *J Biol Chem* **271**:30840-30846.
3. Tuttle JV, Krenitsky TA. (1980) *J Biol Chem* **255**:909-916.
4. Ullman, B. and Carter, D. (1995) *Infectious Agents and Disease* **4**:29-40.
5. Schwartzman, JD., and Pfefferkorn, ER (1982) *Experimental Parasitology* **53**:77-86.
6. Xu Y, Eads J, Sacchettini JC, Grubmeyer C (1997) *Biochemistry* **36**(12):3700-3712.
7. Schumacher, M., personal communication.
8. Yuan L, Craig SP 3d, McKerrow JH, Wang CC (1992) *Biochemistry* **31**(3):806-810.
9. Eads JC, Scapin G, Xu Y, Grubmeyer C, Sacchettini JC. (1994) *Cell* **78**:325-334.
10. Somoza JR, Chin MS, Focia PJ, Wang CC, Fletterick RJ. (1996) *Biochemistry* **35**:7032-7040.
11. See also chapter 2.1.

2.4. Mutagenesis Studies

2.4.1. Manuscript:

The Active Site Aromatic Residue Stabilizes Substrate Binding to the *Leishmania donovani*

Hypoxanthine-Guanine Phosphoribosyltransferase

by

Darrick Carter and Buddy Ullman §

Department of Biochemistry and Molecular Biology

Oregon Health Sciences University

Portland, OR 97201-3098

Telephone (503) 494-8437 - FAX (503) 494-8393

Internet: ullmanb@ohsu.edu

Abbreviations: GPRT, guanine phosphoribosyltransferase; HGPRT, hypoxanthine-guanine phosphoribosyltransferase; HGXPRT, hypoxanthine-guanine-xanthine phosphoribosyltransferase; LPIM, low phosphate induction medium; mLPIM, modified low phosphate induction medium; PRPP, 5-phosphoribosyl-1-pyrophosphate; PRT, phosphoribosyltransferase; PAGE, polyacryl-amide gel electrophoresis; TMD, 50 mM Tris, pH 7.5, 5 mM MgCl₂, and 2 mM dithiothreitol; XGPRT, xanthine-guanine phosphoribosyltransferase; XPRT, xanthine phosphoribosyltransferase.

§ To whom correspondence should be addressed

Abstract

A conserved aromatic amino acid in the active site of all hypoxanthine-guanine phosphoribosyltransferase (HGPRT) enzymes for which 3-dimensional structures have been crystallographically determined has been implicated in the binding of the purine substrate via π - π stacking interactions. The role of this residue in mediating substrate binding to the active site and in restricting the substrate specificity of this group of enzymes has now been evaluated genetically by the creation and biochemical characterization of site-directed mutants of the *Leishmania donovani* HGPRT. Mutant HGPRTs, F178Y, F178W, and F178L, were purified to homogeneity along with the wild type enzyme and displayed diminished enzyme efficiencies (k_{cat}/K_m) in both the forward and reverse directions with k_{cat}/K_m ratios proportional to the degree of structural conservation with $k_{\text{cat}}/K_m(\text{Phe}^{178}) > k_{\text{cat}}/K_m(\text{Tyr}^{178}) > k_{\text{cat}}/K_m(\text{Trp}^{178}) > k_{\text{cat}}/K_m(\text{Leu}^{178})$. The decrease in efficiencies of the mutant enzymes could be attributed primarily to increased K_m values, while k_{cat} values were largely unchanged. No alterations in substrate specificity were observed with any mutant, i.e., the enzymes did not phosphoribosylate xanthine or adenine. Only the wild type and F178Y HGPRTs could functionally complement a genetic lesion of S ϕ 609 *E. coli*, a purine auxotroph lacking the corresponding phosphoribosylating activities. These studies reveal the role of the conserved aromatic residue in binding of the purine ring to the active site and demonstrate that genetic alterations at this site do not alter substrate specificity of the enzyme.

Key words: Hypoxanthine-guanine phosphoribosyltransferase; Phosphoribosyltransferase; Purine salvage; *Leishmania donovani*; Enzyme kinetics; Enzyme structure.

1. Introduction

All protozoan parasites studied to date lack an intact purine biosynthetic pathway and are, therefore, auxotrophic for purines (1). Consequently, each parasite genus expresses a unique complement of purine salvage enzymes that enables it to scavenge purines from the host milieu. Central to the salvage of purines by most parasites are the phosphoribosyltransferase (PRT) enzymes that convert preformed purines bases to the nucleotide level. There are two basic classes of purine PRTs in parasites; one that recognizes adenine exclusively and one that recognizes purines containing a 6-exocyclic oxygen. The latter group consists of enzymes that exhibit distinct and occasionally overlapping substrate specificities. There exist hypoxanthine-guanine PRTs (HGPRT), hypoxanthine-guanine-xanthine PRTs (HGXPRT), xanthine PRTs (XPRT), and at least one guanine-specific PRT (GPRT). These PRT enzymes share a number of conserved motifs implicated in substrate recognition or in transition state stabilization (2-8). Crystal structures of the human HGPRT (4), *Tritrichomonas foetus* (5) and *Toxoplasma gondii* (6) HGXPRTs, and *E. coli* xanthine-guanine PRT (XGPRT) (7) have revealed the presence of a completely conserved aromatic residue within the catalytic binding pocket that presumably forms aromatic-aromatic interactions with the purine ring of both the substrate and product. This residue is a Phe in all PRT enzymes that recognize hypoxanthine and guanine exclusively but is a Tyr in the *T. foetus* HGXPRT and a Trp in the *T. gondii* HGXPRT, the *G. lamblia* GPRT, and the *E. coli* XGPRT enzymes. The Phe→Tyr and Phe→Trp changes in these PRTs might implicate a role of this residue in the unusual substrate specificities of these enzymes (9). To evaluate the role

of this conserved aromatic amino acid in governing PRT specificity and stabilizing substrate binding, the Phe¹⁷⁸ of the *L. donovani* HGPRT has been genetically altered by site-directed mutagenesis. Biochemical and functional analysis of the mutated proteins revealed that this residue is involved in stabilization of substrate binding to the active site of the enzyme but that none of the genetic modification created at this site amends the limited specificity of the *L. donovani* HGPRT for hypoxanthine and guanine.

2. Materials and Methods

2.1. Chemicals, materials, and reagents

[8-¹⁴C]hypoxanthine (56 mCi mmol⁻¹) was purchased from Moravек Biochemicals (Brea, CA). 5-phosphoribosyl-1-pyrophosphate (PRPP), hypoxanthine, guanine, xanthine, IMP, and GTP-agarose were obtained from Sigma Chemicals Co. (St. Louis, MO). DE-53 anion exchange matrix was from Whatman (Hillsboro, OR). All restriction and DNA modifying enzymes were acquired from either Bethesda Research Laboratories Life Technologies Inc. (Gaithersburg, MD) or Boehringer Mannheim Biochemicals (Indianapolis, IN). The pAlter-1 mutagenesis vector from Promega (Madison, WI) was used to generate site-directed mutants. All other chemicals, materials, and reagents were of the highest quality commercially available.

2.2 Molecular Modelling

Using the Homology module of the Biosym molecular modelling package InsightII 2.2.0, the *L. donovani* HGPRT primary sequence was aligned to the human HGPRT sequence and coordinates from semi-conserved regions were transferred directly to the *L. donovani* model from the human HGPRT crystal structure (4). Loops were modelled between semi-conserved regions by minimizing the rms deviations of distances from energetically favorable conformations of *L. donovani* model peptides to the human crystal structure. The completed model was energy minimized using the Discover package of InsightII, and alternative conformations were explored using dynamics simulations. The most favorable structure was chosen for final rounds of energy minimization and a Brookhaven pdb file was written out for the native model structure. The mutations described above were inserted using the molecular modelling package Sybyl by Tripos, and regions within 5 Å of the mutant residue were energy minimized.

2.3 Site-directed mutagenesis

The *EcoRI/XbaI* fragment from the *L. donovani* HGPRT-pBAce expression construct described by Allen *et al.* (10) was excised and subcloned into the corresponding sites within pAlter-1. This *EcoRI/XbaI* fragment contained the entire HGPRT protein coding region and the *phoA* promoter thus enabling expression of the mutated *hgprt* genes without further

subcloning. Site-directed mutagenesis was performed with 25 nucleotide mutagenic primers according to the brochure provided by Promega.

2.4. Complementation analysis

S Φ 609 (Δ *pro-gpt-lac*, *hpt*, *thi*, *pup*, *purHJ*) *E. coli*, a purine auxotroph that lacks the bacterial hypoxanthine and xanthine-guanine phosphoribosylating activities (11), was transformed with each of the expression constructs described above and grown overnight in LB broth containing 30 μ g ml⁻¹ streptomycin, 10 μ g ml⁻¹ tetracycline, and 100 μ g ml⁻¹ ampicillin. Cells were harvested by centrifugation, washed twice in low phosphate induction medium (LPIM), and then diluted 100-fold into a modified LPIM supplemented with 30 μ g ml⁻¹ streptomycin and 100 μ M adenine (mLPIM) to which either no additional purine, 100 μ M guanine, 100 μ M hypoxanthine, 100 μ M xanthine, or 100 μ M guanosine was added. The composition of LPIM has been reported (12,13). Growth was monitored by measurements of optical density at 600 nm as a function of time.

2.5 HGPRT Purification

Mutated *hgprt*-pAlter-1 constructs were expressed in S Φ 606 (Δ *pro-gpt-lac*, *thi*, *hpt*) *E. coli*, a bacterial line lacking the same PRT activities as the S Φ 606 cells (11). The wild type *HGPRT* enzyme was expressed in S Φ 606 cells in parallel from the previously described *HGPRT*-pBAce construct (10). Overnight cultures grown in mLPIM to which 100

μ M guanosine was added were harvested by centrifugation at 4000 X g, resuspended in 50 mM Tris, pH 7.5, 5 mM MgCl₂, and 2 mM dithiothreitol (TMD50) buffer, and lysed by French press at 16,000 psi. Crude lysates were centrifuged at 30,000 X g for 30 min at 4°C and the supernatant fractions from the wild type F178Y, F178W, and F178L transformants loaded onto GTP-agarose affinity columns equilibrated in TMD50 buffer. Unbound protein was removed by washing with 20 column volumes of TMD50 buffer, and bound HGPRT was eluted with TMD50 containing 5mM PRPP as described (10,13). The F178W mutant did not bind to the affinity column and was purified by a combination of DEAE-cellulose chromatography and ammonium sulfate precipitation. All purified protein preparations were dialyzed overnight against 3 X 4 l of TMD50 buffer and concentrated with a Centricon concentration unit (Amicon, Beverly, MA). All enzyme preparations were frozen and stored at -20°C without loss of activity. SDS-polyacrylamide gel electrophoresis (PAGE) was performed on 15% acrylamide slab gels as described (14).

2.6. *Fluorescence melting*

Proteins were diluted in 50 mM Tris, pH 7.5, 5 mM MgCl₂, and 0.1 mM DTT to a concentration of 80 μ g ml⁻¹. Fluorescence was monitored on a Phototechnology Inc. fluorometer. Cuvettes were equilibrated for 10 min at 20°C followed by a linear temperature gradient from 20°C to 80°C for 1 h. The time-dependent fluorescence curves were then normalized and superimposed.

2.7. Steady-state kinetic measurements of HGPRT for both the forward and reverse reactions

Initial rates for the forward reaction were determined in 1.0 ml of TMD buffer on a Beckman DU640 spectrophotometer at 37°C equipped with a kinetics software package. Hypoxanthine and guanine phosphoribosylation were measured by increases in absorbance at 234 nm and 255 nm, respectively. Reaction conditions were as described (8). Extinction coefficients of 2200 M⁻¹ cm⁻¹ and 4200 M⁻¹ cm⁻¹ were used for the formation of IMP and GMP respectively. K_m values for hypoxanthine and guanine were determined with 5 mM PRPP, and purine concentrations were varied from 2 to 100 μM. PRPP kinetics were evaluated with 50 μM hypoxanthine and PRPP-Mg concentrations ranging between 20 μM and 4.5 mM. As the high K_m of the F178L mutant for hypoxanthine hindered an accurate determination of the PRPP K_m with the spectrophotometric assay, the previously described radiometric assay was implemented with [¹⁴C]hypoxanthine (10,13). The reverse reaction in which hypoxanthine is generated from IMP and PP_i was monitored using the previously reported xanthine oxidase-coupled reaction assay (15). PP_i K_m values were determined by varying PP_i between 50 μM and 1 mM and maintaining the IMP concentration constant at 500 μM. The K_m value for IMP was determined at 1 mM PP_i and varying IMP concentrations from 20 μM to 500 μM. Kinetic data were plotted and analyzed by the method of Hanes (16).

3. Results

3.1. Molecular modelling of HGPRT proteins

Structures of HG(X)PRT proteins have revealed a conservative aromatic residue in the active site pocket, which appears to participate in π - π stacking interactions with the purine ring (4-7). This amino acid is Phe in most HGPRTs (Phe¹⁷⁸ in the *L. donovani* HGPRT) but is a Tyr in *T. foetus* HGXPRT and a Trp in *T. gondii* HGXPRT, *G. lamblia* GPRT, and *E. coli* XGPRT. To visualize the role of this residue in purine binding to the active site, a molecular model of the *L. donovani* HGPRT was computationally constructed using the atomic coordinates of the human HGPRT as a backbone. This model predicted that the Phe at position 178 was enveloped within the active site pocket of the protein, as is the equivalent residue in the human HGPRT structure (4). Molecular modeling of the mutant proteins predicted that the F178Y mutant was virtually identical in structure to the wild type protein, while the bulky side chains in the F178W and F178L HGPRTs were observed to extend into the active site of the enzyme. Major perturbations of the overall 3-dimensional structure of the *L. donovani* HGPRT were not envisioned from any of the three amino acid substitutions.

3.2. Functional complementation of *E. coli*

To ascertain experimentally the role of this active site aromatic residue in substrate binding, the F178Y, F178W, and F178L mutations were inserted into *HGPRT* by site-directed mutagenesis. These mutations were initially evaluated for their ability to

complement the *hpt* and *gpt* lesions in the S ϕ 609 *E. coli*. As S ϕ 609 cells are purine auxotrophs, they cannot survive in mLPIM in the absence of a 6-exocyclic purine source, i.e., either hypoxanthine, guanine, or xanthine (8,10,11). However, S ϕ 609 cells transformed with the wild type *HGPRT* are capable of growth in mLPIM supplemented with either hypoxanthine or guanine, but not with xanthine (Fig. 1). If mLPIM is not supplemented with a purine base containing a 6-exocyclic oxygen, the wild type *HGPRT* S ϕ 609 transformants cannot proliferate. It should be noted that the adenine supplement (see Materials and Methods) in the mLPIM cannot be used as a source of guanylate nucleotides by the *purHJ E. coli* (11). The F178Y transformant exhibited essentially the same growth phenotype as the wild type transformant, i.e., it grew in mLPIM augmented with hypoxanthine or guanine but not with xanthine (Fig. 1). Conversely, neither F178W nor F178L were capable of growth in mLPIM when hypoxanthine or guanine was a purine source (Fig. 1). All strains grew at equivalent rates in mLPIM supplemented with guanosine, a purine nucleoside whose conversion to the nucleotide level bypasses *HGPRT*. The differences in the abilities of various *HGPRT* constructs to complement S ϕ 609 cells could not be ascribed to differential *HGPRT* expression, as the amount of *HGPRT* protein produced after induction in mLPIM was roughly equivalent among all S ϕ 609 transformants (data not shown).

3.3 Protein purification

Wild type and mutant *HGPRT* genes were overexpressed in S ϕ 606 *E. coli*, and the

recombinant proteins were each purified to homogeneity. Wild type, F178Y, and F178L HGPRTs all bound to the GTP-agarose resin and could be virtually quantitatively eluted in TMD buffer containing 1 mM PRPP. The F178W mutant adhered poorly to the affinity matrix and was subsequently purified in an empirical fashion by ion exchange chromatography and salt precipitation. Yields for all HGPRT proteins were $> 50 \text{ mg l}^{-1}$ bacterial culture.

3.4. Kinetic analyses

The consequences of single site mutations at Phe¹⁷⁸ on substrate recognition and steady state kinetics of both the forward and reverse reactions were then evaluated. HGPRTs encompassing the F178Y, F178W, and F178L mutations all retained the capacity to recognize both hypoxanthine and guanine but did not acquire the ability to phosphoribosylate other naturally occurring purines, i.e., xanthine or adenine. Wild type HGPRT displayed K_m values for hypoxanthine and guanine of $4.8 \mu\text{M}$ and $6.1 \mu\text{M}$, respectively (Table I). These values coincide with K_m values previously reported for the native (17) and recombinant (10) *L. donovani* HGPRTs. The effect of an individual mutation on nucleobase affinities was proportional to the structural conservation at position 178 of the protein. The F178Y mutation hardly influenced the K_m value of the enzyme, the F178W mutant exhibited a 2-3 fold increase in the K_m value for both purine bases, while the F178L mutation conferred a 25-30 fold reduction in the affinity of the enzyme for both hypoxanthine and guanine (Table I). K_m values for PRPP were also determined. K_m values

for the F178Y, F178W, and F178L mutants were ~2-, ~7-, and ~3-fold greater, respectively, than that for the wild type enzyme. Under all assay conditions, k_{cat} values never varied for any of the 3 mutants more than 2-fold from that obtained with wild type HGPRT. The relative efficiencies of each enzyme for each substrate were obtained from the ratio of the k_{cat} to K_m values (Table I). Calculated catalytic efficiencies were k_{cat}/K_m (Phe¹⁷⁸) > k_{cat}/K_m (Tyr¹⁷⁸) > k_{cat}/K_m (Trp¹⁷⁸) > k_{cat}/K_m (Leu¹⁷⁸).

The kinetics of the reverse reaction, i.e., the formation of hypoxanthine and PRPP from IMP and pyrophosphate, were also assessed using the xanthine oxidase-coupled enzyme assay (15). The relative affinities of the mutants for nucleotide product paralleled those obtained in the forward reaction for the nucleobase. The F178Y and F178W mutants exhibited K_m values for IMP ~3- and ~4-fold greater than that obtained for wild type protein (Table II). K_m values for pyrophosphate were within 2-fold of the K_m determined for wild type HGPRT. Accurate K_m values for either product could not be calculated for the F178L protein, as the activity of the mutant enzyme at any IMP concentration was too low to evaluate accurately.

3.5. Fluorescence melting

Due to the bulky sidechains of the amino acids at position 178 in the wild type and mutant HGPRT proteins, the premise that the F178W and F178L mutations might affect the stability of the enzyme was evaluated by fluorescence measurements. The *L. donovani* enzyme is amenable to fluorescence measurements as it contains a single Trp residue at

position 34 of the protein (10). The wild type protein displayed a sharp decrease in Trp fluorescence at 65°C as a function of time, presumably due to precipitation of the enzyme as the protein unfolds and aggregates. The F178L mutant exhibited a reduced rate of fluorescence decay, indicating no clear transition from a folded to unfolded state. The F178W mutant presented a complex profile in which a peak of Trp fluorescence was observed, as the enzyme approached its transition temperature. This peak is associated with a decrease of quantum transfer of energy from the excited Trp¹⁷⁸ as it is released from the core of the protein (Fig. 2).

4. Discussion

The role of a conserved aromatic amino acid that is found among all H(G)(X)PRT proteins and that has been implicated in purine binding within the active site after crystallographic resolution of product-bound HG(X)PRT structures (4-6) has now been analyzed. These X-ray structures intimate that π - π interactions between the aromatic side chain of this residue and the purine base in the active site are critical for binding and positioning of the purine ring during catalysis. However, as these crystal structures only provide static representations of the enzyme bound to the product, the role of this residue in catalysis and purine binding could only be conjectured. Thus, site-directed mutants at this position were constructed in the *L. donovani* HGPRT and evaluated kinetically. Clearly, the aromatic-aromatic interactions between the side chain at position 178 and the purine

base in the active site are critical for substrate binding, as the F178L mutation dramatically diminished the capacity of the enzyme to recognize both hypoxanthine and guanine in the forward direction and IMP in the reverse direction and precluded functional complementation of the S ϕ 609 *E. coli*. The k_{cat} value of the F178L HGPRT, however, was equivalent to that of the wild type enzyme, indicating that Phe¹⁷⁸ is unlikely to play a major catalytic role in the PRT reaction. The relatively conservative changes introduced into the F178Y and F178W mutants, mutations that mimicked amino acids present at the equivalent site in other PRT enzymes (9), affected the affinities of the enzyme for nucleobase and IMP only slightly, 2-4 fold. Somewhat unexpected was the substantially increased K_m value of the F178W mutant. This can be ascribed to the increased size of the side chain which can only be accommodated inside the catalytic pocket, thereby interfering with binding of both the PRPP and purine substrate. This hindrance to substrate binding presumably accounts for the failure of the F178W HGPRT to complement the genetic lesions in S ϕ 609 *E. coli* and may also contribute to the failure of this mutant enzyme to bind to the GTP-agarose affinity matrix. Interestingly, the *T. gondii* HGXPRT that accommodates a Trp in this position also binds the nucleotide affinity resin poorly (18).

Introduction of the Trp residue at position 178 of the *L. donovani* HGPRT conveniently introduced a fluorescent probe into the purine binding region of the enzyme enabling studies on the domain structure of the enzyme. Melting of the F178W protein was biphasic consistent with the two domain structure of HG(X)PRT proteins determined crystallographically (4-7). These two domains consist of a core region encompassing the PRPP binding site and a hood region that contains Phe¹⁷⁸ counterparts in other HGPRTs.

As the hood region denatures, the fluorescence signal from Trp¹⁷⁸ increases when the indole side chain becomes solvent exposed. This liberation of Trp from the enveloped solvent-protected active site precedes complete unfolding of the protein, indicating that melting of the hood region precedes denaturation of the core.

Finally, it should be noted that none of the mutations introduced at Phe¹⁷⁸ influenced the substrate specificity of the enzyme. Among the naturally occurring purine bases, each of the mutants recognized only hypoxanthine and guanine. Xanthine and adenine, as for the wild type enzyme (10), were not substrates. Both xanthine and adenine are converted to the nucleotide level in *L. donovani* by genetically and biochemically distinguishable PRT enzymes (19). Thus, genetic alterations in the Phe¹⁷⁸ of the *L. donovani* HGPRT do not alter the substrate specificity of the enzyme and imply that the Tyr at this position in the *T. foetus* HGXPRT and the Trp in the *T. gondii* HGXPRT, the *G. lamblia* GPRT, and the *E. coli* XGPRT are not critical determinants in governing the unusual substrate specificities of these PRTs. Although untested genetically, the crystal structures of the human, *T. foetus*, *T. gondii*, and *E. coli* H(G)(X)PRTs suggest that it is the backbone geometry at Asp¹⁸⁵ that serves as the critical determinant in regulating specificity at the 2 position of the purine ring, while hydrogen bonds formed between the side chain of Lys¹⁵⁷, an invariant amino acid among all H(G)(X)PRTs, and the 6-exocyclic oxygen are the presumptive key factors enabling recognition of 6-oxypurine bases and precluding adenine binding from the active site. Thus, this conserved aromatic amino acid corresponding to Phe¹⁷⁸ in the *L. donovani* HGPRT does not govern which purines are recognized by the enzyme but clearly plays a major role in substrate binding to the active site.

Acknowledgements

This work was supported by Grant AI-23682 from the National Institute of Allergy and Infectious Disease. D.C. was supported in part by an N.L. Tartar Trust Fellowship from the Medical Research Foundation of Oregon. B.U. is a Burroughs Wellcome Fund Scholar in Molecular Parasitology, and this work was supported in part by a grant from the Burroughs Wellcome Fund.

References

- [1] Berens RL, Krug EC, Marr JJ. Purine and pyrimidine metabolism. In: Marr, JJ, Müller, M, editors. Biochemistry and molecular biology of parasites. London: Academic Press, 1995;89-117.
- [2] Argos P, Hanei M, Wilson JM, Kelley WN. A possible nucleotide-binding domain in the tertiary fold of phosphoribosyltransferases. *J Biol Chem* 1983;258:6450-6457.
- [3] Hershey HV, Taylor M. Nucleotide sequence and deduced amino acid sequence of *Escherichia coli* adenine phosphoribosyltransferase and comparison with other analogous enzymes. *Gene* 1986;43:287-293.
- [4] Eads JC, Scapin G, Xu Y, Grubmeyer C, Sacchettini JC. The crystal structure of human hypoxanthine-guanine phosphoribosyltransferase with bound GMP. *Cell* 1994;78:325-334.
- [5] Somoza JR, Chin MS, Focia PJ, Wang CC, Fletterick RJ. Crystal structure of the

- hypoxanthine-guanine-xanthine phosphoribosyltransferase from the protozoan parasite *Tritrichomonas foetus*. *Biochemistry* 1996;35:7032-7040.
- [6]. Schumacher MS, Carter D, Roos DS, Ullman B, Brennan RG. Crystal structures of the *Toxoplasma gondii* HGXPRTase reveal the catalytic role of a long flexible loop. *Nature Struct Biol* 1996;3:881-887.
- [7] Vos S, de Jersey J, Martin, JL Crystal structure of *Escherichia coli* xanthine phosphoribosyltransferase. *Biochemistry* 1997;36:4125-4134.
- [8] Jardim A, Ullman B. The conserved serine-tyrosine dipeptide in *Leishmania donovani* hypoxanthine-guanine phosphoribosyltransferase is essential for catalytic activity. *J Biol Chem* 1997;271:30840-30846.
- [9] Sommer JM, Ma H., Wang, CC. Cloning, expression and characterization of an unusual guanine phosphoribosyltransferase from *Giardia lamblia*. *Mol Biochem Parasitol* 1996;78:185-193.
- [10] Allen TE, Hwang H-Y, Jardim A, Olafson R, Ullman B. Cloning and expression of the hypoxanthine-guanine phosphoribosyltransferase from *Leishmania donovani*. *Mol Biochem Parasitol* 1995;73:133-145.
- [11] Jochimsen B, Nygaard P, Vestergaard T. Location on the chromosome of *Escherichia coli* of genes governing purine metabolism. *Mol Gen Genet* 1975;143:85-91.
- [12] Craig SP, Yuan L, Kuntz DA, McKerrow JH, Wang CC. High level expression in *E. coli* of soluble, enzymatically active schistosomal hypoxanthine/guanine phosphoribosyltransferase and trypanosomal ornithine decarboxylase. *Proc Natl Acad Sci USA*. 1991;88:2500-2504.

- [13] Allen TE, Ullman B. Cloning and expression of the hypoxanthine-guanine phosphoribosyltransferase gene from *Trypanosoma brucei*. Nucl Acids Res 1994;21:5431-5438.
- [14] Laemmli UK. Cleavage of structural proteins during the assembly of the head of bacteriophage T4. Nature 1970;227:680-685.
- [15] Giacomello A, Salerno, C. Human hypoxanthine-guanine phosphoribosyltransferase. Steady state kinetics of the forward and reverse reactions. J. Biol. Chem. 1978;253:6038-6044.
- [16] Cornish-Bowden A. Fundamentals of Enzyme Kinetics. London: Portland Press, 1995.
- [17]. Allen TE, Henschel EV, Coons T, Cross L, Conley J, Ullman B. Purification and characterization of the adenine phosphoribosyltransferase and hypoxanthine-guanine phosphoribosyltransferase activities from *Leishmania donovani*. Mol Biochem Parasitol 1989;33:273-281.
- [18] Donald RGK, Carter D, Ullman B, Roos DS. Insertional tagging, cloning and expression of the *Toxoplasma gondii* hypoxanthine-xanthine-guanine phosphoribosyltransferase gene: characterization of a new genetic marker for stable transformation. J Biol Chem 1996;271:14010-14019.
- [19] Tuttle JV, Krenitsky TA. Purine phosphoribosyltransferase from *Leishmania donovani*. J Biol Chem 1980;255:909-916.

Table I

Forward Reaction Kinetics *L. donovani* HGPRT mutants

	Wildtype		F178Y		F178W		F178L	
	K_m	V_{max}	K_m	V_{max}	K_m	V_{max}	K_m	V_{max}
Hypoxanthine	4.8	15.6	8.1	10.0	14.5	13.5	152.8	18.9
Guanine	6.1	13.5	7.4	14.7	15.9	27.0	166.7	15.2
PRPP-Mg	43.6	13.7	86.0	8.3	278.8	12.0	122.1	7.8

V_{max} are nmol/min/ μ g; K_m values are μ M

Table II

Reverse Reaction Kinetics *L. donovani* HGPRT mutants

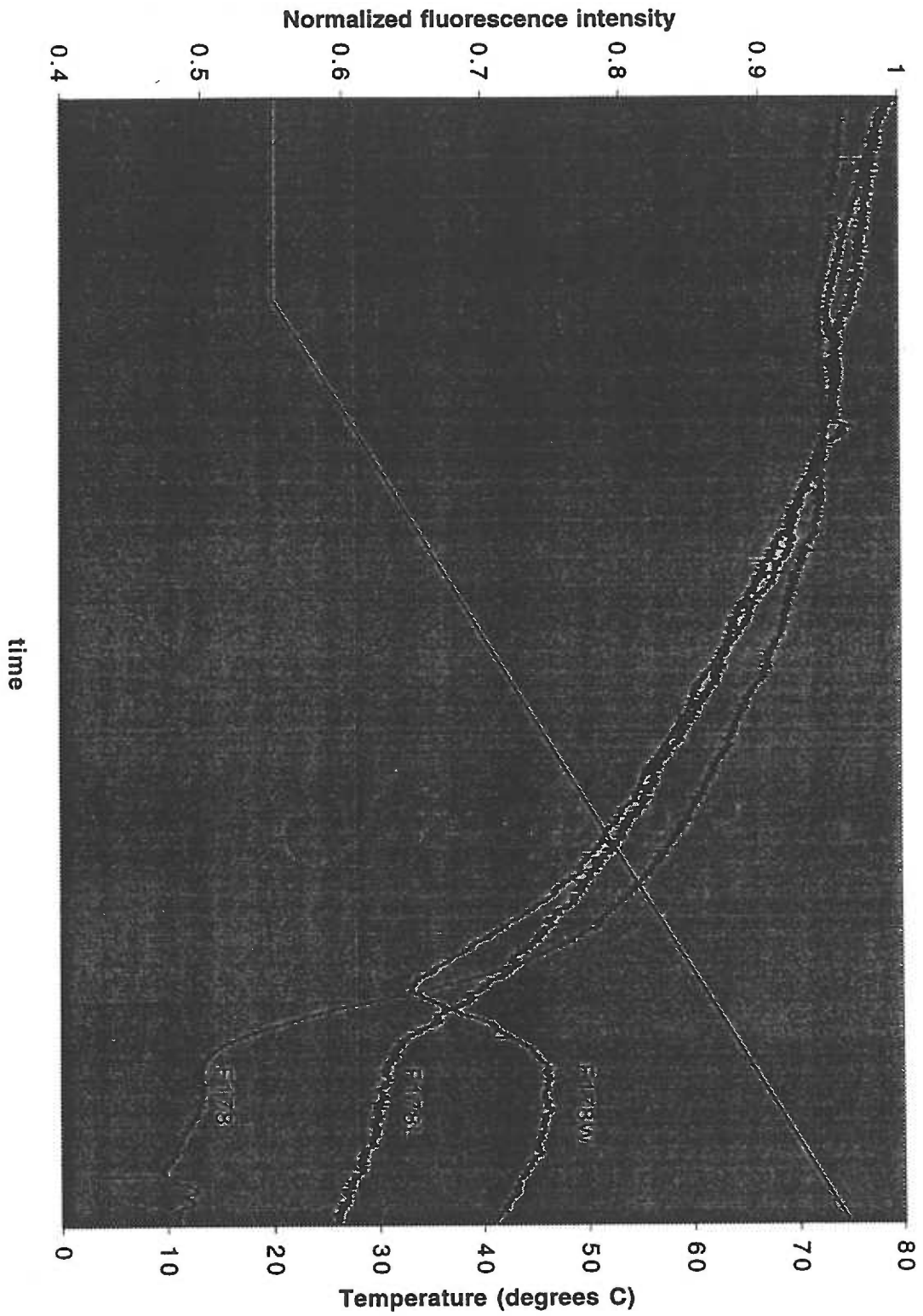
	Wildtype		F178Y		F178W		F178L	
	K_m	V_{max}	K_m	V_{max}	K_m	V_{max}	K_m	V_{max}
IMP	38.8	53	118	143	153	90.0	n.d.	n.d.
PPi-Mg	96.0	117	58.3	163	183	81.0	n.d.	n.d.

V_{max} are pmol/min/ μ g; K_m values are μ M

Fig. 1. Complementation analysis for wild type *HGPRT* and mutant *hgprt* constructs. S ϕ 609 *E. coli* transformed with either wild type *HGPRT* (\square) or with *HGPRT* constructs encoding the F178Y (Δ), F178W (\circ), or F178L (\diamond) mutations were inoculated into mLPIM containing either no 6-oxypurines, hypoxanthine, guanine, xanthine, or guanosine. All purines were present at a concentration of 125 μ M. Cells were incubated at 37 $^{\circ}$ C with vigorous shaking for 6-9 h, conditions under which exponential growth was continuously maintained. Culture densities were then measured spectrophotometrically at 600 nm at frequent intervals.

Fig. 2. Tryptophan fluorescence of wild type, F178W, and F178L HGPRTs.

Temperature Dependent Melting of F178 Mutants



2.4.2. Site-directed Mutagenesis at Asp206 Reveals the Role of the Conserved Aspartate in Purine Specificity of HG(X)PRT proteins

Darrick Carter, Erika Dahl, and Buddy Ullman

1. Introduction

The functional roles of many highly conserved residues in hypoxanthine-guanine-(xanthine) phosphoribosyltransferases (HG(X)PRTs) has been speculated about since the determination of X-ray crystal structures of these proteins in the presence and absence of the nucleoside monophosphate product [1,2,3]. These structures intimated the roles of a number of residues in purine recognition and catalysis, but could not explain the differences in specificity of some of these enzymes. HGXPRT enzymes have been cloned and characterized from numerous organisms [4] and have been reported to recognize hypoxanthine and guanine in most cases. However, a few of these enzymes can also convert xanthine, while some of these proteins only recognize either hypoxanthine, or guanine, or xanthine. These purines all have an oxygen bonded to the 6-position of the purine ring and differ from each other only by the substituent at the 2-position, which is hydrogen in hypoxanthine, an amine in guanine, and an oxygen in xanthine. Binding to the substituent at the two position of the purine ring in the HGXPRT enzymes appears to occur via hydrogen bonds from backbone atoms of a conserved aspartate residue in the purine binding site of these enzymes. As all of these

enzymes have an aspartate at this position, specificity must be governed by the local conformation of this residue. This local geometry may be shifted by either mutating and perturbing residues adjacent to this one, or as reported here, by mutating this conserved aspartate to various amino acids including asparagine, glutamate, and glycine.

2. Materials and Methods

2.1. Chemicals, materials and reagents: [¹⁴C] hypoxanthine was bought from Moravick Biochemicals (Brea, CA). All restriction and DNA modifying enzymes were acquired from either Bethesda Research Laboratories Life Technologies Inc. (Gaithersburg, MD) or Boehringer Mannheim Biochemicals (Indianapolis, IN). For mutagenesis, the pAlter-1 site-directed mutagenesis system from Promega (Madison, WI) was used. 5-phosphorylribose-1-pyrophosphate (PRPP), hypoxanthine, guanine, and xanthine, were from Sigma Chemicals Co. (St. Louis, MO). DE-53 anion exchange matrix was from Whatman (Hillsboro, OR). All other materials, chemicals, and reagents were of the highest purity commercially available.

2.2. Site-Directed Mutagenesis of the T. gondii hgxpri: The EcoRI/XbaI fragment of the *T. gondii hgxpri*-pBAce construct described by Donald *et al.* [5] was subcloned into the corresponding site of the pAlter-1 vector and site-directed mutagenesis was performed according to the protocol provided by Promega. This EcoRI/XbaI fragment contains the entire coding region of the *T. gondii* HGXPRT as well as the *phoA* promoter enabling

mutagenesis and expression to occur off of this single construct [6].

2.3. HGXPRT-I expression and purification: The pAlter-hgxprt-I constructs described above were transformed into the hgxprt deficient SΦ606 cell line [7] and cultures were induced in low phosphate induction medium and purified as described. An additional hydrophobic interaction chromatography step was included to achieve highly purified proteins which were then dialyzed against 50 mM Tris pH 7.5, 5 mM MgCl₂ and 2 mM Dithiothreitol (DTT) to remove residual ammonium sulfate.

2.4. Polyacrylamide gel electrophoresis. SDS-polyacrylamide gel electrophoresis was performed as described [8] on 15% acrylamide slab gels.

2.5. Complementation analysis of mutant constructs: SΦ609 cells were transformed with the expression constructs described above and grown overnight in LB broth with 30μg/ml streptomycin, 10μg/ml tetracyclin and 100 μg/ml ampicillin. Cells were harvested by centrifugation, washed two times in LPI medium and expression of the mutant proteins was induced by growing these cells for 1h in LPI medium with 200μM guanosine. The cultures were harvested by centrifugation and washed again two times in LPI medium. Cells were then diluted 100 fold in LPI medium supplemented with streptomycin (30 μg/ml) and either no additional purine, 100 μM guanine, 100 μM hypoxanthine, 100 μM xanthine, or 100 μM guanosine. Growth proceeded overnight at 37°C and was quantified

by measuring optical density at 600 nm.

2.6. Steady state kinetic measurements: For kinetic analysis, purified HGXPRT proteins were incubated in 1 ml assay cocktails at 37°C and the increase in absorbance at 255nm (guanine), 234nm (hypoxanthine) or 250nm (xanthine) was monitored using a Beckman DU640 spectrophotometer. Kinetic parameters for PRPP were determined by measuring rates at saturating concentration of purine base with PRPP-Mg concentrations ranging from 20 μ M to 20 mM. For the purine base kinetics, rates were measured at saturating PRPP concentrations and base concentrations were varied from 2 μ M to 200 μ M.

Extinction coefficients of 2200 $M^{-1}cm^{-1}$, 4200 $M^{-1}cm^{-1}$ and 3900 $M^{-1}cm^{-1}$ were used for the formation of IMP, GMP, and XMP respectively [9]. Kinetic data were plotted and analyzed by the method of Hanes [10].

3. Results

3.1. Mutagenesis and protein purification: Site-directed mutagenesis and expression was performed successfully to yield three mutant proteins, D206N, D206E, and D206G, and the native *T. gondii* HGXPRT-I. The proteins were successfully purified to apparent homogeneity by the biochemical means described (Figure 1) and used for further analysis.

3.2. Complementation studies: S Φ 609 cells are purine auxotrophs which are deficient in HG(X)PRT activity. Growth of these cells can be made conditional on having an expression

construct which allows for the expression of functional PRT enzymes. In the presence of guanosine these cells can grow without additional PRT activity. None of the mutated expression constructs could complement the genetic lesion in SΦ609 cells, while the native construct did so efficiently (Figure 2). All cells showed expression of the mutant proteins (Data not shown) indicating that the mutant proteins are not efficient enough to support growth *in vivo*, a finding which may explain the high degree of conservation found at this aspartate (Figure 3).

3.3. Kinetic studies on mutant HGXPRT proteins: As seen in Table 1, none of the mutant PRT proteins was as active as the wildtype protein, although some recognized their substrates with an equivalent or even lower K_m than the wildtype. The specificity profiles of these enzymes were altered. The D206G mutant did not catalyze any detectable reaction with xanthine, but appreciably recognized hypoxanthine and guanine, while the D206E mutant efficiently recognized xanthine, but did not accept hypoxanthine or guanine as well. Even a slight change from a carboxylate to an amide as found in the D206N mutant had a profound effect on the catalytic constants of this enzyme, elevating all of the K_m values and drastically reducing the v_{max} values. Interestingly, in the D206N and D206E mutants the apparent K_m value for PRPP was also increased.

4. Discussion

HG(X)PRT enzymes have a highly conserved aspartate in their purine binding region. Even highly conservative mutations of this aspartate abolish the proteins capacity to complement genetic PRT lesions in *E. coli* which may explain why this residue is invariable in this class of proteins. The inability of these mutant constructs to complement in *E. coli* is likely due to the drastic decrease in the maximal velocity these enzymes achieve. These proteins still recognize their substrates efficiently as seen in the reasonable K_m values determined for most of the mutant proteins. Thus decreased catalytic capability may be due to inefficient positioning of the bound purine base over its reaction partner, PRPP. Two of the three mutant proteins had dramatically increased K_m values for PRPP. It is interesting to note that in the crystal structure of the *T. gondii* HGXPRT the aspartate side chain points into the active site, toward the PRPP binding site, and that the two proteins with side chains were the ones which affected the PRPP K_m , while the glycine mutant, which lacks a side chain, did not. This may indicate that the length and electrochemical properties of this residue are chosen to select for both the local backbone geometry which governs purine base specificity and for non-interference with the PRPP binding region. The drastic variability seen in the K_m profiles of each one of these mutants supports the hypothesis that this region is governing specificity for the purine base at the 2 position. Notably, the proteins were engineered to either behave like an HGPRT (D206G) or like an XPRT (D206E) enzyme. It is noteworthy that an enzyme from the organism *Leishmania donovani* which has recently been cloned [11] and is also specific for xanthine has a glutamate at the equivalent position in D206E.

Figure 1: Representative purification of the expressed HGXPRT proteins. Lane A: Crude lysate of *E. coli* overexpressing HGXPRT-I. Lane B: DEAE-cellulose chromatography pool. Lane C: ammonium sulfate precipitated pool. Lane D: Hydrophobic interaction chromatography pool.

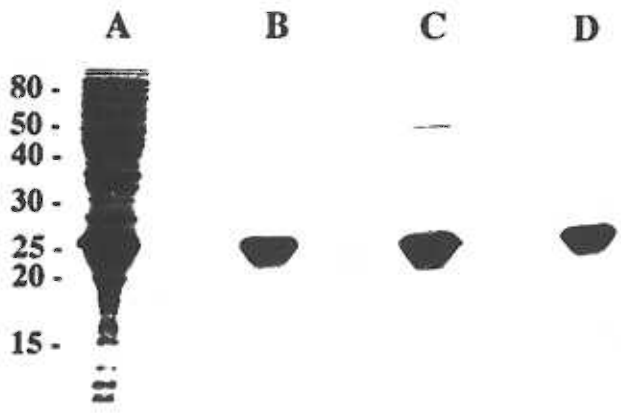


Figure 2: Complementation analysis of mutant constructs

Complementation of S ϕ 609 cells by HGXPRT mutant constructs

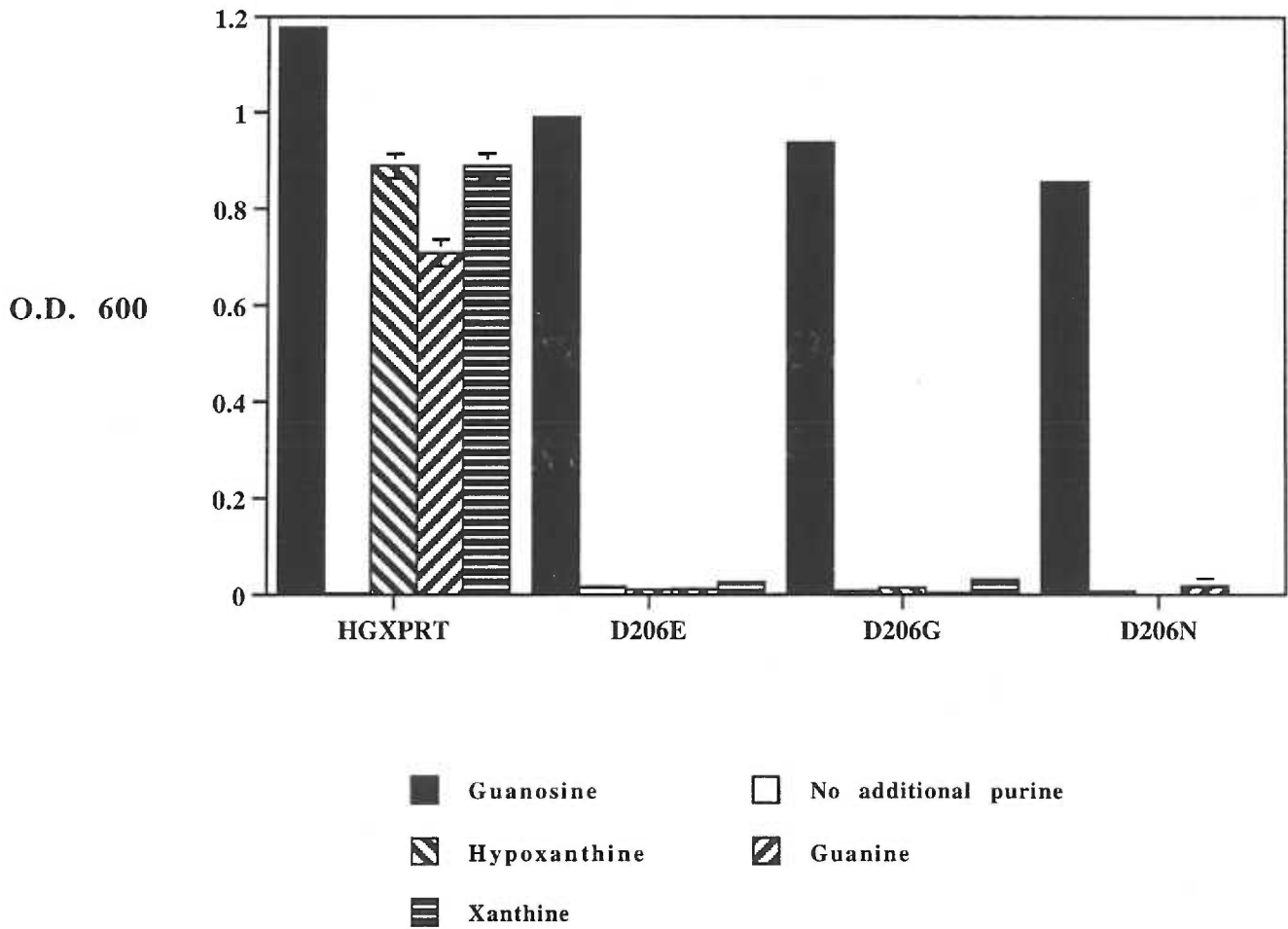


Figure 3: Alignment of the purine binding regions from various HG(X)PRT proteins and their specificities.

<i>L. donovani</i>	(HG)	173	...TIPHAFVIGYGMDYAESYRE...	193
<i>C. fasciculata</i>	(HG)	170	...TIPHAFVIGYGMDFAEAYRE...	190
<i>T. brucei</i>	(HG)	161	...DVPNVFVVG YGLDYDQSYRE...	181
<i>T. cruzi</i>	(HG)	159	...NIPNAFVIGYGLDYDDTYRE...	179
<i>S. mansoni</i>	(HG)	188	...EVPNRFVVG YALDYNDNFRD...	208
Human	(HG)	182	...EIPDKFVVG YALDYNEYFRD...	202
<i>P. falciparum</i>	(HGX)	192	...SIPDHFVVG YSLDYNEIFRD...	212
<i>T. gondii</i>	(HGX)	194	...SIEDVWIVGCCYDFNEMFRD...	214
<i>T. foetus</i>	(HGX)	151	...VVENRYIIGYGFDFHNKYRN...	171
<i>M. tuberculosis</i>	(HG)	170	...DIPKTFVVG YGLDYDERYRD...	190

Table 1: Kinetic parameters for D206 mutants

	PRPP		hypoxanthine		guanine		xanthine	
	K_m^1	V_{max}^2	K_m	V_{max}	K_m	V_{max}	K_m	V_{max}
wildtype	0.14 ± 0.01	23.4 ± 1.26	0.78 ± 0.3	19.2 ± 0.403	2.10 ± 1.3	21.2 ± 2.000	6.3 ± 1.2	29.8 ± 0.650
D206N	2.67 ± 0.67	0.16 ± 0.014	>> 131	≈ 0.29	42.4 ± 1.5	0.12 ± 0.008	57.0 ± 15.0	0.19 ± 0.022
D206E	7.54 ± 1.81	0.35 ± 0.027	15.9 ± 3.1	0.40 ± 0.021	17.4 ± 2.7	0.23 ± 0.013	3.1 ± 2.4	0.06 ± 0.003
D206G	0.28 ± 0.18	0.29 ± 0.069	34.8 ± 1.6	0.13 ± 0.003	20.6 ± 4.4	0.83 ± 0.036	>>200	<0.001

¹ K_m values are mM for PRPP and μ M for the purines

² V_{max} values are nmol/min/ μ g

³ determinations are averages from triplicate experiments

1. Schumacher MA, Carter D, Roos DS, Ullman B, and Brennan RG (1996) *Nature Structural Biology* **3**(10):881-887.
2. Eads JC, Scapin G, Xu Y, Grubmeyer C, Sacchettini JC. (1994) *Cell* **78**:325-334.
3. Somoza JR, Chin MS, Focia PJ, Wang CC, Fletterick RJ. (1996) *Biochemistry* **35**:7032-7040.
4. Ullman, B. and Carter, D. (1995) *Infectious Agents and Disease* **4**:29-40.
5. Donald RGK, Carter D, Ullman B, and Roos DS (1996) *J Biol Chem* **271**:14010-14019.
6. Jardim A, Ullman B. (1997) *J Biol Chem* **271**:30840-30846.
7. Jochimsen B, Nygaard P, Vestergaard T.
8. Laemmli UK. (1970) *Nature* **227**:680-685.
9. Tuttle JV, Krenitsky TA. (1980) *J Biol Chem* **255**:909-916.
10. Cornish-Bowden A. (1995) *Fundamentals of Enzyme Kinetics*. London: Portland Press.
11. Ullman B, personal communication.

3. Inhibitor Design Targeting the *T. gondii* HGXPRT-I enzyme

Darrick Carter and Buddy Ullman

1. Introduction

Enzymes in the purine salvage pathways of parasitic protozoans have long been touted as targets for the rational development of new antiparasitic drugs. A requisite for this type of targeted drug development is the development of new inhibitors which are either subversive substrates of an enzyme, or inhibit the enzyme directly. Many of the rationally developed subversive substrates are derivatives of an enzyme's natural substrates and are discovered by trial and error. These classes of compounds are usually activated by the protein's action on them and are not strictly enzyme inhibitors. Once converted, the active form of the compound usually inhibits downstream enzymes or interferes with other important metabolic functions to exert its therapeutic effect. An example of this form of compound which is activated by a hgprt enzyme is the drug allopurinol, a purine analog, which is used in veterinary medicine to treat Leishmaniasis. This chemical is converted by the enzyme's HGPRT to allopurinol riboside monophosphate, which is then metabolized to adenyly nucleotides and incorporated into RNA. A second method for the development of new classes of inhibitors requires knowledge of the enzyme's mechanism of action. Generally, mechanism-based inhibitors target the transition-state of an enzyme and thus bind tightly to the active site. This class of inhibitors usually is not converted by an enzyme and

show competitive inhibition kinetics. A new approach to rational inhibitor design, structure-based inhibitor design, is currently gaining more and more attention as this approach is beginning to show promise in the therapeutic field for the development of new therapeutic leads. This method can lead to the discovery of completely new chemical classes of inhibitors which bind tightly to the targeted enzyme and are completely unrelated to the substrate. An impediment to this type of inhibitor design is the requirement for a three-dimensional structure of the target. Advances in the fields of molecular modeling, X-ray crystallography and nuclear magnetic resonance spectroscopy have accelerated the resolution of target structures and will greatly facilitate structure based drug design.

2. Materials and Methods

2.1. HGXPRT-I expression and purification: The pBAce-hgxpirt-I construct was transformed into the hgxpirt deficient S Φ 606 cell line and cultures were induced in low phosphate induction medium and purified as described [1].

2.2. PRTase activity: Assay cocktails contained a [C-14] labeled purine base and 2mM 5-phosphorylribosepyrophosphate in TMD50 buffer. Reactions were initiated by addition of enzyme to the cocktail at 37°C and time points were taken by spotting aliquots on DE-81 paper (Whatman). Free purine base was then removed by washing twice with water and once with 70% ethanol. Filters were dried in a 80°C oven and bound radioactive isotopes quantified with a Beckman scintillation counter in the presence of aqueous fluor.

2.3. *Bacterial screen for inhibitors of HGXPRT: E. coli* SΦ606 cells [2] were transformed with the pBAce-HGXPRT I construct and grown overnight in LB broth. 1 μl of each of these saturated cultures was then added to 1 ml low phosphate induction medium in Linbro cell culture plates. Various purine analogs kindly provided by Dr. Rich Miller were then added to a final concentration of 1mM. The plates were incubated overnight at 37°C and growth was scored by visual inspection of the plates. The most potent analog was then retested in a dose-dependent manner for its effect on both SΦ606 and SΦ609 cells transformed with the pBAce-HGXPRT I construct and compared to the effect on SΦ606 cells carrying the vector, pBAce, alone.

2.4. *Mechanism-based Inhibitor:* The phosphorylribosepyrophosphate (PRPP) analog, carbocyclic-phosphorylribosepyrophosphate (cPRPP), which differs from PRPP by the substitution of the sugar ring oxygen by a carbon atom [3], was used as an alternative substrate in a radiolabeled assay as described above. Additionally, kinetic studies were performed in the presence and absence of 5 μM cPRPP and analyzed by the method of Hanes *et al.* [4]. The K_m^{app} values determined in these studies were used to calculate a K_i value for cPRPP:

$$K_i = \frac{|i|}{\left(\frac{K_m^{APP}(+cPRPP)}{K_m^{APP}(-cPRPP)} - 1 \right)}$$

2.4. Structure based inhibitor design: Using the program suite Dock 3.5 and the coordinates of the crystal structure of the *T. gondii* HGXPRT apoenzyme [5], a sphere model of the active site containing 50 spheres was generated and used to screen a structural database provided by the National Cancer Institute (NCI). Geometric scoring was used to rank the compounds in the database and the top 100 compounds were collected into a pdb-type coordinate file. 23 of these compounds were available through the NCI and used for preliminary screening. An initial screen was performed by an activity assay such as the one described above containing 50 μ M PRPP, 5 μ M [C-14] hypoxanthine, and 1mM of the experimental compound in dimethylsulfoxide (DMSO). Those compounds which inhibited the enzyme under these conditions were further characterized and K_i values determined towards PRPP.

3. Results

3.1. Bacterial screen for inhibitors: Of the 28 compounds tested for activity against bacteria expressing the *T. gondii* HGXPRT-I, 8 showed inhibition of growth (Figure 1). Of these, the two isothiocyanopurines, 6-isothiocyano-2-amino-purine and 6-isothiocyanopurine showed the strongest effect. 6-isothiocyano-2-amino-purine was chosen for further investigation and diminished growth of both bacterial strains at concentrations as low as 20 μ M, the lowest concentration tested. Cells which did not express the HGXPRT were not affected by this compound (Figure 2.).

3.2. Mechanism-based inhibition: As predicted, the HGXPRT could not utilize cPRPP as an alternative substrate to any detectable level. cPRPP did bind to the active site of the enzyme and showed competitive inhibition kinetics with a K_i of 970 nM (Figure 3.).

3.3. Structure-based inhibitor design: One hundred compounds were collected by the DOCK3.5 program for evaluation. Inspection of these compound indicated that they fit well into the active site geometrically, but may encounter electrochemical repulsions as could be expected for a DOCK run utilizing only geometric scoring. Despite of this drawback, 48% of the chemicals which were chosen by DOCK and available through the NCI showed greater than 50% inhibition of activity under the conditions employed. Two of these (9%) abolished all detectable HGXPRT activity in the primary screen (Figure 4.). These two compounds were reasonable inhibitors of the HGXPRT-I: 1,1,5,5-tetraphenyl-3-pentanone showed a K_i of 411 μ M, while 7,7' iminobis[4-hydroxy-2-naphthalenesulfonic acid] exhibited strong inhibition with a K_i of 18 μ M (Figure 5.).

4. Discussion

Three methods for the discovery of inhibitors were successfully employed to identify new compounds which interfere with catalysis by the *T. gondii* HGXPRT-I enzyme. Purine analogs were randomly tested as subversive substrates of the HGXPRT in a bacterial screen which provided 7 lead compounds. Of these, three were potent inhibitors of bacterial growth. Isothiocyanopurine and 8-azahypoxanthine have since been shown to inhibit *T. gondii* growth and 8-azahypoxanthine is now used as a convenient pH-stabile selectable

marker for HGXPRT expression in *Toxoplasma* [6]. The mechanism-based inhibitor, cPRPP, is not likely to be a useful anti-toxoplasmodic agent as it is highly charged and unlikely to cross the parasites membrane. However the high levels of inhibition by this compound and its resistance to hydrolysis by the enzyme will be useful in future X-ray crystallographic studies aimed at understanding the individual steps in HG(X)PRT catalysis as the PRT enzymes may be co-crystallized with this analog. Thus, it may be possible to determine crystal structures of the enzyme in its (c)PRPP bound form and in a transition-state like form in which both (c)PRPP and purine base are bound to the active site of the enzyme. The inability of the HGXPRT to utilize this compound as a substrate sheds light on the chemical mechanism of the protein and provides further evidence for the proposed oxycarbonium intermediate. The successful identification of new inhibitors by the structure-based program DOCK is a major step in the development of new rationally design drugs against *Toxoplasma* as inhibitors of both the HGXPRT and adenosine kinase should prove to be potent and specific therapeutic agents. These newly identified inhibitors are still weak, but co-crystallization with the HGXPRT and chemical modification to improve the identified modes of binding in an iterative process such as that utilized for the thymidylate synthase [7] should allow for the development of tightly binding, specific inhibitors. 7,7' iminobis[4-hydroxy-2-naphthalenesulfonic acid] is a promising lead and exhibits antitoxoplasmodic effects which may be in part mediated by inhibition of the HGXPRT [8]. Future studies will improve the potency of the purine analogs, allow insights in PRT catalysis and possibly open an avenue for the development of new therapeutic regimens.

Figure 1: Efficacy of purine analogs in the recombinant bacterial screen

Purine Analog	Inhibition of Growth
Mercaptopurine	-
6-thioguanine	-
8-azaguanine	+
8-azaxanthine	-
8-aza-hypoxanthine	+++
2-thioxanthine	-
Allopurinol	-
6-SCH ₃ -guanine	-
6-cyano-purine	-
7-deaza-8-aza-guanine	-
Imuran	+
8-methyl-purine	-
2-aminoethyl-purine	-
8-phenyl-guanine	-
6-isothiocyano-purine	+++
8-mercapto-guanine	-
6-CONH ₂ -purine	-
6-CSNH ₂ -guanine	-
6-SOCH ₃ -purine	-
9-deaza-8-aza-purine	-
6-isothiocyano-guanine	+++
6-iodo-guanine	+
6-O-phenyl-purine	-
8-methyl-guanine	-
6-carboxyl-purine	-
8-Thio-purine	-
6-iodopurine	-
6-CHNO-purine	+

Figure 2: Inhibition of bacterial growth by different concentrations of 2-amino-6-isothiocyanopurine

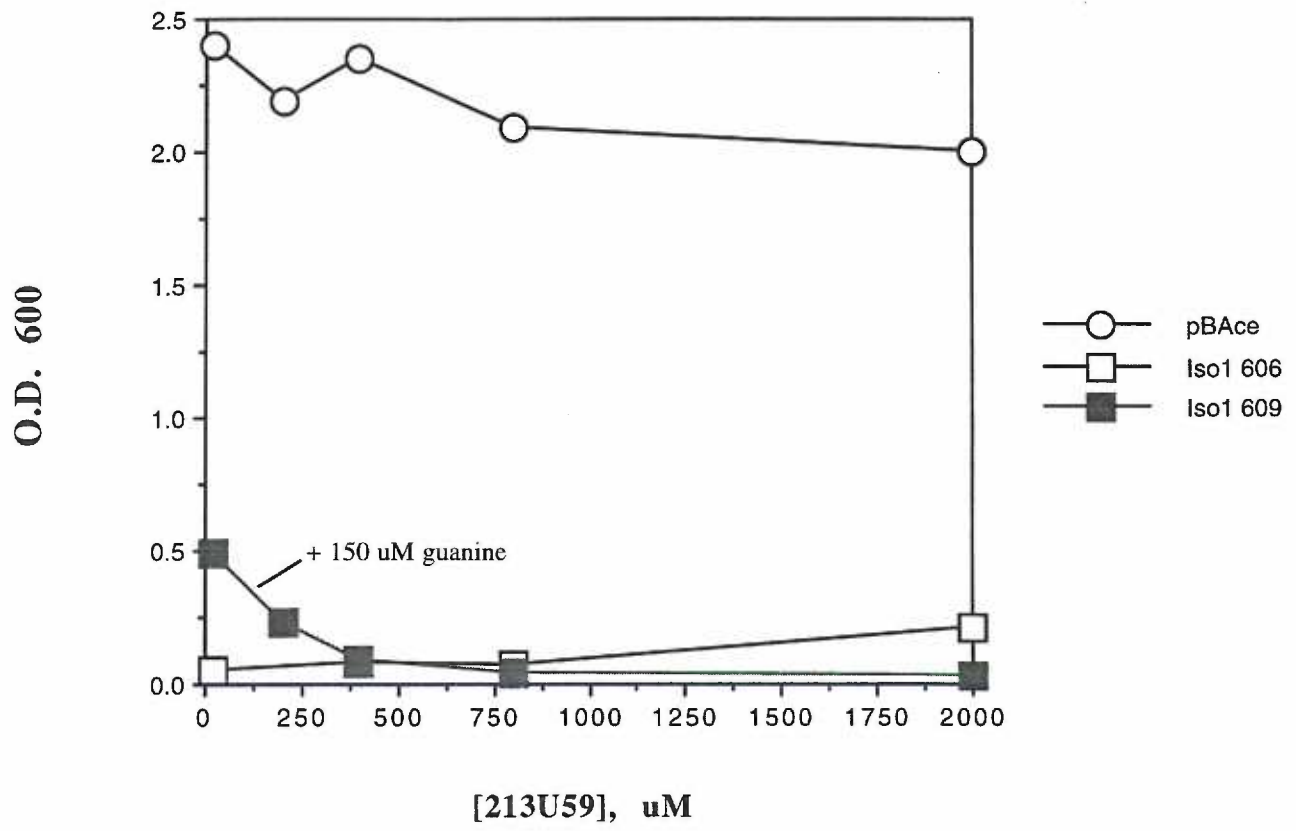
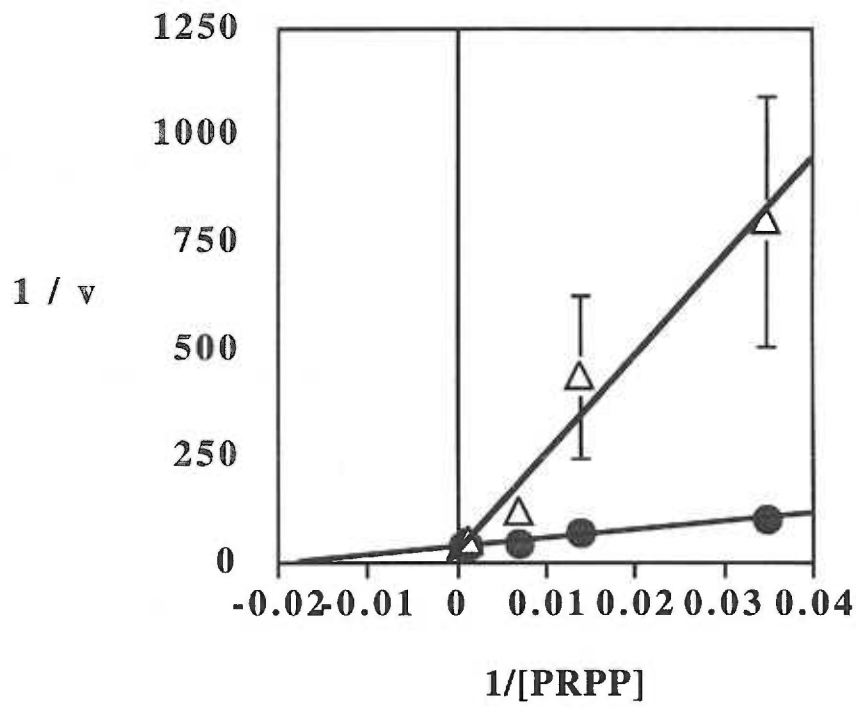


Figure 3: Inhibition kinetics of cPRPP. triangles: 5 μ M cPRPP added to reactions. solid circles: Uninhibited HGXPRT.



HGXPRT
Activity (%)

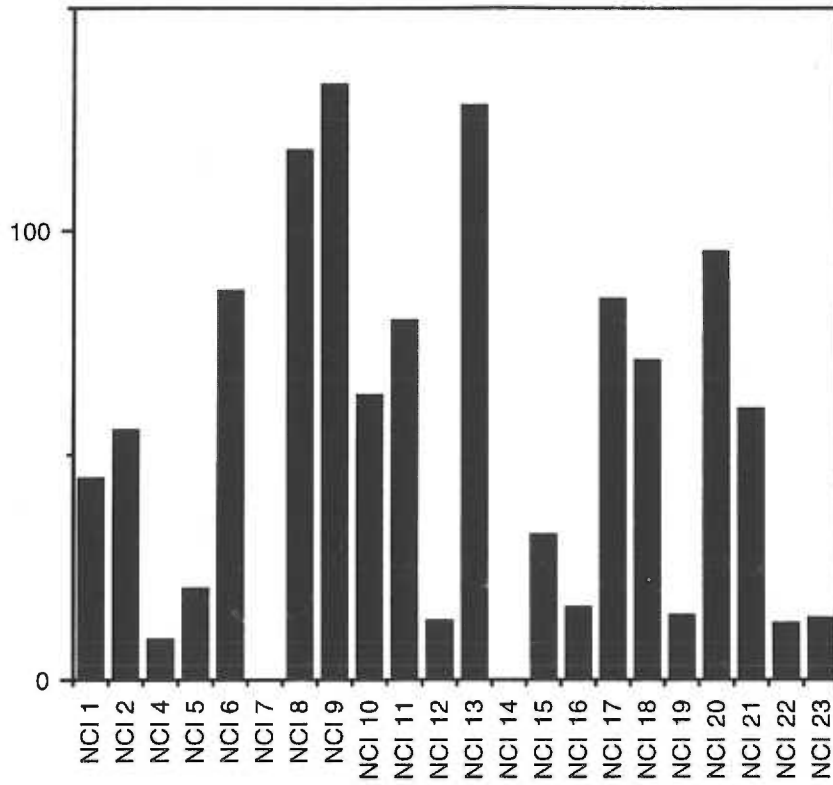
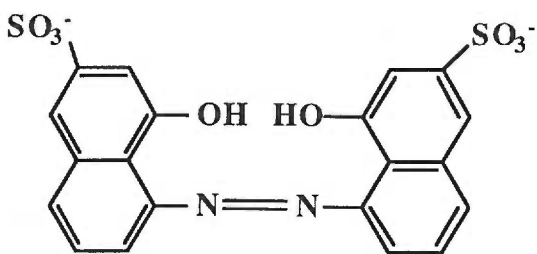


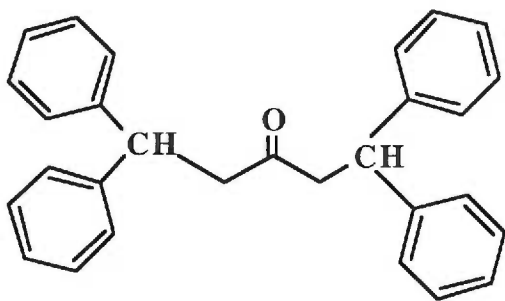
Figure 5: Strong inhibitors identified by DOCK 3.5 and their K_i values



7,7' iminobis[4-hydroxy-2-naphthalenesulfonic acid]

$K_i = 18 \mu\text{M}$

M.W. 461
Sum: C₂₀H₁₅NO₈S₂
DOCK score: #26
NCI: 14
CAS: 87-03-6



1,1,5,5-tetraphenyl-3-pentanone

$K_i = 411 \mu\text{M}$

M.W. 391
Sum: C₂₉H₂₆O
DOCK score: #31
NCI: 7
CAS: 87351-03-9

1. Donald RGK, Carter D, Ullman B, and Roos DS (1996) *J Biol Chem* **271**:14010-14019.
2. Jochimsen B, Nygaard P, Vestergaard T. (1975) *Mol Gen Genet* **143**:85-91.
3. Parry R, personal communication.
4. Cornish-Bowden A. (1995) *Fundamentals of Enzyme Kinetics*. London: Portland Press.
5. Schumacher MA, Carter D, Roos DS, Ullman B, and Brennan RG (1996) *Nature Structural Biology* **3(10)**:881-887.
6. Roos DS, personal communication.
7. Shoichet, B.K., Stroud, R.M., Santi, D.V., Kuntz, I.D., and Perry, K.M. (1993) *Science* **259**:1445-1450.
8. Bohne W, personal communication.

Abstract

The coding region derived from a full-length cDNA spanning the uracil phosphoribosyltransferase (UPRT) gene of *Toxoplasma gondii* has been ligated into a bacterial expression vector and overexpressed in *E. coli*. Recombinant UPRT protein migrated with a molecular mass of 27 kD on SDS polyacrylamide gels and was purified to homogeneity by conventional protein purification techniques. In solution, UPRT behaved as a monomer and exhibited K_m^{app} values of 3.5 μM for uracil and 243 μM for phosphoribosylpyrophosphate, respectively. Other naturally occurring pyrimidine or purine bases were not recognized as substrates. [^{14}C]Uracil phosphoribosylation was inhibited by 5-fluorouracil with a K_i value of 25 μM and was not activated by GTP. Ample quantities of recombinant enzyme are now available for biochemical and structural studies, facilitating evaluation of UPRT as a possible therapeutic target.

Keywords: Uracil phosphoribosyltransferase; Phosphoribosyltransferase; *Toxoplasma gondii*; Pyrimidine metabolism; Protein purification; Enzyme kinetics

1. Introduction

The obligate intracellular protozoan parasite *Toxoplasma gondii* is a prominent cause of neurological birth defects and a common opportunistic infection associated with AIDS. Current therapies for treatment and prophylaxis are far from ideal due to the complications of treating congenital infection and the high incidence of toxic and/or allergic reactions during chronic treatment of immunodeficient patients [1-3]. The purine and pyrimidine salvage pathways offer a multiplicity of potential targets for therapeutic manipulation through the incorporation of cytotoxic analogs into cellular nucleotide pools. This paradigm has been widely and successfully employed in antineoplastic, antiviral, antiparasitic, and immunosuppressive chemotherapies [4]. In particular, cytotoxic analogs of naturally-occurring purines and pyrimidines are recognized by members of the nucleobase phosphoribosyltransferase family, which catalyze the phosphoribosylation of pyrimidine and purine bases to the nucleotide level, and these enzymes are, therefore, touted as rational targets [4-6]. For instance, structure-function studies have indicated that the *T. gondii* uracil phosphoribosyltransferase (UPRT) and hypoxanthine-guanine-xanthine phosphoribosyltransferase (HGXPRT) activities recognize a variety of pyrimidine [7] and purine [8] nucleobase analogs, respectively. These investigations were, however, conducted only with crude parasite extracts.

Metabolic studies have demonstrated that *T. gondii* can incorporate uracil into pyrimidine nucleotides using the UPRT enzyme [9,10]. As *Toxoplasma* can synthesize pyrimidines *de novo* [11], UPRT is not essential for the parasite, and mutants deficient in

UPRT activity have been isolated by both chemical mutagenesis and molecular genetic strategies [12,13]. The ability of the *T. gondii* UPRT enzyme to recognize a wide variety of pyrimidines, including cytotoxic analogs [7,12,13], coupled with the lack of a human UPRT counterpart [14], suggests that this enzyme may be a candidate for rational drug design. Due to the minute quantities of UPRT expressed in *T. gondii* parasites, however, the native enzyme has not been purified for detailed biochemical and structural characterization. This barrier has recently been surmounted by molecular means. The *T. gondii* UPRT locus has been identified using insertional tagging and plasmid rescue, and full-length cDNAs are now available [13]. We now report the overexpression of UPRT coding sequence in *E. coli* and the purification of recombinant UPRT protein to homogeneity for biochemical and kinetic studies.

2. Materials and Methods

2.1. Chemicals, materials and reagents.

[6-¹⁴C]uracil (56 mCi mmol⁻¹) was purchased from Moravек Biochemicals (Brea, CA), while 5-fluoro[6-¹⁴C]uracil (55 mCi mmol⁻¹) was bought from Amersham International plc (United Kingdom). All restriction and DNA modifying enzymes were acquired from either Bethesda Research Laboratories Life Technologies Inc. (Gaithersburg, MD) or Boehringer Mannheim Biochemicals (Indianapolis, IN). Site-directed mutagenesis was performed with the pAlter-1 site-directed mutagenesis system from Promega (Madison, WI). 5-phosphorylribose-1-pyrophosphate (PRPP) and Sephadex G-150-120 matrix were obtained from the Sigma Chemical Co. (St. Louis, MO), and DE-53 anion exchange matrix was from Whatman (Hillsboro, OR). All other materials, chemicals, and reagents were of the highest purity commercially available.

2.2. Expression of *T. gondii* UPRT in *E. coli*.

The isolation and characterization of the *T. gondii* UPRT cDNA and gene have been described previously [7]. The cDNA was ligated into the *Xba*I site of the pAlter-1 vector, and an *Nde*I site was created at the ATG initiation codon by site directed mutagenesis using the mutagenic primer 5'-CACAGGGCTTCTCATATGGCGCAGGTC-3' (restriction site

underlined). The coding region of the *UPRT* cDNA was subcloned into the *NdeI/XbaI* sites of bacterial expression vector pBAce [15] and transformed into *E. coli* JM109. *UPRT* expression was induced at 37°C for 16 h in a low phosphate induction medium as previously reported [16].

2.3. *UPRT* purification

1-2 liter cultures of *E. coli* transformed with the pBAce-*UPRT* construct were harvested by centrifugation at 4000 x g and resuspended in TMD buffer: 50 mM Tris, pH 7.5/ 5 mM MgCl₂/ 2 mM dithiothreitol. Cells were lysed in a French press at 16,000 psi. The crude lysate was centrifuged at 30,000 x g for 30 min at 4°C and the supernatant fraction loaded onto a DE53 anion exchange column equilibrated in TMD50 buffer. Protein in the void volume was collected, and solid ammonium sulfate was added to 35% saturation. Protein which precipitated after 15 min at 4°C was removed by centrifugation at 30,000 x g for 20 min and discarded. The supernatant was brought to 50% saturation with solid ammonium sulfate, and precipitation was allowed to proceed overnight. Protein was pelleted by centrifugation at 30,000 x g for 20 min at 4°C and the pellet redissolved in TMD50 buffer containing 10% glycerol. Resolubilized protein was chromatographed on a Sephadex G-150-120 column equilibrated in TMD50 buffer, and fractions containing *UPRT* activity were combined. SDS polyacrylamide gel electrophoresis was performed on 15 % slab gels according to the method of Laemmli [17].

2.4. UPRT assay

Both spectrophotometric and radiometric assays for measuring UPRT activity were employed. The spectrophotometric assay was a modification of that described by Natalini *et al.* [18] and was used to monitor protein purification and for the enzyme denaturation studies. The assay mixture consisted of TMD50 buffer, 125 μM uracil, and 1.0 mM PRPP, and the reaction was initiated by enzyme addition. Assays were performed at 37°C on a DU640 spectrophotometer with a kinetics/time module by monitoring increases in absorbance at 252 nm. All other studies with the enzyme were conducted at 37°C in TMD50 buffer containing various concentrations of [6- ^{14}C]uracil and PRPP as indicated. Radiometric measurements were terminated by spotting onto Whatman DE81 filter paper, and the filters were washed 3 times with H_2O followed by a single wash with 95% ethanol. Filters were dried at 60°C and bound radiolabel quantitated by liquid scintillation spectrometry.

The K_m^{app} value of UPRT for PRPP was determined at 100 μM [6- ^{14}C]uracil (56 mCi mmol^{-1}) and PRPP concentrations ranging from 80 μM to 8.0 mM. The K_m^{app} value for uracil was ascertained at 5.0 mM PRPP and concentrations of [6- ^{14}C]uracil varying from 0.25 μM to 42 μM . Kinetic parameters were determined by Hanes analysis [19]. The substrate specificity of UPRT for nucleobases was evaluated at 100 μM [^{14}C]-uracil and 5mM PRPP in the presence of 1.0 mM concentrations of nonradiolabeled nucleobase. A K_i value for 5-fluorouracil (FUra) was calculated from inhibition data using 200 μM FUra, 5 mM PRPP, and 8-200 μM [^{14}C]-uracil according to the following formula [19], where [i] is the inhibitor concentration and K_m^{uracil} and K_m^{App} are the apparent K_m values determined for uracil in the

absence and presence of FUra.

$$K_i = \frac{|i|}{\left(\frac{K_m^{App}}{K_m^{uracil}} - 1 \right)}$$

In addition, conversion of FUra to the nucleotide level was determined directly using [6-¹⁴C]FUra (55 mCi mmol⁻¹) in place of [6-¹⁴C]uracil (56 mCi mmol⁻¹) as described above. To determine the cation specificity of UPRT, purified protein was dialyzed overnight against 4 liters of 50 mM Tris, pH 7.5 containing 2 mM dithiothreitol. Enzyme activity was then measured in the absence and presence of 5 mM divalent cation.

2.5. Size exclusion chromatography

The molecular size and subunit composition of UPRT was determined by high performance liquid chromatography using a Protein Pak 125 gel permeation column. The column was equilibrated in TMD50 buffer containing 100 mM NaCl and 0.05% sodium azide. 100 µg pure UPRT was then chromatographed over the column at a flow rate of 0.5 ml min⁻¹. 100 µg carbonic anhydrase (M_r = 29 kd) or bovine serum albumin (M_r = 67 kd) were used as molecular weight standards.

3. Results

3.1. *UPRT* expression and enzyme purification

High level expression of *T. gondii* UPRT was observed in *E. coli* following induction of the pBAce-*UPRT* vector in low phosphate medium (Fig. 1, lane A). The recombinant UPRT appeared as a band migrating at ~27 kd on SDS polyacrylamide gels. Sequential purification steps involving an anion exchange resin, ammonium sulphate precipitation, and gel sieving, resulted in purification of the *T. gondii* UPRT to virtual homogeneity as judged by the SDS gel electrophoretogram (Fig. 1, lane D). The overall yield was 43% (Table 1). The protein band was excised from the gel and subjected to five rounds of NH₂-terminal sequencing, yielding the sequence Ala-Gln-Val-Pro-Ala. This pentapeptide corresponds to amino acids 2-6 predicted from translation of the *UPRT* cDNA [13], indicating that the initiation Met had been cleaved.

3.2. Biochemical characterization of *T. gondii* UPRT

Size exclusion chromatography revealed that the recombinant UPRT behaved as a monomer in solution (Fig. 2). The retention time of the protein was slightly longer than that of the 29 kD carbonic anhydrase standard, consistent with a molecular mass of ~24 kD. This experimental value is compatible with the predicted size of 27.6 kD for the UPRT protein coding region [13]. Purified UPRT enzyme was stable for >1 week in TMD50 buffer

at 4°C. The protein rapidly precipitated from the solution in the absence of thiol reducing agents, however, presumably due to oxidation and crosslinking of the six Cys residues in the protein. Thermal inactivation curves revealed that UPRT begins to unfold irreversibly at 50°C and is completely inactivated by heating for 5 min at 65°C (Fig. 3). The *T. gondii* UPRT exhibited an absolute requirement for metal cofactors (not shown), but as reported for other phosphoribosyltransferase enzymes [20,21], UPRT can utilize a variety of divalent cations, including Mn^{2+} and Co^{2+} in place of Mg^{2+} (Fig. 4). Neither Ca^{2+} nor Ba^{2+} could fulfill the divalent cation requirement. As UPRT enzymes from a number of prokaryotes can be activated by GTP [22-24], the effects of the nucleotide on the *T. gondii* UPRT were tested. *T. gondii* UPRT activity was not, however, affected by the addition of 1 mM GTP. In three separate determinations, UPRT activity in the absence of GTP was $2.03 \pm 0.66 \mu\text{mol min}^{-1} (\text{mg protein})^{-1}$, whereas UPRT activity in the presence of 1.0 mM GTP was $1.53 \pm 0.55 \mu\text{mol min}^{-1} (\text{mg protein})^{-1}$.

3.3. Kinetic studies with *T. gondii* UPRT

Steady-state kinetic analysis (Fig. 5) indicated that *T. gondii* UPRT exhibited a high affinity for uracil ($K_m^{\text{app}} = 3.5 \mu\text{M}$), and a lower affinity for PRPP ($K_m^{\text{app}} = 243 \mu\text{M}$). A V_{max} value of $0.45 \pm 0.13 \mu\text{mol min}^{-1} (\text{mg protein})^{-1}$ was also calculated for the enzyme.

Competition experiments with other nucleobases revealed that [6- ^{14}C]-uracil phosphoribosylation was not inhibited by thymine, orotic acid, cytosine, or hypoxanthine. However, the UPRT activity could convert FUra to the nucleotide level and was inhibited by FUra in a competitive manner with a K_i value of 25 μM (data not shown).

4. Discussion

Recombinant UPRT from *T. gondii* was overexpressed in *E. coli* and purified by standard biochemical techniques. Among naturally occurring substrates, the enzyme exhibited a high affinity and narrow specificity for uracil. Other pyrimidine nucleobases, as well as the hypoxanthine, were not substrates for *T. gondii* UPRT, as has been found for the *E. coli* [22] and *Saccharomyces cerevisiae* [25] counterparts. The conversion of FUra to the nucleotide level by the UPRT enzyme has been suspected from genetic evidence, as UPRT-deficient *T. gondii* are resistant to the analog [9]. This has now been confirmed using the purified recombinant enzyme and radiolabeled substrate. The K_m determined for FUra using purified enzyme, however, is an order of magnitude lower than that determined using cell lysates [7]. Recognition of FUra could possibly be attributed to the small van der Waals radius of the fluorine substituent on the pyrimidine ring, as the *T. gondii* UPRT recognizes 5-chlorouracil - but not 5-bromouracil or 5-iodouracil - as a substrate [7].

The *T. gondii* UPRT holoenzyme exists as a monomer in solution, unlike UPRTs that have been studied from other organisms. *S. cerevisiae* [18], *Crithidia luciliae* [20], and *E. coli* [22] UPRTs behave as a heterodimer, a homodimer, and homotrimer respectively. Whether the *in vitro* conditions for assessing quaternary structure of the enzyme reflect the native oligomeric state in intact parasites is unknown. If the native *T. gondii* enzyme is a multimer, however, this oligomerization is not required for catalysis - in contrast to the obligatorily dimeric orotate phosphoribosyltransferase (OPRT) enzyme, which requires residues in both subunits for activity [26].

At 3.5 μM , the measured K_m^{app} of *T. gondii* UPRT for uracil is lower than those determined for other purified UPRT enzymes [18,20,22,27], possibly reflecting the intracellular milieu of the parasite, where steady-state uracil levels are extremely low. The apparent K_m value for PRPP, the ribose-phosphate donor, is similar to those determined for other UPRTs, as is the divalent cation specificity [18,20,22]. Unlike some prokaryotic UPRTs [22-24], however, the *T. gondii* UPRT is not activated by GTP.

UPRT is the most important pyrimidine salvage enzyme for *T. gondii*, as the parasite funnels extracellular pyrimidines into uracil [9,12]. The enzyme does not play an indispensable function for the parasite, however, as *T. gondii uprt* mutants have been isolated by both direct selection [9,12] and insertional mutagenesis [13]. These mutants cannot access the host pyrimidine pool and cannot incorporate radiolabeled uracil [9,11]. The viability of *uprt* mutants establishes that *T. gondii* -- unlike certain other genera of protozoan parasites [28-30] -- are prototrophic for pyrimidines. Thus, the parasite must contain an OPRT activity, the penultimate enzyme in *de novo* pyrimidine nucleotide biosynthesis, and the substrate specificities of the *T. gondii* OPRT and UPRT for pyrimidine nucleobases must be nonoverlapping.

The *T. gondii* UPRT is a logical target for therapeutic validation, as no counterpart is expressed in mammalian cells and tissues [31]. Mammalian cells can, however, convert uracil to UMP through the sequential actions of uridine phosphorylase [32] and uridine kinase [33]. The mammalian OPRT can also recognize uracil, albeit inefficiently, and only at alkaline pH [34]. Thus, pyrimidine nucleobase analogs that can be selectively incorporated into the nucleotide

pool of the parasite serve as potential 'lead' compounds for selective anti-Toxoplasma chemotherapy. The one subversive substrate of UPRT used in this study (FUra) cannot be implemented against *T. gondii*, as this analog is very toxic to mammalian cells (and widely employed as an antineoplastic agent in humans [6,35]). Iltsch and Tankersley [7] have shown that other uracil analogs can also interfere with uracil phosphoribosylation in *T. gondii* extracts. However, these compounds are not good candidates for antiparasitic drugs, as they are very inefficient substrates. Future development of better drug candidates that target UPRT will be greatly facilitated by the availability of effectively limitless quantities of purified recombinant protein for biochemical and structural studies.

Acknowledgements

This work was supported by Grant AI-31808 (D.S.R. and B.U.) from the National Institute of Allergy and Infectious Disease. D.C. was supported in part by an N.L. Tartar Trust Fellowship from the Medical Research Foundation of Oregon. D.S.R. and B.U. are both Burroughs Wellcome Fund Scholars in Molecular Parasitology, and this work was supported in part by grants from the Burroughs Wellcome Fund.

References

- [1] Brooks, R.G., Remington, J.S., and Luft, B.J. (1987) Drugs used in the treatment of toxoplasmosis. *Antimicrob. Agents Annu.* 2, 297-306.
- [2] Haverkos, H.W. (1987) Assessment of therapy for toxoplasmic encephalitis. *Am. J. Med.* 82, 907-914.
- [3] Luft, B.J. and Remington, J.S. (1992) Toxoplasmic encephalitis in AIDS. *Clin. Infect. Dis.* 15, 211-222.
- [4] Chabner, B.A., Allegra, C.J., Curt, G.A., and Calabresi, P. (1996) Antineoplastic agents. In: Goodman & Gilman's *The pharmacological basis of therapeutics* (Handman, J.G., Limbird, L.E., Molinof, P.B., Ruddon, R.W., and Gilman, A.G., eds.), pp 1247-1257. McGraw-Hill Co., Inc., New York.
- [5] Ullman, B. and Carter, D. (1995) Hypoxanthine-guanine phosphoribosyltransferase as a therapeutic target in protozoal infections. *Infect. Agents Dis.* 4, 29-40.
- [6] Ullman, B. and Kirsch, J. (1979) Metabolism of 5-fluorouracil in cultured cells: protection from fluorouracil cytotoxicity by purines. *Mol. Pharmacol.* 15, 357-366.
- [7] Iltzsch, M.H. and Tankersley K.O. (1994) Structure activity relationship of ligands of uracil phosphoribosyltransferase from *T. gondii*. *Biochem. Pharmacol.* 48, 781-792.
- [8] Naguib, F.N., Iltzsch, M.H., el Kouni, M.M., Panzica, R.P., and el Kouni, M.H. (1995) Structure-activity relationships for the binding of ligands to xanthine or guanine phosphoribosyltransferase from *Toxoplasma gondii*. *Biochem. Pharmacol.* 50, 1685-1693.

- [9] Pfefferkorn, E.R. and Pfefferkorn, L.C. (1977) *Toxoplasma gondii*: characterization of a mutant resistant to 5-fluorodeoxyuridine. *Exp. Parasitol.* 42, 44-55.
- [10] Roos, D.S., Donald, R.G.K., Morrissette, N.S., and Moulton, A.L.C. (1994) Molecular tools for genetic dissection of the protozoan parasite *Toxoplasma gondii*. In: *Methods in Cell Biology* Vol. 45 pp. 25-61 Academic Press.
- [11] Schwartzman, J.D. and Pfefferkorn, E.R. (1981) Pyrimidine synthesis by intracellular *Toxoplasma gondii*. *J. Parasitol.* 67, 150-156.
- [12] Pfefferkorn, E.R. (1978) *Toxoplasma gondii*: the enzymic defect of a mutant resistant to 5-fluorodeoxyuridine. *Exp. Parasitol.* 44, 26-35.
- [13] Donald, R.G.K. and Roos, D.S. (1995) Insertional mutagenesis and marker rescue in a protozoan parasite: cloning of the uracil phosphoribosyltransferase locus from *Toxoplasma gondii*. *Proc. Natl. Acad. Sci. USA* 92, 5749-5753.
- [14] Schneider, E.L., Stanbridge, E.J., and Epstein, C.J. (1974) Incorporation of ³H-uridine and ³H-uracil into RNA. A simple technique for the detection of mycoplasma contamination of cultured cells. *Exp. Cell. Res.* 84, 311-318.
- [15] Craig, S.P., Yuan, L. Kuntz, D.A., McKerrow, J.H. and Wang, C.C. (1991) High level expression in *E. coli* of soluble, enzymatically active schistosomal hypoxanthine/guanine phosphoribosyltransferase and trypanosomal ornithine decarboxylase. *Proc. Natl. Acad. Sci. USA* 88, 2500-2504.
- [16] Allen, T.E. and Ullman, B. (1994) Cloning and expression of the hypoxanthine-guanine phosphoribosyltransferase gene from *Trypanosoma brucei*. *Nucl. Acids Res.* 21, 5431-5438.

- [17] Laemmli, U.K. (1970) Cleavage of structural proteins during the assembly of the head of bacteriophage T4. *Nature* 227, 680-685.
- [18] Natalini, P., Ruggieri, S., Santarelli, I., Vita, A., and Magni, G. (1979) Baker's yeast UMP:pyrophosphate phosphoribosyltransferase. purification, enzymatic and kinetic properties. *J. Biol. Chem.* 254, 1558-1563.
- [19] Cornish-Bowden A. (1995) *Fundamentals of enzyme kinetics*. Portland Press London, U.K.
- [20] Asai, T., Lee, C.S. Chandler, A. and O'Sullivan, W.J. (1990) Purification and characterization of uracil phosphoribosyltransferase from *Crithidia luciliae*. *Comp. Biochem. Physiol.* 95B:1, 159-163.
- [21] Kidder, G.W., Nolan, L.L., and Dewey, V.C. (1979) The purine phosphoribosyltransferases of *Crithidia fasciculata*. *J. Parasitol.* 65, 520-525.
- [22] Rasmussen, U.B., Mygind, B. and Nygaard, P. (1986) Purification and some properties of uracil phosphoribosyltransferase from *Escherichia coli* K12. *Biochim. Biophys. Acta* 881, 268-275.
- [23] Jyssum, S. and Jyssum, K. (1979) Metabolism of pyrimidine bases and nucleosides in *Neisseria meningitidis*. *J. Bacteriol.* 138, 320-323.
- [24] Mitchell, A. and Finch, L.R. (1979) Enzymes of pyrimidine metabolism in *Mycoplasma mycoides* subsp. *mycoides*. *J. Bacteriol.* 137, 1073-1080.
- [25] Natalini, P., Fioretti, E., Ruggieri, S., Vita, A., and Magni, G. (1975) Presence of a specific uridine 5'-monophosphate pyrophosphorylase in baker's yeast. *Experientia* 31, 1008-1010.

- [26] Henriksen, A., Aghajari, N., Jensen, K.F., and Gajhede, M. (1996) A flexible loop at the dimer interface is a part of the active site of the adjacent monomer of *Escherichia coli* orotate phosphoribosyltransferase. *Biochemistry* 35, 3803-3809.
- [27] McIvor, S., Wohlhueter, R.M., Plagemann, P.G.W. (1983) Uracil phosphoribosyltransferase from *Acholeplasma laidlawii*: partial purification and kinetic properties. *J. Bacteriol.* 156, 192-197.
- [28] Lindmark, D.G. and Jarroll, E.L. (1982) Pyrimidine metabolism in *Giardia lamblia* trophozoites. *Mol. Biochem. Parasitol.* 5, 291-296.
- [29] Wang, C.C., Verham, R., Tzeng, S.F., Aldritt, S. and Cheng, H.W. (1983) Pyrimidine metabolism in *Tritrichomonas foetus*. *Proc. Natl. Acad. Sci. USA* 80, 2564-2568.
- [30] Heyworth, P.G., Gutteridge, W.E., and Ginger, C.D. (1984) Pyrimidine metabolism in *Trichomonas vaginalis*. *FEBS Lett.* 176, 55-60.
- [31] Schneider, E.L., Stanbridge, E.J., and Epstein, C.J. (1974) Incorporation of ³H-uridine and ³H-uracil into RNA. A simple technique for the detection of mycoplasma contamination of cultured cells. *Exp. Cell Res.* 84, 311-318.
- [32] Watanabe, S.-I., Hino, A., Wada, K., Eliason, J.F., and Uchida, T. (1995) Purification, cloning, and expression of murine uridine phosphorylase. *J. Biol. Chem.* 12191-12196.
- [33] Cheng, N., Payne, R.C., and Traut, T.W. (1986) Regulation of uridine kinase. Evidence for a regulatory site. *J. Biol. Chem.* 261, 13006-13012.
- [34] Reyes, P. and Guganig, M.E. (1975) Studies on a pyrimidine phosphoribosyltransferase from murine leukemic P1534J. Partial purification,

substrate specificity, and evidence for its existence as a bifunctional complex with orotidine 5'-phosphate decarboxylase. *J. Biol. Chem.* 250, 5097-5108.

- [35] Heidelberger, C. (1965) Fluorinated pyrimidines. *Prog. Nucl. Acid Res.* 4, 1-50.

Fig. 1. Fractionation of UPRT by SDS polyacrylamide gel electrophoresis. *T. gondii* UPRT was overexpressed in *E. coli* and purified as described in Materials and Methods. Lane A, soluble fraction of crude lysate; lane B, combined void volume fractions from the DE-53 column; lane C, proteins precipitated by 50% ammonium sulphate; lane D, peak fractions after gel permeation chromatography. 5-10 μ g of each fraction were loaded onto each lane of the gel. Numbers at left indicate molecular weight standards.

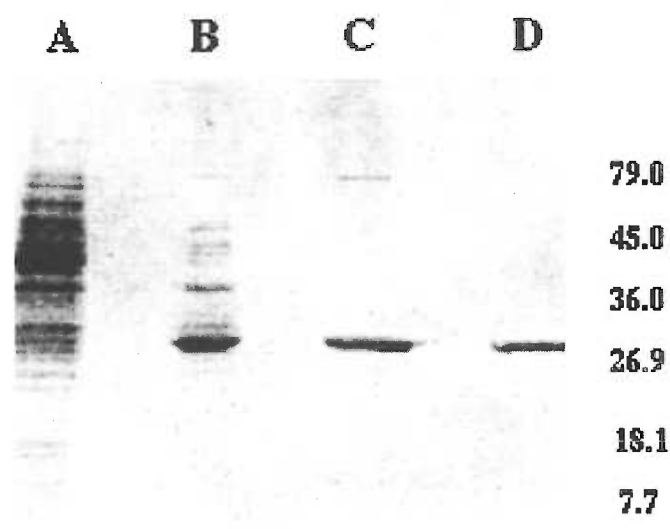


Fig. 2. Size exclusion chromatography of purified UPRT. Purified *T. gondii* UPRT was chromatographed over a gel permeation column as reported in Materials and Methods. Protein in the eluate was monitored by absorbance at 280 nm. Molecular weight standards for bovine serum albumin ($M_r \approx 66$ kd) and carbonic anhydrase ($M_r \approx 29$ kd) are indicated by the arrows. Column inclusion volume (determined using GMP) is indicated by the double arrow.

Absorbance at 280 nm

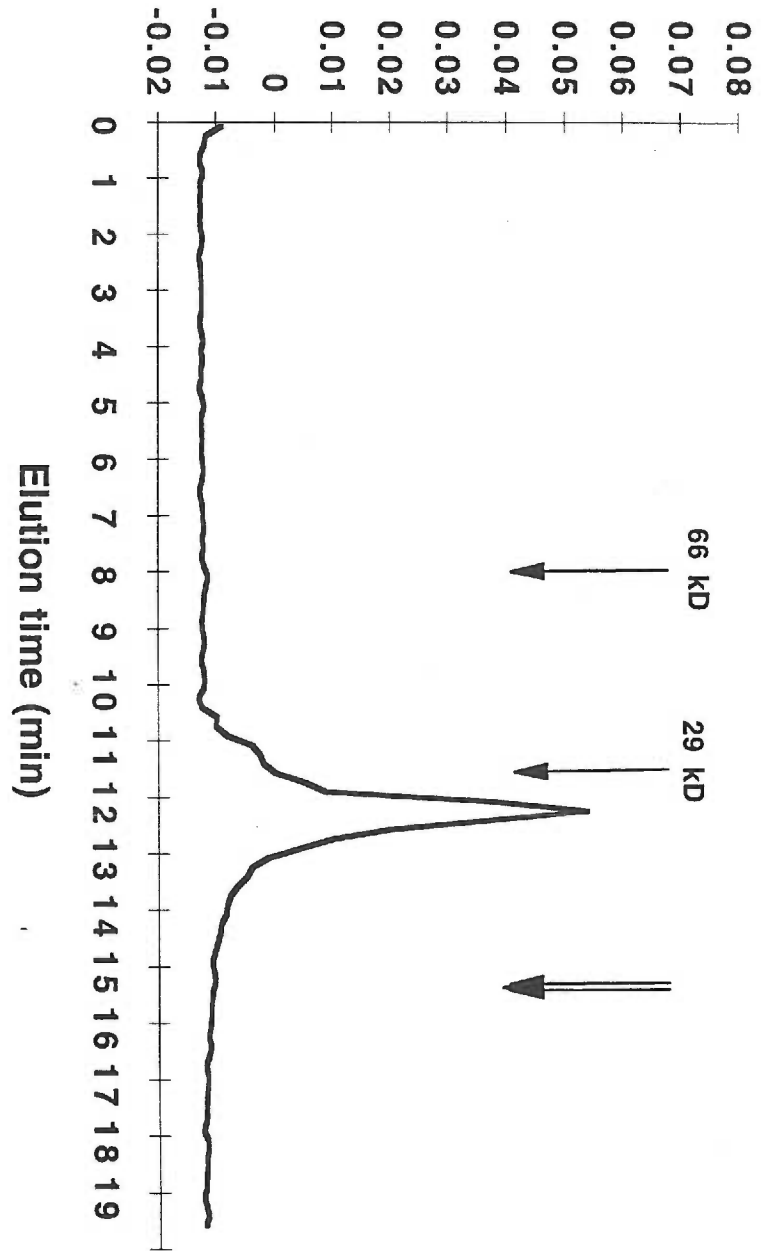


Fig. 3 Heat inactivation of *T. gondii* UPRT. Enzyme was incubated for 5 min at various temperatures and residual enzyme activity quantitated spectrophotometrically. The change in absorbance at 252 nm min⁻¹ is plotted as a function of temperature.

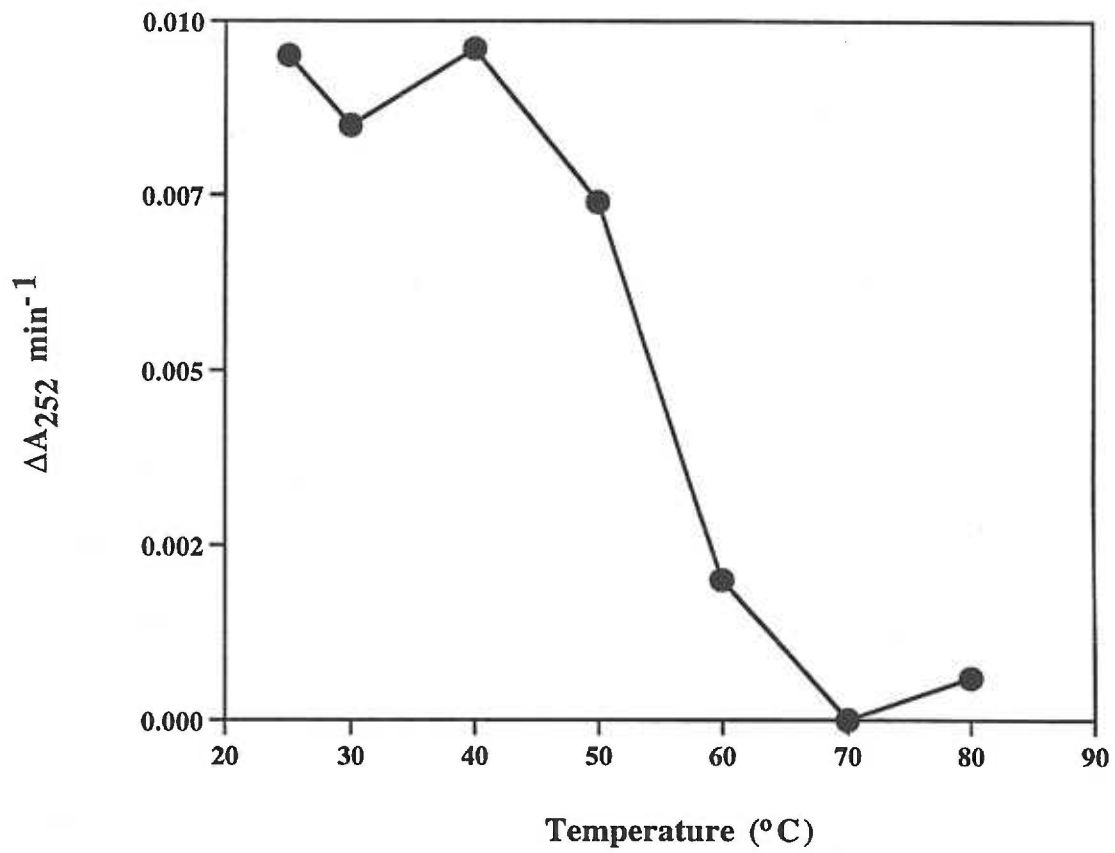


Fig. 4. Effects of sundry divalent cations on UPRT activity. UPRT activity was monitored by radiometric assay in the presence of different divalent cations. The activities are the averages \pm standard errors from 3 different determinations.

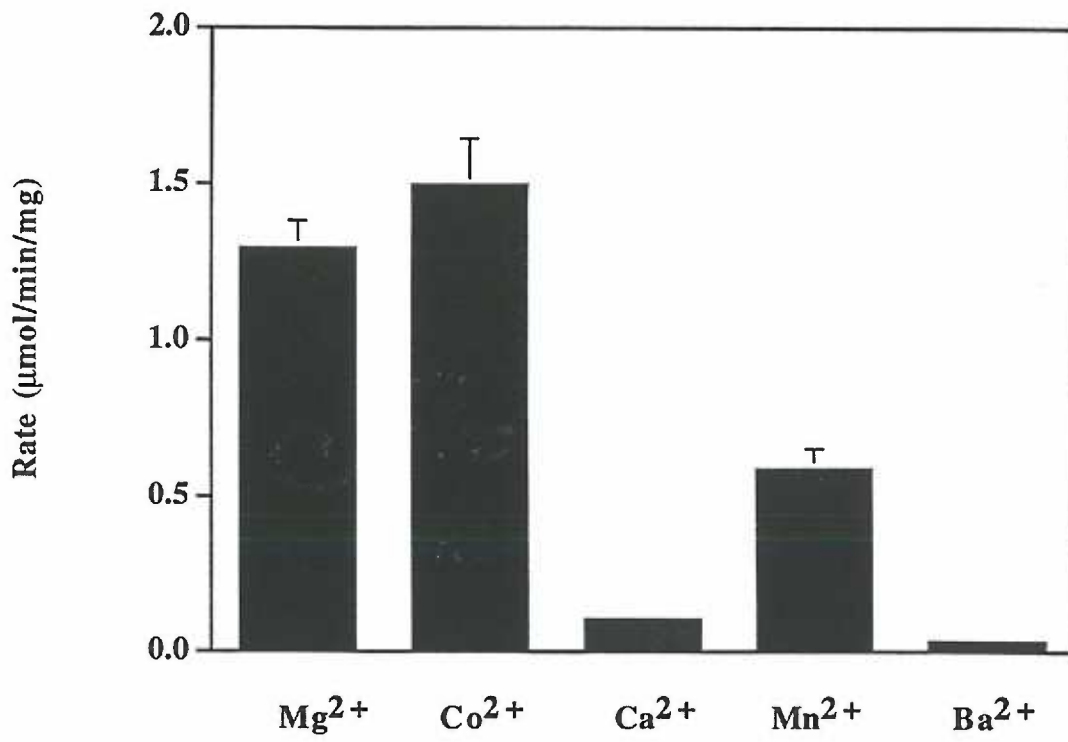


Fig. 5. Hanes analysis of UPRT activity as a function of substrate concentration. The steady state kinetics of the *T. gondii* UPRT were determined using the radiometric assay as a function of substrate concentration and analyzed as described in Materials and Methods. At left, PRPP concentrations were fixed at 5.0 mM when uracil was varied between 0.25 - 42 μM ; at right, the uracil concentration was maintained at 100 μM when PRPP fluctuated between 80 μM and 8.0 mM.

4.2. Chemical modifications and mutagenesis of the *T. gondii* UPRT enzyme

Darrick Carter, Erika Dahl, Daniel Scott and Buddy Ullman

1. Introduction

The uracil phosphoribosyltransferase (UPRT) enzyme has been touted as a selectable marker in *T. gondii* [1] and as an attractive target for antitoxoplasmodic agents [2]. As humans are deficient in this enzyme and rely completely on *de novo* synthesis for pyrimidine nucleotides, compounds which are activated by the UPRT may be specific drugs with little adverse reactions in the human host. A specific inhibitor or substrate analog can be designed after extensive biochemical and structural analyses on the targeted protein which allow insight into the structure-function relationships governing catalysis. Chemical modifications targeting specific residues can provide data on the type and accessibility of amino acids involved in catalysis, while site-directed mutants can be utilized to study the function of a specific residue, or to alter the chemical properties of a protein to favor structural analyses. Little is known about the family of UPRT enzymes and no structural information is available for this class of proteins. To assist in the determination of the X-ray crystal structure of the UPRT, a C128V mutant was created which would circumvent the reported oxygen sensitivity of the protein [3] and chemical modifications were performed to study which type

of amino acids are involved in UPRT catalysis. Valine was chosen over the more common serine to replace C128 as there is a valine at this position in the homologous yeast enzyme.

2. Materials and Methods

2.1. Chemicals, materials and reagents.

Uracil was purchased from Aldrich chemicals. All restriction and DNA modifying enzymes were acquired from either Bethesda Research Laboratories Life Technologies Inc. (Gaithersburg, MD) or Boehringer Mannheim Biochemicals (Indianapolis, IN). Site-directed mutagenesis was performed with the pAlter-1 site-directed mutagenesis system from Promega (Madison, WI). 5-phosphorylribose-1-pyrophosphate (PRPP) and octyl agarose matrix were obtained from the Sigma Chemical Co. (St. Louis, MO). DE-53 anion exchange matrix was from Whatman (Hillsboro, OR). All other materials, chemicals, and reagents were of the highest purity commercially available.

2.2. Site-directed mutagenesis

The *T. gondii* UPRT cDNA construct in the mutagenesis vector pAlter-1 was utilized to create a Cys to Val mutation in the protein coding region of the *T. gondii* UPRT at position 128 by site directed mutagenesis. The coding region of the mutant UPRT cDNA was subcloned into the *NdeI/XbaI* sites of bacterial expression vector pBAce [4] and transformed into *E. coli* JM109.

2.3. *UPRT expression and purification*

The pBAce-*UPRT* mutant and wild-type constructs were overexpressed and purified by DEAE chromatography and ammonium sulfate precipitation as described. However, the gel permeation chromatography step was replaced with hydrophobic interaction chromatography on octyl agarose (Sigma) and UPRT protein was bound at 1.5 M ammonium sulfate and eluted with a decreasing gradient of ammonium sulfate. The purified fractions of UPRT were then pooled and dialyzed for further studies. SDS polyacrylamide gel electrophoresis was performed on 15 % slab gels according to the method of Laemmli [5].

2.4. *UPRT assay and kinetics of the UPRT C128V mutant*

The spectrophotometric assay for measuring UPRT activity was employed as described [3]. The assay mixtures consisted of TMD50 buffer, 50 μ M uracil, and 1.0 mM PRPP, and the reaction was initiated by enzyme addition. Assays were performed at 22°C on a DU640 spectrophotometer with a kinetics/time module by monitoring increases in absorbance at 262 nm. The K_m^{app} value of UPRT for PRPP was determined at 100 μ M uracil and PRPP concentrations ranging from 80 μ M to 8.0 mM. The K_m^{app} value for uracil was ascertained at 5.0 mM PRPP and concentrations of uracil varying from 1 μ M to 42 μ M. Kinetic parameters were determined by Hanes analysis [6].

2.5. Chemical modification of UPRT protein

Purified UPRT protein was diluted to 200 μM in 50 mM Tris and 5mM MgCl_2 (pH 7.5) and protein modifying reagents were added to 100 fold excess. The reactions proceeded at 20°C or on ice for 100 minutes and UPRT activity was assessed as described above.

2.6. 7-diethylamino-3-(4'-maleimidyl phenyl)-4-methylcoumarin (CPM) labeling of UPRT

UPRT protein was covalently modified on cysteine residues by the fluorescent label CPM (Molecular Probes) as described above and modified protein was tested for UPRT activity. The modified UPRT was then fractionated on SDS-PAGE and UPRT was visualized by UV fluorescence.

2.7. TNM dependent inactivation of UPRT

UPRT protein was diluted to 40 μM and tetranitromethane (TNM) added in methanol to 0.2 mM (5 fold excess) The inactivation of UPRT was followed by taking aliquots and determining UPRT activity as a function of time. Protection of UPRT by its substrate PRPP was monitored under the conditions described above with the addition of 2.5 mM PRPP. The number of tyrosines modified by TNM was determined by incubating UPRT in 100 fold excess TNM for 100 minutes and determining the A_{426} of the protein after acetone precipitation, ethanol washing, and redissolving in 6M urea. The molar absorption per modified tyrosine was 4100 $\text{M}^{-1}\text{cm}^{-1}$.

3. Results

3.1. Improved purification of the UPRT enzyme: The purification protocol used is a modification of the one previously reported for UPRT in Chapter 4.1. The substitution of the gel permeation chromatography step by a hydrophobic interaction chromatography column resulted in highly purified protein (Figure 1) more reproducibility and higher yields than prior purification protocols. Using the conditions described, the UPRT protein elutes at 1.1 M ammonium sulfate.

3.2. Chemical modifications of UPRT: The UPRT enzyme was resistant to most chemical modifying reagents (Table 1.). It was completely inactivated by tetranitromethane, which targets tyrosyl residues and by phenylglyoxal, which is an arginine modifying reagent.

Table 1. Chemical modifiers of the UPRT enzyme

Reagent	Amino acids targeted	% UPRT activity remaining
Iodomethane	Cys	110
CPM	Cys	90
Iodoacetamide	Cys	88
EDPC	Asp, Glu	75
Diisopropylfluorophosphate	Ser	83
DEPC	His, Tyr, Lys	85
TNM	Tyr	0
Phenylglyoxal	Arg	0
Control	--	100

3.3. TNM dependent inactivation of the UPRT enzyme: TNM inactivated the UPRT in a time dependent fashion with 50% inactivation after five minutes under the conditions employed. This inactivation was not hindered by the presence of 2.5 mM PRPP (Figure 2). At saturation, 3.07 ± 0.39 mols tyrosine were modified per mol protein indicating that 3 tyrosyl residues are accessible to the reagent out of the nine tyrosyls present in the protein.

3.4. Cysteine tagging by CPM: As there was little modulation of UPRT activity upon modification with Cys specific reagents, a fluorescent probe was used to determine whether the sulfhydryl groups are accessible to protein modifying reagents. Following modification by CPM the UPRT protein was still completely active. However, when the modified protein was fractionated on an SDS-PAGE gel fluorescent bands on the gel corresponding to the UPRT protein were found indicating that the protein is modified, but that this modification does not affect enzymatic activity (Figure 3)

3.5. C128V mutant kinetics: Mutant UPRT protein purified similarly to the native protein, but eluted at 0.6 M ammonium sulfate from the hydrophobic interaction column. Consistent with the resistance of the protein to Cys modifying reagents, the protein was still highly active and the kinetic parameters did not differ significantly from the wild type protein. K_m^{app} values for uracil were 13.4 μ M for the C128V protein and 11.4 μ M for the wild type enzyme under the conditions employed. Similarly, K_m^{app} values for PRPP were 401 μ M for the C128V protein and 413 μ M for the wild type.

4. Discussion

The purification scheme for UPRT has been modified to include a hydrophobic interaction chromatography step which simplifies the procedure and improves the purity of the resulting protein. The importance of a number of residue types was ascertained by chemical modifications. The result of these studies seems to indicate that the UPRT utilizes a tyrosyl residues and arginanyl residues in its active site. Tyrosyl residues have been implicated in PRT catalysis in a number of cases and the presence of a catalytically active tyrosine may be a common motif for the catalysis of the purine / pyrimidine PRTs. Unlike reports for the *L. donovani* HGPRT [7], the tyrosyl residue in the *T. gondii* UPRT is not protected by the substrate PRPP. There are six cysteines present in the primary sequence of the UPRT protein. However, none of these residues seem vital for catalysis as the protein was not affected by any of the cysteine modifying reagents tested. If any of these Cys residues are important, this residue must be in a position in the apo-enzyme which does not allow modifying reagents to access it. At least one of the cysteine residues is not vital for catalysis and is accessed by the reagents used as can be seen by the fluorescent tagging of the UPRT protein with the Cys-specific reagent CPM. Modification of one of the residues from a cysteine to a valine, the residue found in an equivalent position in the homologous protein from yeast, does not affect activity of the protein, but does seem to improve the protein's stability and resistance to atmospheric oxygen [8]. This new, stable protein may prove vital for future crystallographic studies which will be useful in delineating the role of the residues, Tyr and Arg, found to be important in catalysis.

Figure 1: Purification of the UPRT protein by hydrophobic interaction chromatography.

Lane A: UPRT protein purified as described previously prior to the gel permeation chromatography step. Lane B: Molecular weight standards.

[ammonium sulfate], M

A B 1.2 1.1 1.1 1.1 1.0 0.5 0.0 0.0

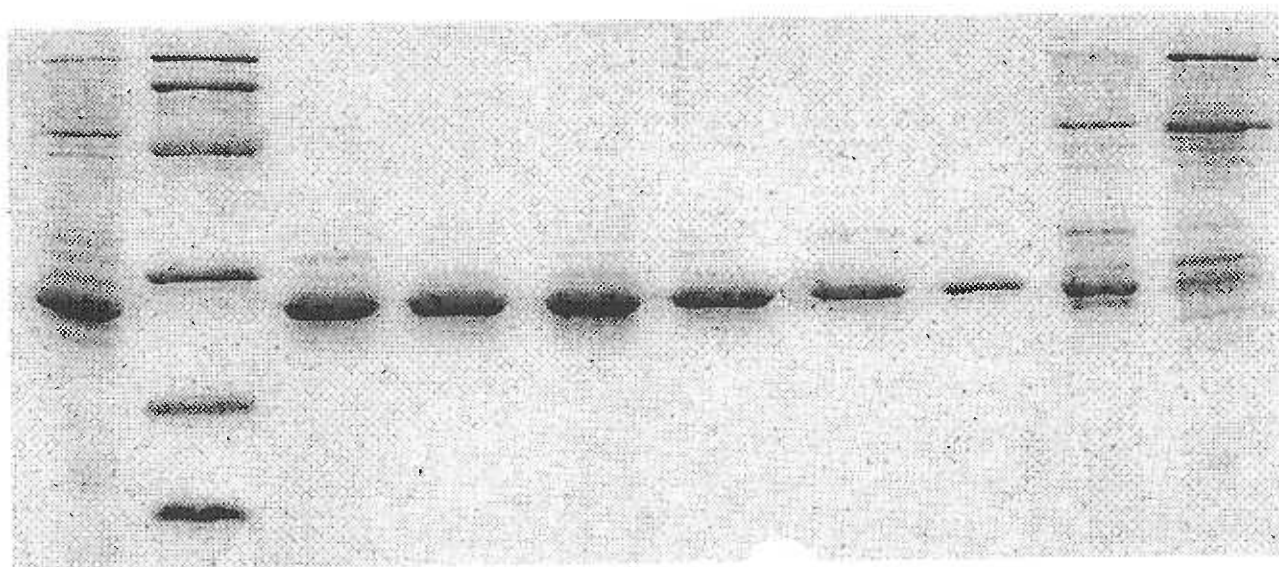


Figure 2: Time dependent inactivation of the *T. gondii* UPRT by the protein modifying reagent, TNM

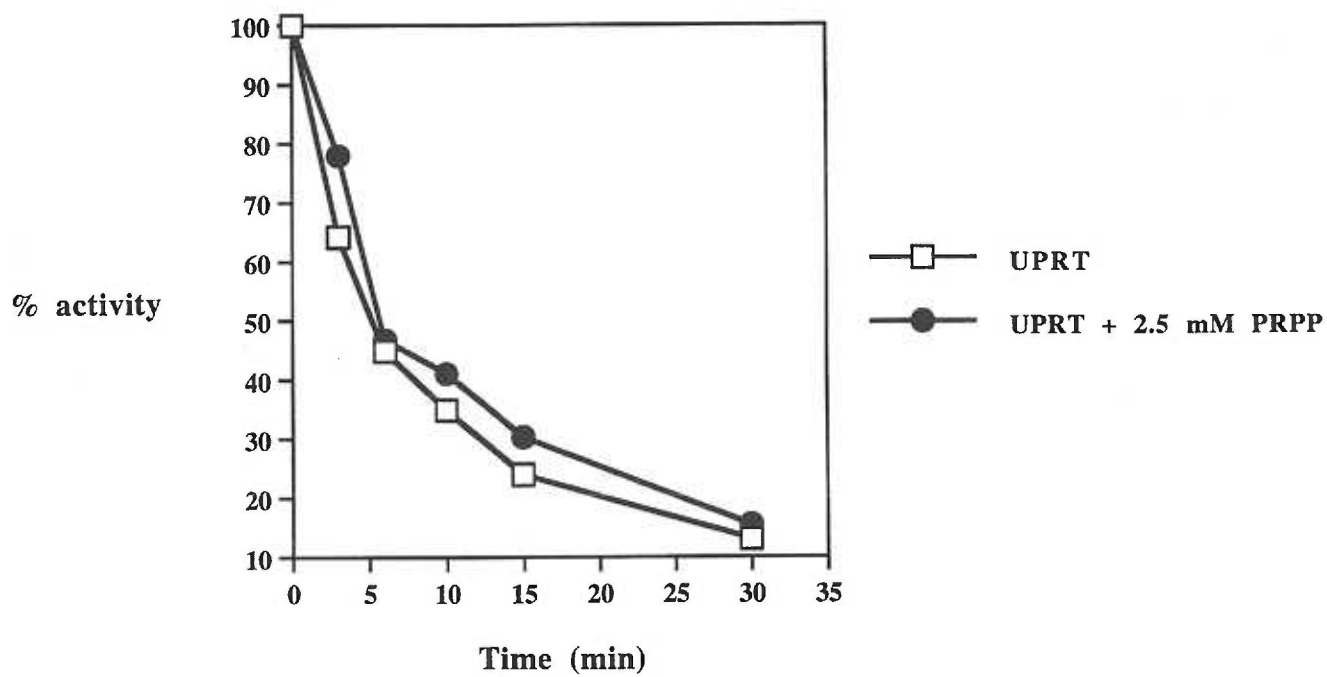
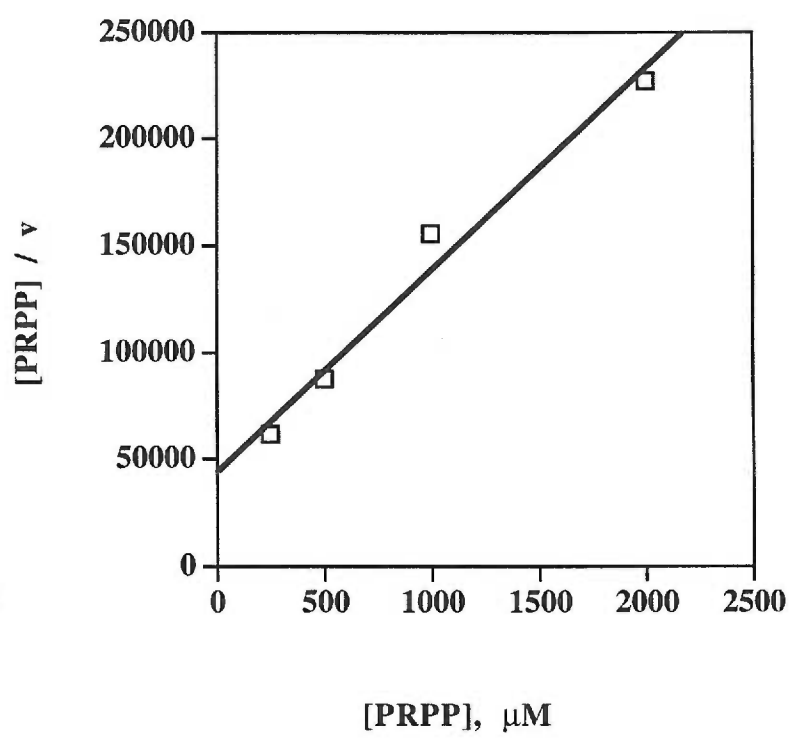
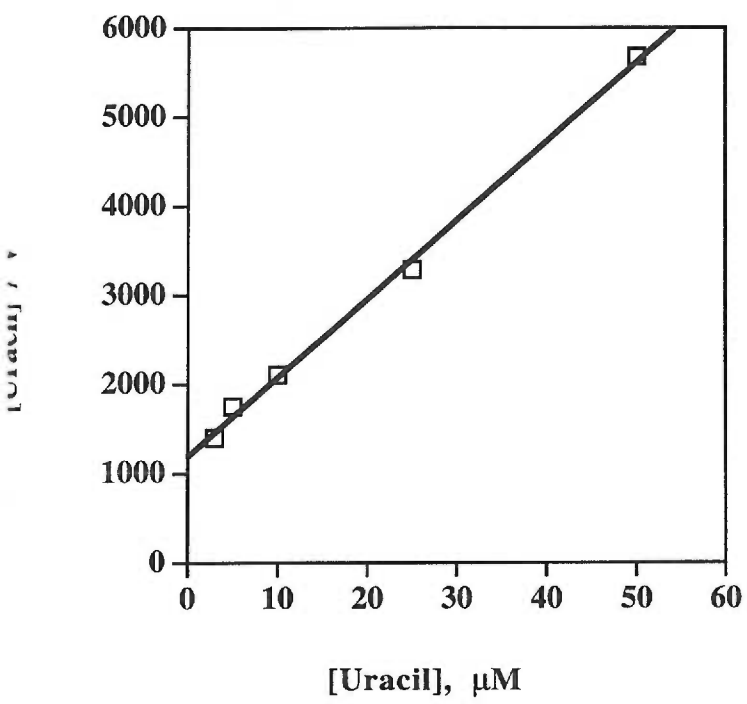


Figure 3. Fluorescent tagging of the UPRT enzyme by the Cys-specific reagent, CPM. Left lane: 10 μ l modified UPRT protein. Right lane: 5 μ l of the same protein preparation.



Figure 4. Kinetics of the C128V mutant in UPRT



1. Donald, R.G.K. and Roos, D.S. (1995) *Proc. Natl. Acad. Sci. USA* **92**:5749-5753.
2. Iltzsch, M.H. and Tankersley K.O. (1994) *Biochem. Pharmacol.* **48**:781-792.
3. Carter D, Donald RGK, Roos DS, Ullman B (1997) *Mol Biochem Parasit* **87**:137-144.
4. Craig, S.P., Yuan, L. Kuntz, D.A., McKerrow, J.H. and Wang, C.C. (1991) *Proc. Natl. Acad. Sci. USA* **88**:2500-2504.
5. Laemmli UK. (1970) *Nature* **227**:680-685.
6. Cornish-Bowden A. (1995) *Fundamentals of Enzyme Kinetics*. London: Portland Press.
7. Jardim A, Ullman B. (1997) *J Biol Chem* **271**:30840-30846.
8. Schumacher M, personal communication.

5. Future Directions

Many questions pertaining to the function of the PRTs investigated have been answered using a wide variety of approaches to study these enzymes. The development of a high-yield expression and purification system for the uracil PRT (UPRT) should allow for the determination of the X-ray crystal structure of this PRT and may answer questions pertaining to structure-function relationships governing the mechanism of this protein. A three dimensional model of this protein may be used to discover new classes of inhibitors using the structure-based inhibitor design approaches discussed in the introduction. Additionally, site-directed mutants selected by inspecting the crystal structure will lead to a dynamic understanding of the interaction of residues in this protein.

The novel inhibitors of the HGXPRT can now be improved upon by combining biochemical and crystallographic approaches to increase the selectivity and effectiveness of these compounds. Crystal structures of the HGXPRT in various mechanistic states will provide insight into the conformational changes occurring during catalysis and structures of mutants will help explain the biochemical data presented in the body of this thesis. Taken together these studies should allow for the design of tight binding inhibitors of HGXPRT which, in combination with inhibitors of the adenosine kinase, may prove to be the basis for an effective combinational therapy for toxoplasmosis.

Appendix A

Cloning and Expression of the *P. falciparum* HGXPRT enzyme

Darrick Carter and Buddy Ullman

Introduction

The malaria parasite, *Plasmodium falciparum* is the causative agent of acute malaria in humans and has been a scourge of mankind for centuries [1]. An effective drug regimen for acute malaria has only been developed in this century and already strains of malaria around the world have developed high levels of resistance to commonly used drugs such as the sulfa drugs, pyrimethamine and chloroquine [2,3,4]. Spreading resistance accompanied by a high mortality rate make it imperative that new treatment methods be developed.

Similarly to *T. gondii*, *P. falciparum* cannot synthesize the purine ring de novo [5] and relies on a battery of salvage enzymes to supply itself with purine nucleotides. Perhaps the most important salvage enzyme for this organism is the HGXPRT [6] which is thought to play an indispensable nutritional role for the parasite [7]. This makes the malarial HGXPRT an attractive target for structure based inhibitor design as tight-binding enzyme inhibitors would be thought to be lethal to *Plasmodium*. A prerequisite for this inhibitor design is the ability to reproducibly generate high quantities of purified protein, a task which would be gargantuan if one were to culture *P. falciparum in vitro* and attempt to extract the native

protein. Thus one needs a recombinant system in which to overexpress the *hgxpri* gene to create large quantities of recombinant enzyme. Due to the high A/T bias in *Plasmodium* genes, many sequences have been very difficult to express and some groups have gone through great lengths to achieve acceptable levels of expression in *E. coli* [8].

Materials and Methods

Primer design: An oligonucleotide primers were designed based on the known *P. falciparum* *hgxpri* cDNA sequence [GENBANK Accession # Y00519], one of which would introduce an NdeI site at the initiating methionine codon and one reverse primer downstream of the stop codon containing a Sall site.

rtPCR: mRNA from *P. falciparum* was generously provided to the lab by Dr. J. Feagin and used to make cDNA using the SuperscriptII kit by Life Technologies. The cDNA was then used as a template for PCR with Tfl polymerase with standard protocols. Briefly, DNAs were denatured in a hot-start for 5 mins at 94° C followed by thirty-five cycles of 30 second denaturation at 94°C, 90 seconds of annealing at 50°C and 60 seconds of synthesis at 72°C. At the end of the cycles a five minute extension at 72°C was performed and PCR products were separated by electrophoresis in 1% agarose/TAE and visualized with ethidium bromide under UV light.

Subcloning, transformation and overexpression: rtPCR products were digested with NdeI

and SalI and ligated into a similarly treated pBAce vector. Ligation reactions were transformed into XL1-blue cells and minicultures were screened for the correct insert. Positive cultures were maxiprepped with the Quiagen maxiprep kit and DNAs further mapped by restriction digest. The pBAce-*hgxpirt* construct was then transformed into the *hgxpirt* deficient SΦ606 cell line and cultures were induced in low phosphate induction medium as described [9].

Protein extraction and assay: Overnight cultures were harvested by centrifugation at 4°C and lysed in 50mM Tris, 5mM MgCl₂, 2mM DTT buffer pH=7.5 (TMD50 buffer) with a French press at 16,000 psi. Cell extracts were clarified by centrifugation at 30,000 x g and the supernatants were analyzed by SDS-PAGE. Additionally, hypoxanthine phosphoribosyltransferase activity was monitored using 30μM [C-14] labeled hypoxanthine and 2mM 5-phosphorylribosepyrophosphate as described [10].

Results and Discussion

A bright band of approximately 760 b.p. was amplified in the PCR reaction containing the *P. falciparum* cDNA (Figure 1) consistent with the predicted size of 738 b.p. for this fragment. Subcloning and restriction mapping of the 760 b.p. fragment verified its identity as the *Plasmodium hgxpirt* coding sequence. Subcloning into the pBAce vector (Figure 2) and induction of SΦ606 cells transformed with this construct gave rise to a prominent band at about 27 kD in crude protein extracts which was not seen in bacterial cultures of SΦ606 cells

transformed with vector alone. (Figure 3) The crude extract instantly converted all the radiolabel in the hypoxanthine assay cocktail, while no such activity was observed in the *E. coli* control. Interestingly, the enzyme seemed to be quite unstable and quickly precipitated from solution over the course of a week. Concomitantly, no HPRT activity was observed in supernatants which were stored for more than a week. The subcloning of the *P. falciparum* *hgprt* coding sequence and high level overexpression has been achieved by use of rtPCR and low phosphate induction. This will greatly facilitate structural and biochemical studies aimed at designing inhibitors for this enzyme. Unfortunately, this protein seems to be prone to precipitation from solution and apparently loses activity upon precipitation. This instability may be inherent to the *P. falciparum* enzyme or may be due to incorrect posttranslational processing in the recombinant system. Interestingly, the HGXPRT from *P. falciparum* differs in many N-terminal residues found in a closely related protein, the *T. gondii* HGXPRT-isoformI (Figure 4). In the crystal structure and by expression of a truncated version of HGXPRT Isoform-I it is found that these residues stabilize the *T. gondii* protein in solution. Possibly, a chimeric construct containing the coding sequence for the N-terminal residues from the *T. gondii* protein could be used to express a stable HGXPRT to use for biochemical and structural studies.

Figure 1. rtPCR products using the *P. falciparum* *hgxpri* primers. A: 123 b.p. molecular size standards; B: PCR reaction containing no *P. falciparum* cDNA template; C: PCR reaction containing the cDNA template, putative *hgxpri* gene fragment is indicated by arrow.

A

B

C



Figure 2. Restriction map of the pBAce-PfHGXPRT expression construct.

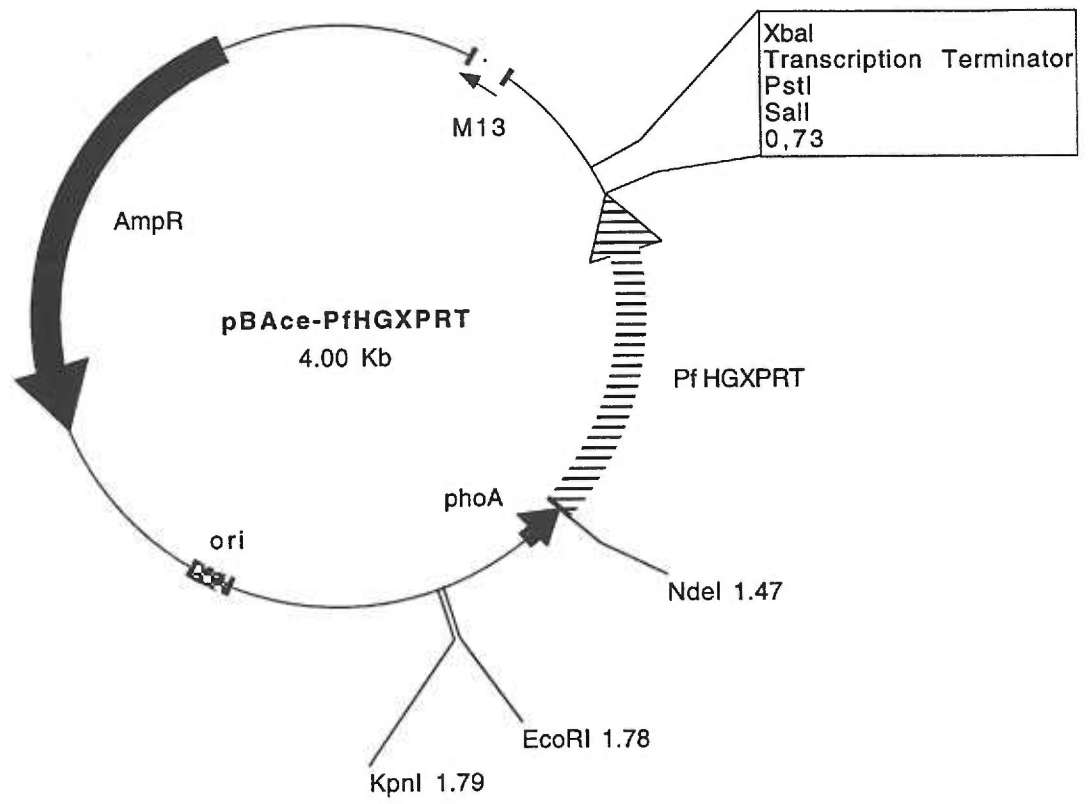


Figure 3. Fractionation of the overexpressed *P. falciparum* HGXPRT protein by SDS-PAGE. Lane A: 10 μ g crude extract from S Φ 606 cells transformed with the pBAce-PfHGXPRT construct. Lane B: Molecular size standards.

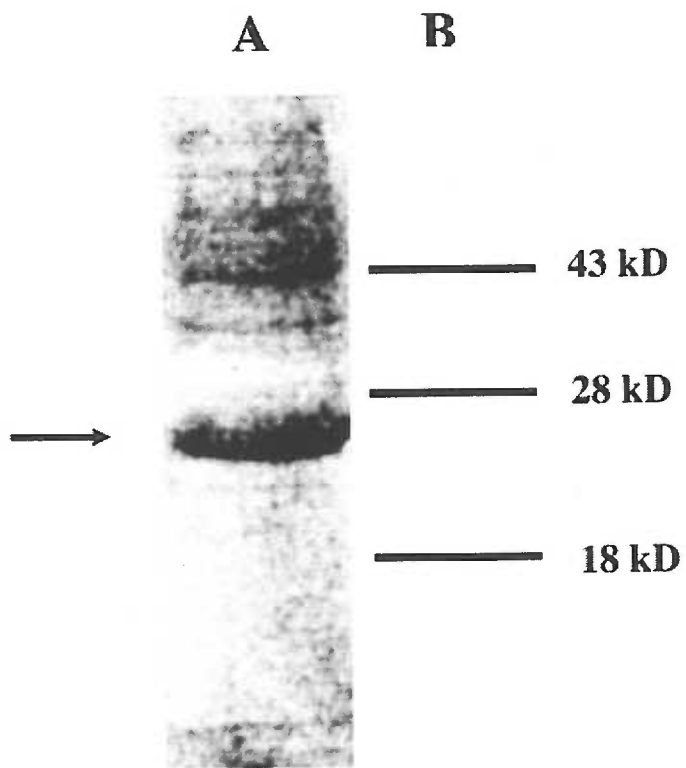


Figure 4. : Alignment of the *T. gondii* and *P. falciparum* HGXPRT peptide sequences.

Bolded residues are those suggested for use in the chimeric HGXPRT construct.

P. falciparum ---MPIPNNPGAGENAFDPVFVKDDDGYPDLDSEFMIPAHYKKYLTQVLPNGVIKRNRIEKL
 T. gondii **MASKPIEDY-GKGGRIEPMYIPDNTFYNAADDFLVPPHCKPYIDKILLPGGLVKDRVEKL**

Consensus ----PI----G-G-----P----D---Y--D-F--P-H-K-Y--K---P-G--K-R-EKL

P. falciparum AYDIKKVYNNEEFHILCLLKGSRGFFTALLKHLRSRIHNYSAVEMSKPLFGEHYVVRVKSQC
 T. gondii AYDIHRTYFGEELHIICILKGSRGFFNLLIDYLATIQKYSGRESSVPPFFEHYVRLKSYQ

Consensus AYDI---Y--EE-HI-C-LKGSRGFF--L---L--I--YS--E-S-P-F-EHYVR-KSY-

P. falciparum NDQSTGTLEIVSEDLSCCLKGKHLVIVEDIIDTGKTLVKFCEYLKKFEIKTVAIACLFIKR
 T. gondii NDNSTGQLTVLSDDLISIFRDKHLVIVEDIVDTGFTLTFEGERLKAAGPKSMRIATLVEKR

Consensus ND-STG-L---S-DLS-----KHLVIVEDI-DTG-TL--F-E-LK----K---IA-L--KR

P. falciparum TPLWNGFKADFVGFSSIPDHFVVGYSLDYNEIFRDLDHCCLVNDGKKKYKATSL
 T. gondii TDRSNSLKGDFVGFSIEDVWIVGCCYDFNEMFRDFDHVAVLSDAARKKFEK---

Consensus T---N--K-DFVGFSI-D---VG---D-NE-FRD-DH-----D---KK-----

1. Desowitz RS (1991) *The Malaria Capers* W.W. Norton & Co. New York London
2. Wang P, Read M, Sims PF, Hyde JE, (1997) *Mol Microbiol* **23 (5)**: 979-986
3. Alin MH, (1997) *Parasitology* **114 (Pt 6)**: 503-506
4. Wooden JM, Hartwell LH, Vasquez B, Sibley CH, (1997) *Mol Biochem Parasitol* **85(1)**: 25-40
5. Hassan HF, Coombs GH (1988) *FEMS Microbiol Rev* **4(1)**:47-83
6. Ullman B, Carter D (1995) *Infect Agents Dis* **4 (1)**:29-40
7. Asahi H (1996) *Parasitology* **113 (Pt 1)**:19-23
8. Hall SJ, Sims PF, Hyde JE (1991) *Mol Biochem Parasitol* **45(2)**:317-330
9. Allen TE, Ullman B (1994) *Mol Biochem Parasitol* **65(2)**:233-245
10. Allen TE, Hwang HY, Jardim A, Olafson R, Ullman B (1995) *Mol Biochem Parasitol* **73(1-2)**:133-143

Appendix B

Subcloning, Expression, and Purification of the *T. gondii* Dihydrofolate Reductase - Thymidylate Synthase (DHFR-TS) Enzyme

Darrick Carter and Buddy Ullman

Introduction

The DHFR enzymes have traditionally been targets for antifolate regimens used in the therapy of a number of diseases. *Toxoplasma gondii*, an obligate intracellular parasite and the etiologic agent of acquired and congenital toxoplasmosis, relies heavily on the folate pathway and is sensitive to folate antagonists such as pyrimethamine, which are commonly used in the treatment of acute toxoplasmosis. The parasite expresses a bifunctional dihydrofolate reductase - thymidylate synthase enzyme with 610 amino acids and a predicted molecular mass of 68,707 Da [1]. The DHFR-TS from *T. gondii* is important as a drug target [2], as a model for drug resistance in malaria [3], and as a selectable marker for molecular transformation of *Toxoplasma* [4]. Expression of the enzyme has been achieved in a recombinant system and biochemical and kinetic studies on recombinant DHFR-TS have been reported [5]. However for further understanding of inhibitor and ligand binding and for the development of new classes of inhibitors by structure-based inhibitor design, crystallographic structure determination will be necessary. To this end, the coding sequence

of the *T. gondii* DHFR-TS has been cloned into a low-phosphate inducible expression vector [6] and high levels of recombinant protein can now be produced and purified for X-ray crystallographic studies.

Materials and Methods

Primer design: An oligonucleotide primer was designed based on the known *T. gondii dhfr-ts* DNA sequence [GenBank™ accession number L08489], which would introduce an NdeI site at the initiating methionine codon: 5'-gtcgtgtctctggg**catatg**cagaaaccg-3' (NdeI site in bold)

Site-directed Mutagenesis: The native DHFR-TS cDNA from *T. gondii* was generously provided to the lab by Dr. David Roos. The XbaI-HindIII fragment of this construct encompassing the entire coding region of the DHFR-TS was ligated into the pSelect vector from Promega. Site-directed mutagenesis was performed as outlined by the Promega manual and mutant constructs containing the 5' NdeI site were identified by restriction digest.

Subcloning, transformation and overexpression: The NdeI fragment of the construct generated above was then ligated into the low-phosphate inducible pBAce vector. Ligation reactions were transformed into DH5 α cells and minicultures were screened for the correct insert. Positive cultures were maxiprepmed with the Quiagen maxiprep kit and DNAs further mapped by restriction digest. The pBAce-*dhfr-ts* construct in DH5 α was induced in low phosphate induction medium and overexpression monitored by fractionation on SDS-PAGE [7].

Protein extraction and assay: Overnight cultures in low phosphate induction medium were harvested by centrifugation at 4°C and lysed by French Press at 16,000 psi in 100mM Tris, 1mM EDTA, 2mM DTT, and 400 mM NaCl at pH 7.0. Cell extracts were clarified by centrifugation at 30,000 x g and the supernatant was assayed for DHFR activity by monitoring the change in absorbance at 340 nm of a solution containing 40 μ M NADPH/H⁺, 40 μ M dihydrofolate, 100 mM potassium phosphate buffer, (pH 7.0) and 1 mM DTT.

Purification of the DHFR-TS : A 5ml column of methotrexate-agarose (Sigma) was equilibrated in 100mM potassium phosphate buffer (pH 7.0) and 1mM DTT (PD buffer). The clarified protein extract from above was then loaded at 1 ml/min and the column washed in 200 ml PD-buffer. The bound protein was then eluted by pulsing with 2ml of PD-buffer with 20 mM dihydrofolate and washing with PD-buffer containing 100 μ M dihydrofolate. Eluted protein was then pooled and chromatographed over a DE-53 column (Whatman, Maidstone United Kingdom) equilibrated in 100 mM NaCl, 10 mM TES (pH 7.0), 1 mM DTT, and 0.1 mM EDTA to remove the dihydrofolate. Purified DHFR-TS eluted from this column in the void volume and was analyzed by fractionation on SDS-PAGE and by activity assay.

Results and Discussion

Creation of an expression construct: A low phosphate inducible expression construct was created by site-direct mutagenesis and ligation into the pBAce vector. (Figure 1)

Transformation of this vector into DH5 α cells and induction of these cells overnight gave rise to an overexpressed 70 kD protein as visualized on SDS-PAGE. (Figure 2 lane A)

Protein assay and purification: DH5 α expressed large amounts of soluble, active DHFR-TS (data not shown) with yields of up to 50 mg purified DHFR-TS per liter of induced bacterial culture. Purified protein was homogeneous as visualized by SDS-PAGE (Figure 2) and exhibited a specific activity of 3.75 ± 2.0 $\mu\text{mol}/\text{min}/\text{mg}$, consistent with the values reported in the literature for this enzyme [5]. Thus large, replenishable quantities of active recombinant DHFR-TS have been produced and can be utilized for future structural studies on this protein. The resolution of the crystal structure of the DHFR-TS will provide a basis for explaining drug resistance in malaria, designing new and better inhibitors for this enzyme and for delineating the binding mode of known inhibitors of the *T. gondii* DHFR-TS.

Figure 1: Vector map of the DHFR-TS expression construct

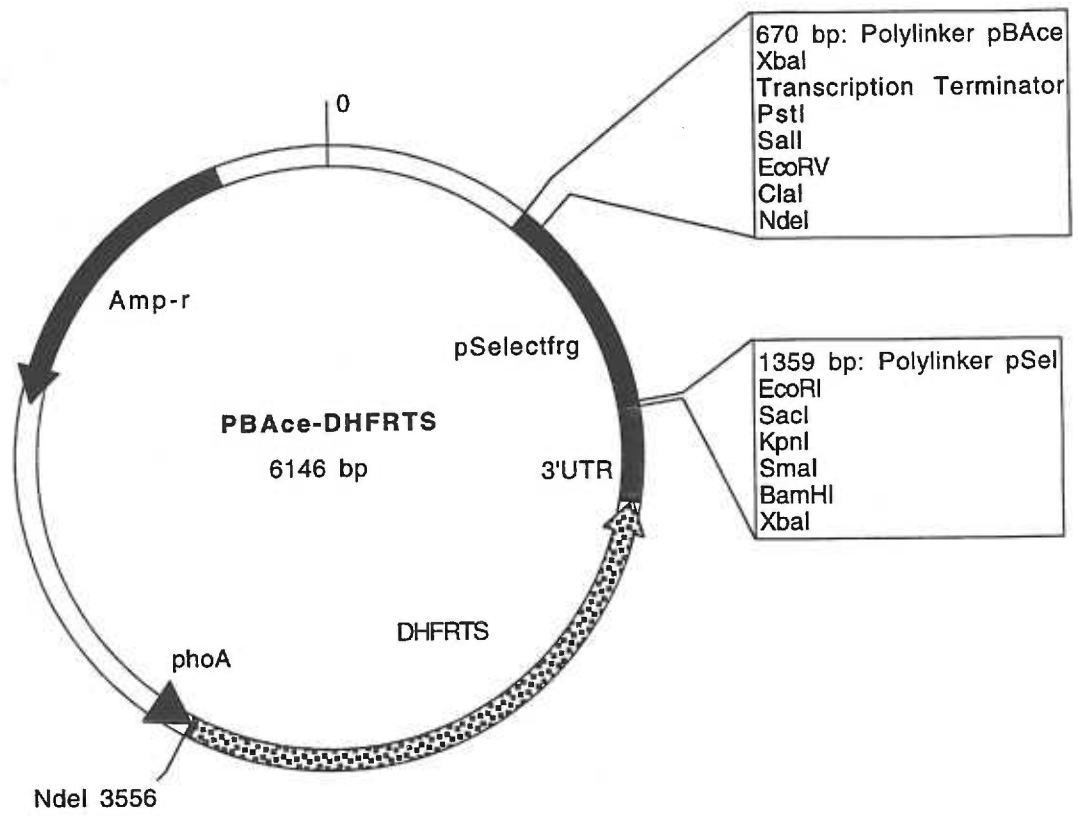
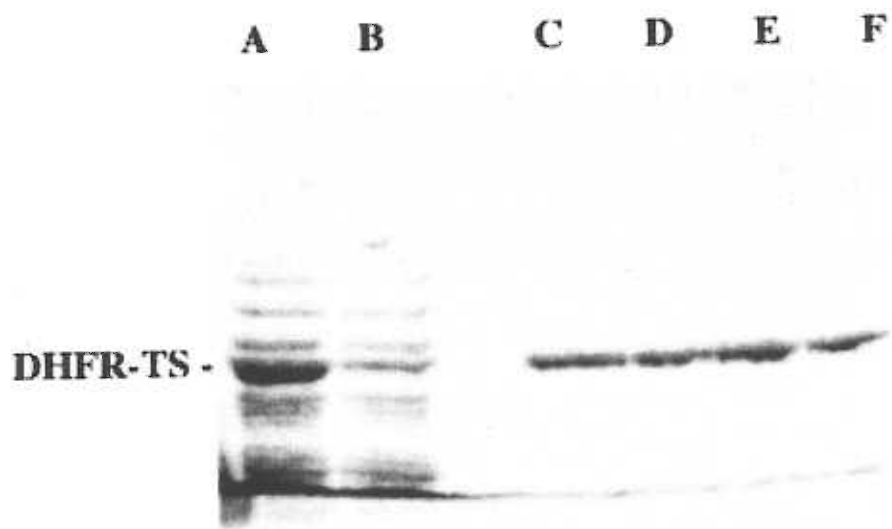


Figure 2: Purification of the DHFR-TS. Lane A: Crude extract of DH5 α cells transformed with the DHFR-TS expression construct. Lane B: Flow through from the methotrexate affinity column. Lanes C-F: Fractions of purified DHFR-TS protein eluted with 20 mM dihydrofolate.



- 1 . Roos DS (1993) *J. Biol. Chem.* **268(9)**: 6269-6280.
- 2 . Dannemann, B., McCutchan JA., Israelski D. et al. (1992) *Ann. Intern. Med.* **116**:33-43.
- 3 . David Roos and Mary Reynolds, personal communication.
- 4 . Donald, RGK, and Roos, DS (1993) *Proc. Natl. Acad. Sci. USA* **90**:11703-11707.
- 5 . Trujillo M, Donald RG, Roos DS, Greene PJ, and Santi DV (1996) *Biochemistry* **35(20)**:6366-6374.
- 6 . Craig SP III, Yuan L, Kuntz DA, McKerrow JH, and Wang CC (1988) *Proc. Natl. Acad. Sci. USA* **88**:2500-2504.
- 7 . Laemmli, UK (1970) *Nature* **227**:680-685.